

TOP SECRET COPY

①

AD-A202 577



THE USE OF CHAFF IN SPACE
AS A JAMMING DEVICE BETWEEN
GROUND STATIONS AND SATELLITES

THESIS

Alan R. Sterns
Captain, USAF

AFIT/GSO/ENP/88D-6

DTIC
ELECTE
S 19 JAN 1989 D
E

DEPARTMENT OF THE AIR FORCE
AIR UNIVERSITY
AIR FORCE INSTITUTE OF TECHNOLOGY

Wright-Patterson Air Force Base, Ohio

This document has been approved
for public release and since its
distribution is unlimited, it is
available to all.

89

1 17 077

AFIT/GSO/ENP/88D-6

THE USE OF CHAFF IN SPACE
AS A JAMMING DEVICE BETWEEN
GROUND STATIONS AND SATELLITES

THESIS

Alan R. Sterns
Captain, USAF

AFIT/GSO/ENP/88D-6

DTIC
ELECTE
S 19 JAN 1989 D
E

Approved for public release; distribution unlimited

AFIT/GSO/ENP/88D-6

THE USE OF CHAFF IN SPACE AS A JAMMING DEVICE
BETWEEN GROUND STATIONS AND SATELLITES

THESIS

Presented to the Faculty of the School of Engineering
of the Air Force Institute of Technology

Air University

In Partial Fulfillment of the
Requirements for the Degree of

Master of Science in Space Operations Engineering



Alan R. Sterns, B.S.

Captain, USAF

December 1988

Accession For	
NTIS GRA&I	<input checked="checked" type="checkbox"/>
DTIC TAB	<input type="checkbox"/>
Unannounced	<input type="checkbox"/>
Justification	
By _____	
Distribution/	
Availability Codes	
Dist	Avail and/or Special
A-1	

Approved for public release; distribution unlimited

Preface

The purpose of this effort was to predict the time evolution of a chaff cloud deployed in orbit around the earth. The idea of using a space-deployed chaff cloud as a jamming device for satellite communications was proposed by Captain Tommy Brown in 1987.

The bulk of the research was in two areas: dissecting and understanding the statistical mechanics approach to satellite breakups as presented by William Heard of the Naval Research Laboratory, and reassembling the information into a useable form in spreadsheet programs so the chaff cloud could be studied at various points in time and for various dispensing velocities. The work is far from complete, however; and further research into this area would be useful. Of particular value would be a computer program which could more efficiently model the chaff cloud over time, thus saving countless hours for any further researcher.

Throughout the course of my research, I have had extensive help from my thesis advisor, Lt Col Howard E. Evans II and will be forever in his debt. I would also be remiss if I did not mention the close friends who were always there to listen to my tirades and helped keep me

focused on the project: Bob Chekan, Wayne Gale, Steve Hildenbrandt, Neil Schoon, Gary Wilson, and Frank Gallagher. These guys collectively spent countless hours letting me bounce questions off them, and just plain listening to me when I wanted to rant and rave in frustration or "strut my stuff" in success. Finally, and most of all, I want to thank two others without whose help I would never have gotten to AFIT, much less completed this thesis: my beautiful wife Brenda and my Lord Jesus Christ.

Alan R. Sterns

Table of Contents

	Page
Preface	ii
List of Figures	vi
List of Tables.	viii
Abstract.	ix
I. Introduction.	1
Background	1
Problem Statement.	4
Scope of Research.	5
Assumptions.	8
Sequence of Presentation	9
II. Review of Literature and Background	
Development	11
Cloud Evolution.	11
Statistical Mechanics.	31
Orbital Mechanics Via Statistical	
Mechanics.	32
Attenuation Through the Chaff Cloud.	46
III. Methodology	50
Applying Heard's Results	50
Graphical Presentation	53
Effectiveness of Attenuation	54
IV. Application of Heard's Results.	56
Dimensional Analysis	56
Velocity Distribution Function.	58
Determining Particle Density	60
Spreadsheet Setup.	64
Attenuation Analysis Using Brown's Thesis	
as a Basis	65

V.	Presentation of Results and Discussion.	72
	Physical Structure of the Chaff Cloud. . .	72
	Signal Attenuation After One Hour.	80
	Attenuation the First Twelve Hours After Dispensing	89
VI.	Conclusions and Recommendations	100
	Conclusions.	100
	Recommendations.	101
	Appendix A: Density Spreadsheet Formulas	114
	Appendix B: Attenuation Spreadsheet Formulas	139
	Appendix C: An Example Calculation	149
	Bibliography.	157
	Vita.	159

List of Figures

Figure	Page
1. Basic Orbital Parameters	
2. Satellite Orientation for Cases I, II, III, and IV	17
3. Chaff Cloud Evolution for Case I	20
4. Chaff Cloud Evolution for Case II.	24
5. Dispensing Setup for Case III.	26
6. Chaff Cloud Evolution for Case III	28
7. "Magnification" of a Subvolume of the Chaff Cloud.	63
8. Numbering Scheme for the Subvolumes Along the Central Column of the Chaff Cloud.	66
9. Effect of Inscribing a Circle Within the Chaff Cloud Model.	68
10. Chaff Cloud Evolution for a 0.01 m/s Dispensing Velocity: 3600 Seconds After Dispensing	73
11. Chaff Cloud Evolution for a 0.01 m/s Dispensing Velocity: 25200 Seconds After Dispensing. . . .	74
12. Chaff Cloud Evolution for a 0.01 m/s Dispensing Velocity: 28800 Seconds After Dispensing. . . .	75
13. Chaff Cloud Evolution for a 0.01 m/s Dispensing Velocity: 39600 Seconds After Dispensing. . . .	76
14. Average Density Through the Centroid of the Chaff Cloud.	79
15. Signal Attenuation at One Hour for Dispensing Velocities Between 0.0115 and 0.0155 m/s	82

16.	Signal Attenuation at One Hour for Dispensing Velocities Between 0 and 0.05 m/s.	83
17.	Signal Attenuation in Ten Minute Increments Up to one Hour	86
18.	Time Until -10 dB Attenuation.	87
19.	Attenuation for the First Twelve Hours: 0.01 m/s Dispensing Velocity	90
20.	Attenuation for the First Twelve Hours: 0.02 m/s Dispensing Velocity	91
21.	Attenuation for the First Twelve Hours: 0.03 m/s Dispensing Velocity	92
22.	Attenuation for the First Twelve Hours: 0.04 m/s Dispensing Velocity	93
23.	Attenuation for the First Twelve Hours: 0.05 m/s Dispensing Velocity	94
24.	Attenuation for the First Twelve Hours: 0.01, 0.02, 0.03, 0.04, and 0.05 m/s Dispensing Velocities.	98
C1.	Initial Downscaling of Cube A.	150
C2.	Central Column at 2.45 km Scaling.	152
C3.	Central Column at 0.35 km Scaling.	153

List of Tables

Table	Page
I. Most Probable Particle Speeds for Various Dispensing Velocities.	59
CI. Number of Particles Along the Central Column at 0.35 km Scaling	154

AFIT/GSO/ENP/88D-6

Abstract

This study predicts the time evolution of the attenuation characteristics of a chaff cloud deployed in orbit around the earth. The study consists of three parts: applying the statistical mechanics solution of a satellite breakup model by William Heard of the Naval Research Laboratory, solving for particle density at any time after dispensing, and calculating the attenuation of an 8 GHz signal through the cloud. The study shows that significant levels of signal attenuation can be achieved, with attenuations of greater than -50 dB lasting for several hours.

(746565) — (R4) 47

THE USE OF CHAFF IN SPACE AS A JAMMING DEVICE BETWEEN GROUND STATIONS AND SATELLITES

I. Introduction

This chapter provides a general background for the problem of deploying a chaff cloud in orbit about the earth with the purpose of jamming satellite communications. It describes why this research effort was needed, and exactly what the problem entailed. Finally, it provides an outline of the scope, assumptions and sequence of presentation which follow.

Background

To fully understand the need for and scope of this research effort, some background knowledge concerning both chaff and statistical mechanics is required. This section provides the basic information needed to understand the orbital chaff cloud jamming problem.

Chaff. Reflective chaff is an electronic countermeasure (ECM) device consisting of a large number of tiny dipoles that are deployed in a rapidly expanding "cloud," and is used to attenuate incident electromagnetic signals. The individual chaff particles affect this

attenuation by reflecting and absorbing portions of the incoming signal (Brown, 1987:4-1). The wavelengths of the incident signal most attenuated by a chaff cloud are those which are approximately double the length of the individual chaff particles (Butters, 1982:197). Some a_priori knowledge of the incident signal is thus required so that the chaff particles can be constructed at the proper length for maximum signal attenuation to occur.

Chaff is routinely deployed in the atmosphere by the Air Force and Navy as a decoy to intercept radar signals targeted for planes and ships, thus allowing the intended targets to avoid detection and subsequent destruction.

Due to the aerodynamic forces which act on the individual chaff particles in the atmosphere, a chaff cloud rapidly blooms (expands) and begins falling to earth shortly after deployment. Therefore, it is a very transient ECM device. In space the aerodynamic forces are minimal, however, so a chaff cloud would be a relatively long-lived entity.

Brown has proposed that chaff in space could be effectively used to jam satellite communications if a cloud of chaff with sufficient density and of the proper resonant wavelength were used (Brown, 1987:4-1 to 4-24). In order to assess the utility of deploying chaff in space, a model

describing the physical blooming characteristics of the chaff cloud needs to be developed.

A blooming model for chaff in outer space would have to include the following information: the size of the cloud in three dimensions at any given time, the particle density of the cloud at any given point in space, and the rate of expansion of the cloud in all directions. The cloud model would also have to be useable from any reference point on the earth to determine whether a signal sent between the ground and a satellite, or vice versa, would be properly attenuated.

Statistical Mechanics Approach. Ideally, the position, velocity, and density of a collection of particles can be described using Newton's Laws of Motion, particularly his Third Law: $F = ma$, where F is the force acting on a given particle, m is the particle's mass, and a is the acceleration vector of the particle in three dimensions. When the number of particles whose motion needs to be described becomes large, however, the use of Newton's Third Law becomes impractical and an approach using statistical mechanics is often taken.

Statistical mechanics refers to the study of the collective properties of a system consisting of a large number of small particles whose exact position and velocity

components are either unknown or difficult to describe (Johnson and McKnight, 1987:56). Since the chaff cloud problem involves billions of individual particles, a statistical mechanics approach is justified.

Problem Statement

This study uses the statistical mechanics approach described by William B. Heard of the Naval Research Laboratory in his paper "Dispersion of Ensembles of Non-Interacting Particles" and describes the time history of the size, shape, and particle density of a space deployed chaff cloud based on stated initial conditions at an ideal spherical deployment. The study then uses the size and shape information for the cloud and the particle densities within the cloud to determine the attenuation of a signal from a ground-based antenna to a satellite located behind the cloud. The attenuation study examines signal attenuation along a column which runs from the part of the cloud closest to the earth, through the center of the cloud, and out the part of the cloud nearest the satellite. Since the cloud is continually changing in size, shape and density, the attenuation study is accomplished by taking "snapshots" of the cloud at various times after initial deployment. The dispensing velocity of the cloud is also varied to determine the dispensing velocity which provides

the most effective attenuation over a specified period of time. This information is then used to determine if jamming occurs, and if so, over what time period and for what dispensing velocities.

Scope of Research

The research effort examines the following:

- 1) existing data which describes the time evolution of a collection of particles in earth orbit;
- 2) the field of statistical mechanics as it applies to the chaff cloud problem;
- 3) Heard's solution to the statistical mechanics problem of numerous particles in orbit about a large body, and its application to the chaff cloud problem;
- 4) Brown's stated requirements for the attenuation of electromagnetic signals through a chaff cloud and equations appropriate for signal attenuation calculations.

Evolution of Particles. A knowledge of the anticipated time history evolution of a chaff cloud is essential in determining if the results obtained via statistical mechanics provides accurate data. Several research efforts have addressed this area in the past. The results of two of them have been examined in this study to provide a basis with which to compare the results of the statistical mechanics solutions.

The first of these studies is the work done by Ross in 1961 which provided a theoretical basis for the evolution of a group of particles deployed from a satellite in earth orbit (Ross, 1961:79-83).

A second research effort entitled "Project Westford" examined the usefulness of a dipole cloud in earth orbit as an aid to long-distance, point-to-point communication. Project Westford got into full swing upon the release of 480 million dipoles into earth orbit on 10 May 1963. The resulting cloud of particles was used to reflect radio signals between a ground-based transmitter and a receiving antenna located at a distant location (Overhage and Radford, 1963:452).

The long-term (days to months) evolution of the chaff cloud, although an interesting aspect of the problem, is not addressed in-depth. Since the current problem involves only whether or not a signal can be attenuated, and if so, for how long, the final shape of the cloud is of no particular interest. After the attenuation of the incident signal drops below a specified value, the evolution of the cloud is no longer pertinent to this study.

Statistical Mechanics Solutions. Statistical mechanics has applications in many wide ranging disciplines. Therefore, a list of some of these applications are provided

to further introduce the subject. First, specific areas of application of statistical mechanics are listed. Then, the Boltzmann equation, which is used to describe the time history of the distribution of a collection of particles, is presented.

Orbital Statistical Mechanics. Several researchers have done work using statistical mechanics which they claim can be used to describe such systems as the rings of saturn, satellite breakups, the asteroid belt, meteor streams, and moving star clusters (Hameen-Antilla, 1976:145; Heard, 1976:63; Johnson and McKnight, 1987:56-57). The results of these efforts, when compared with the results of the two particle evolution studies mentioned previously are used to solve the problem at hand. In particular, the local densities at various points throughout the chaff cloud are determined. This in turn leads to the actual number of particles lying within various subvolumes within the cloud. These particle densities are also examined at various time intervals after deployment of the cloud. The attenuation of the signal through each subvolume (and subsequently the entire cloud) is then determined.

Signal Attenuation. In his 1987 Master's thesis, Brown provided several equations describing the attenuation of a radio signal through a chaff cloud. His procedure depends

.. on the number of particles encountered by the incident signal. Brown also described the size of a chaff cloud required to jam an area the size of Washington D.C, the required altitude of the chaff cloud for this scenario, and time requirements for signal attenuation (Brown, 1987:4-3 to 4-5, 4-13 to 4-17). In order to prevent the unnecessary duplication of effort, his results are applied directly to the above statistical mechanics solutions to determine the attenuation of the signal through each of the subvolumes described above. By examining the attenuation through subvolumes which line up directly with each other along a central column through the chaff cloud, and by multiplying together the percentage of the signal which passes through each of these subvolumes, the percentage of the signal which penetrates through the cloud is determined.

Assumptions

Several general assumptions are made to help simplify the calculations and keep the scope of this research effort manageable. The assumptions are as follows:

- 1) All the chaff particles can be instantaneously and ideally deployed in orbit at the specified time, t_0 .
- 2) The cloud will follow an ideal, circular orbit around a non-rotating earth and will experience no perturbations.

- 3) There will be no physical interaction between individual chaff particles after deployment.
- 4) The initial dispersion pattern will be spherical.
- 5) The electromagnetic signal will always be directed normally to and through the point of initial dispersion (centroid) of the cloud to a geosynchronous satellite.
- 6) The incremental velocity imparted to the chaff particles upon deployment is very much less than the velocity of the parent body in its orbit.

Sequence of Presentation

First, the research is presented beginning with a review of current literature relating to the problem of deploying a chaff cloud in earth orbit. As outlined above, this includes a look at the evolution of the cloud using classical approaches, a discussion of statistical mechanics, a presentation of specific statistical mechanics solutions to orbital problems, and a synopsis of signal attenuation as described by Brown.

A short methodology section briefly describing the process involved in the solution of the problem is next, followed by a section building on the theories outlined in the literature review section. Appropriate adaptations for the chaff cloud problem are included.

Following that is a section that provides the solutions to the chaff cloud problem, including two-dimensional

graphical representations showing the physical dimensions of the chaff cloud as a function of time. These results are then analyzed using the attenuation model to show the time period over which effective jamming by the chaff cloud occurs.

The final section provides some conclusions regarding the chaff cloud problem and recommends some areas of study where future research might be useful.

II. Review of Literature and Background Development

This chapter provides an in-depth review and some development of the background information which forms the basis for this research effort. It is divided into the following sections: discussions of chaff cloud evolution in general, a review of statistical mechanics, solutions to orbital problems similar to the chaff cloud problem using statistical mechanics approaches, and a review of the theory of signal attenuation through a dipole cloud.

Cloud Evolution

As mentioned in the previous chapter, several researchers have addressed the problem of the evolution of a collection of particles that has been released from a parent satellite in earth orbit. Since this paper is mainly concerned with the density of the chaff cloud and an integration across its volume, and since statistical mechanics will be used to provide the actual numbers to be used, this section does not apply any rigorous mathematics. Instead, only a description of the most general aspects of chaff cloud evolution in earth orbit will be discussed.

Orbital Mechanics Review. In order to fully understand a satellite's orbital motion about the earth, a knowledge of

the basic orbital parameters is required. This section provides a review of some of the basic concepts and definitions associated with orbital mechanics.

The coordinate system for an earth-orbit is a right-handed, inertial system with the origin at the center of the earth. The I-axis points in the Vernal Equinox direction and passes through the earth's equator. The J-axis is located 90 degrees from the I-axis along the equatorial plane. The K-axis is orthogonal to the other two principle axes and points through the north pole (Bate and others, 1971:58).

There are six basic orbital parameters: semi-major axis (a), eccentricity (e), inclination (i), longitude of the ascending node (Ω), argument of perigee (ω), and time of perigee passage (T). All of the orbital parameters are described in "Fundamentals of Astrodynamics" by Bate, Mueller, and White (Bate and others, 1971:58). The orbital parameters are represented pictorially in Figure 1.

Three additional aspects of a satellite's motion which are also important to the chaff cloud problem, although not included among the basic orbital parameters, are the period of the satellite's orbit (P), the specific mechanical energy of the orbit (E), and the satellite's mean motion (n).

The period is the amount of time it takes a satellite to complete one revolution about the earth and is usually,

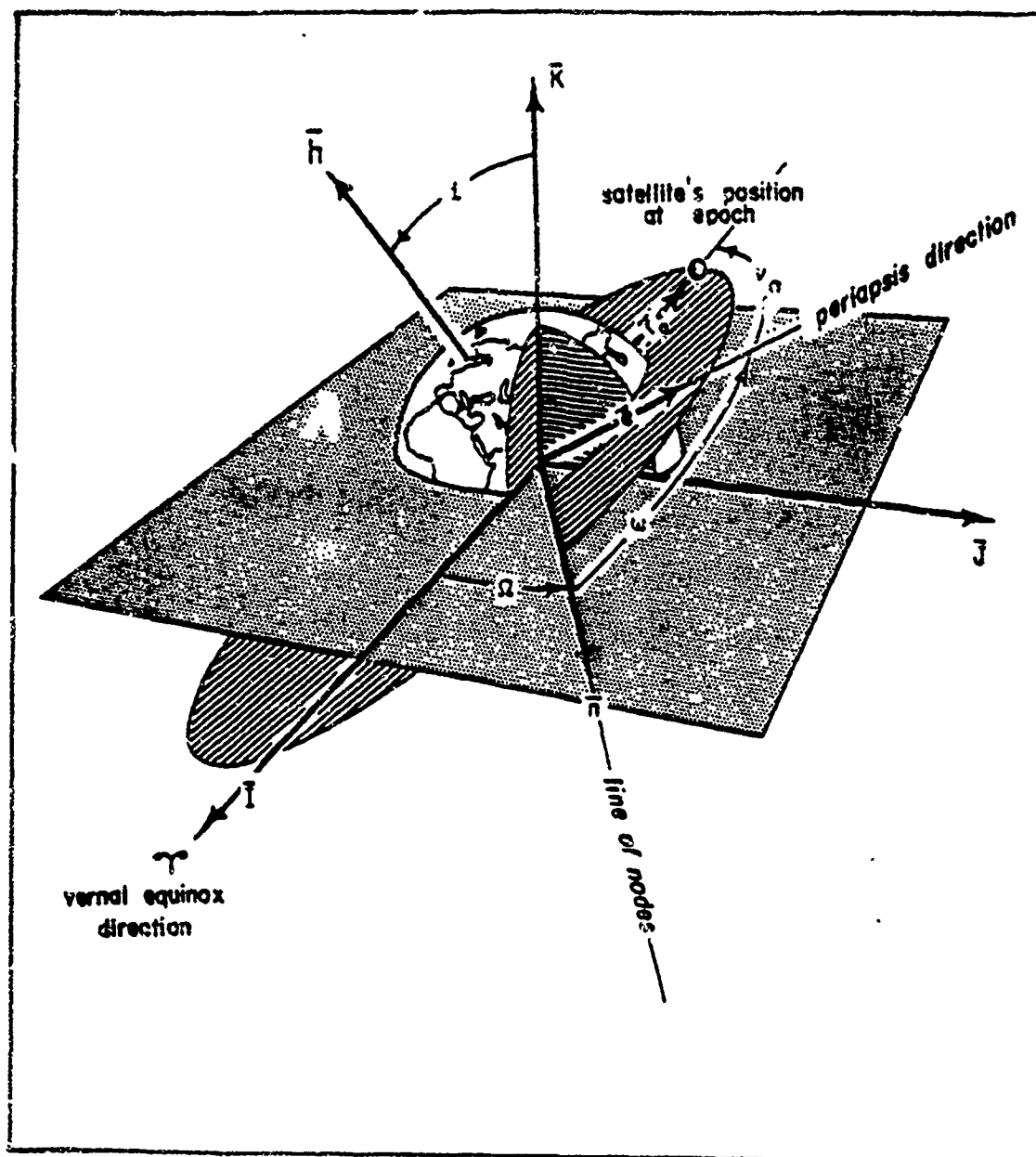


Figure 1. Basic Orbital Parameters
(Bate, 1971:59)

measured in minutes. A satellite's period is defined as follows:

$$P = 2\pi(a^3/K)^{1/2} \quad (1)$$

where a is the semi-major axis and K equals the Universal Gravitational Constant (G) multiplied by the mass of the earth (M) (Bate and others, 1971:33).

The specific mechanical energy of each particular orbit is constant and related to K in the following manner:

$$E = v^2/2 - K/r \quad (2)$$

Here, v is the magnitude of the satellite's velocity and r is the distance from the center of the earth to the satellite (Bate and others, 1971:16).

Mean motion is the time it takes a satellite to complete one revolution of travel about its orbit and is defined as follows:

$$n = (K/a^3)^{1/2} \quad (3)$$

where K and a are the same as in Eq (1) (Bate and others, 1971:185).

From the relationships described above, it can be shown that any change in a satellite's energy directly affects both the satellite's period and the semi-major axis of the satellite's orbit (Thomson, 1986:58). Shapiro states that a

change in satellite velocity will not change the energy of the satellite's orbit unless a component of the velocity is in the direction of satellite motion. Velocity components in the other two orthogonal directions have effects only on the other orbital parameters, particularly 'e' and 'i' (Shapiro and others, 1964:483).

Preliminary Assumptions and Setup. To understand a description of the evolution of a particle cloud in orbit, it is best to begin by looking at simplistic examples and expand the complexity one step at a time. Therefore, it will be assumed that the parent satellite (the satellite which dispenses the chaff particles) starts in a perfectly circular ('e' = 0), equatorial ('i' = 0) orbit about the earth. At this point, the specific values for the other orbital parameters and the values for 'P', 'E', and 'n' are unimportant. As noted in Chapter I, any perturbations to the orbit caused by anything other than the velocity changes noted below are assumed to be negligible.

For these examples, the shape of the parent satellite will be assumed to be cylindrical with the satellite spinning about its longitudinal axis. For simplicity, the cloud will be assumed to consist of small particles initially located inside the spinning parent satellite. Dispensing occurs when the outer shell of the parent

satellite is instantaneously removed. This allows the particles, no longer held in place by the shell but still moving at the angular velocity imparted by the spinning of the parent satellite, to spread radially from the parent.

The rest of this section will examine four types of particle dispensing from the cylindrical particle satellite as described by Ross in his paper "The Orbital Motion of Pellet Clouds" and Shapiro, Jones, and Perkins in their paper "Orbital Properties of the West Ford Dipole Belt" (Ross, 1961:79-83; Shapiro and others, 1964:482-492). Except where noted, all the material for Cases I and II comes from Ross's paper; Cases III and IV are entirely from the Shapiro paper.

The first two cases assume instantaneous dispensing of the particles, and the parent satellite's orientation is as shown in Figure 2. The case where the spin axis is oriented axially in relation to the earth will not be specifically discussed, but will be automatically included in Cases III and IV as discussed below.

Cases III and IV involve dispensing the particles over a period of time and are also shown in Figure 2. The release of particles over time could be accomplished by releasing only a fraction of the outermost particles within the parent at any one instant in time. In these cases, the direction of spin axis orientation is assumed to be time

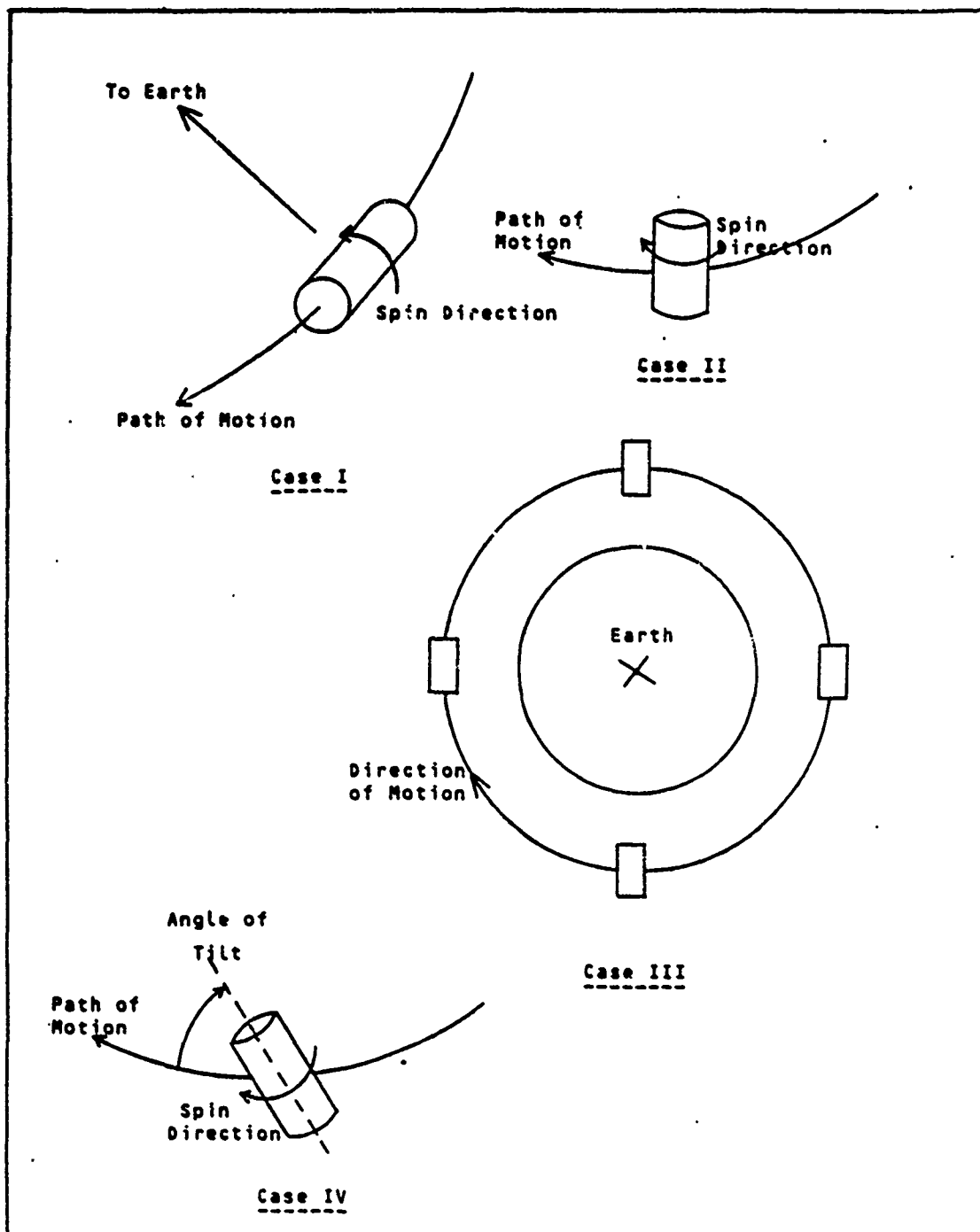


Figure 2. Satellite Orientation for
Cases I, II, III, and IV

independent and, therefore, the spin axis will continually change its orientation angle with respect to the path of satellite motion as the satellite moves around the earth. The resultant dispensing of particles over time causes spreading in all directions relative to the parent satellite.

Case I: Spin Axis Along Satellite's Path of Motion.

In this first case, Ross says that since no incremental velocity is imparted upon the particles in the direction of satellite motion, no energy change is imparted to their respective orbits. Therefore, no changes in their orbital periods occur.

The velocity changes which occur happen only perpendicular to the parent satellite's path with the subsequent effect that both the eccentricity and inclination change. The eccentricity change is caused by the radial component of the particle velocity with respect to the orbital plane of motion, while the inclination change is a result of the velocity component perpendicular to the orbit plane.

Another interesting effect is that since a change in period does not occur, all particles must return to their original locations in the parent orbit at the end of each subsequent revolution about the earth. This means that

although the incremental velocity imparted to the particles causes an expansion of the cloud, the expansion reaches a maximum halfway around the orbit. At this point, the cloud begins to contract and will return to its original size and shape at the original point of dispensing. The combination of the change in values for 'e' and 'i' has the additional effect of causing the "ends" of the cylindrical cloud to tilt sinusoidally with time. Figure 3 illustrates the contracting/expanding/tilting particle cloud over time. In the figure, 'nT' is the portion of the orbit (in radians) the cloud has traversed, the 'S' direction is in the direction of satellite motion, the 'R' direction is pointed radially to the earth, and the 'W' direction is out of the orbital plane.

The effect of the angular velocity of the parent satellite's spin is important to the dispensing in that the outermost particles undergo the biggest changes in velocity (and thus 'e' and 'i') and the innermost particles experience the smallest changes. Because of these variances in the delta velocities, a smear of particles develops between the parent orbit and the orbits of the particles with the maximum eccentricity and inclination changes.

It is important to note that since the velocity changes occur instantaneously and no further accelerations or velocity changes are involved, the changes in 'e' and 'i'

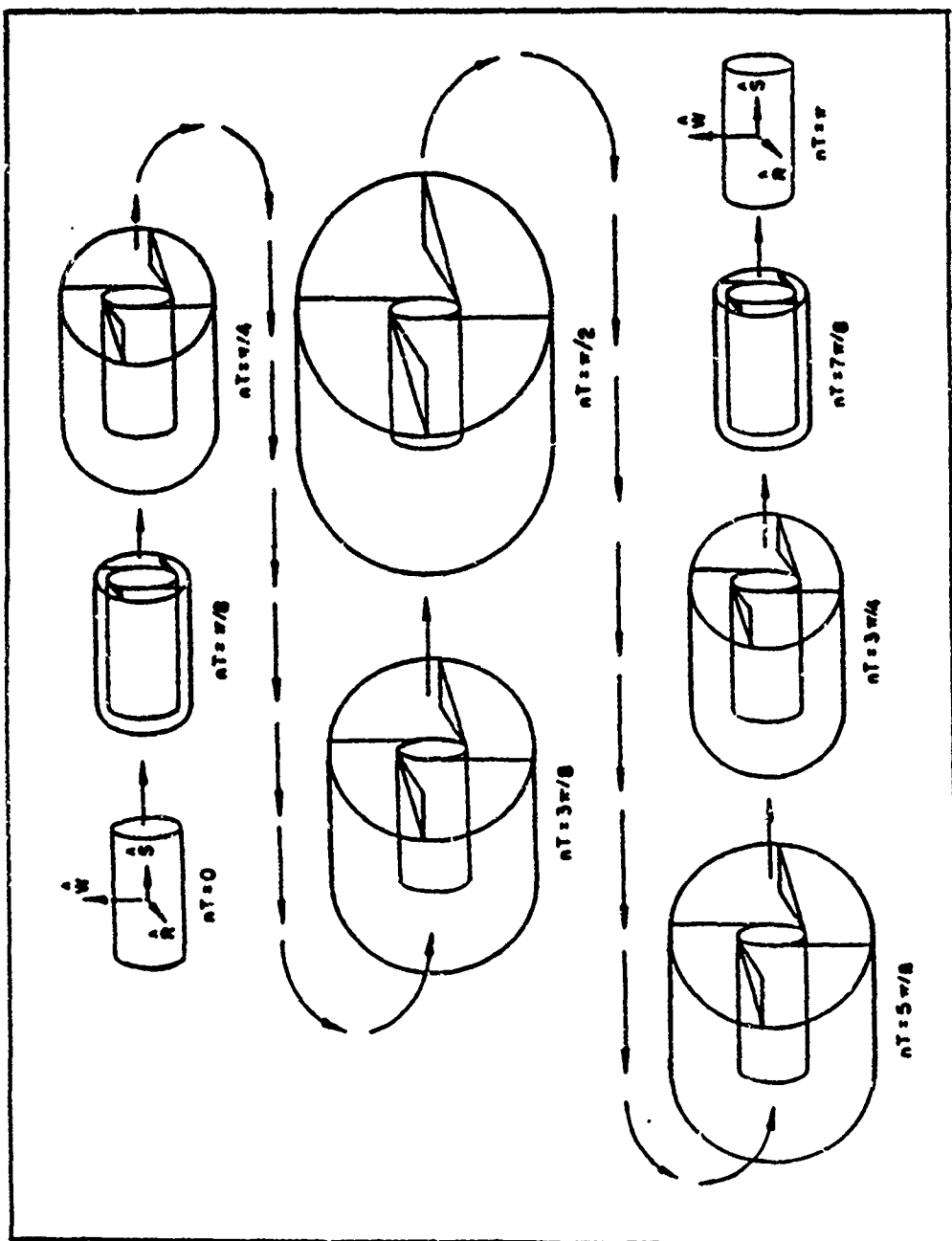


Figure 3. Cheff Cloud Evolution for Case I
(Ross, 1961:82)

have an upper limit. This limit is what causes the cloud to reach its maximum size at the halfway point in the orbit.

Case II: Spin Axis Perpendicular to Orbit Plane. With the spin axis perpendicular to the orbit, there is one component of velocity directed radially from the earth in the orbital plane and one component in the direction of satellite motion. Since no velocity component can cause an inclination change, the spread of the particles out of the orbit plane is solely determined by the initial length of the parent satellite.

The velocity component in the radial direction has the same effect as it had in the previous case, causing a change in the eccentricity of the satellite's orbit. However, the velocity component which acts in the direction of satellite motion introduces a new effect into the problem. By altering the particle velocity in the direction of motion, the energy of the orbit is changed. This alteration in turn causes a change in 'P' and 'a' of the orbit.

The effect of the differences of the angular velocities of the particles, as was noted in Case I, is that the outermost particles undergo larger changes in velocity (and thus 'P' and 'a') than the innermost particles. This causes either an increase or decrease in orbital period depending on the direction of the velocity vector in relation to the

satellite's motion. Again, a smear of particles develops between the parent orbit and the highest and lowest orbits caused by the period changes.

Since the period changes are permanent if no other perturbations are considered, the particles continue to spread forward and backward along the orbit (with respect to the parent satellite) at rates equal to their respective changes in period from the initial orbit. For example, if a period change of one minute is imparted upon a particle, it will move away from the parent satellite at a rate of one minute per orbit. Eventually, the cloud expands to the point that the forward moving particles meet the backward moving particles halfway around the orbit from the parent satellite. Since the expansion due to period changes of the particles continues indefinitely, a toroid ultimately develops around the earth.

The result of the eccentricity and period changes acting together to change the orbit (for those particles that have components of velocity in both the radial direction with respect to the parent satellite and the direction of satellite motion) are different than for Case I because of the period changes involved. The eccentricity causes some oscillations of the height of the apogee and perigee points with a maximum occurring halfway through the first orbit. However, due to the fact that virtually every

particle has at least a small component of velocity along the direction of motion, the overall tendency of the cloud is not to continue oscillating each orbit. Instead, the cloud elongates along the orbit in a manner similar to that shown in Figure 4.

Case III: Long-Term Dispensing with Spin Axis in Orbital Plane. With the spin axis lying in the orbital plane, its orientation is the same as that in Case I exactly twice each orbit. These points are 180 degrees from each other in the orbit. At a point 90 degrees from either of these points, the spin axis is oriented radially with respect to the earth. At any other point in the orbit, the spin axis is at some other orientation.

With the spin axis oriented precisely perpendicular to the path of motion for only an instant of time twice each orbit, only a fraction of the particles receive velocity components exactly in the direction of motion. Therefore, the number of particles with the greatest period change is significantly less than in the previous two cases. However, since the particles are dispensed in all directions, all particles receive some change in period (except in those instances with the spin axis exactly parallel to the satellite's motion), unlike Cases I and II.

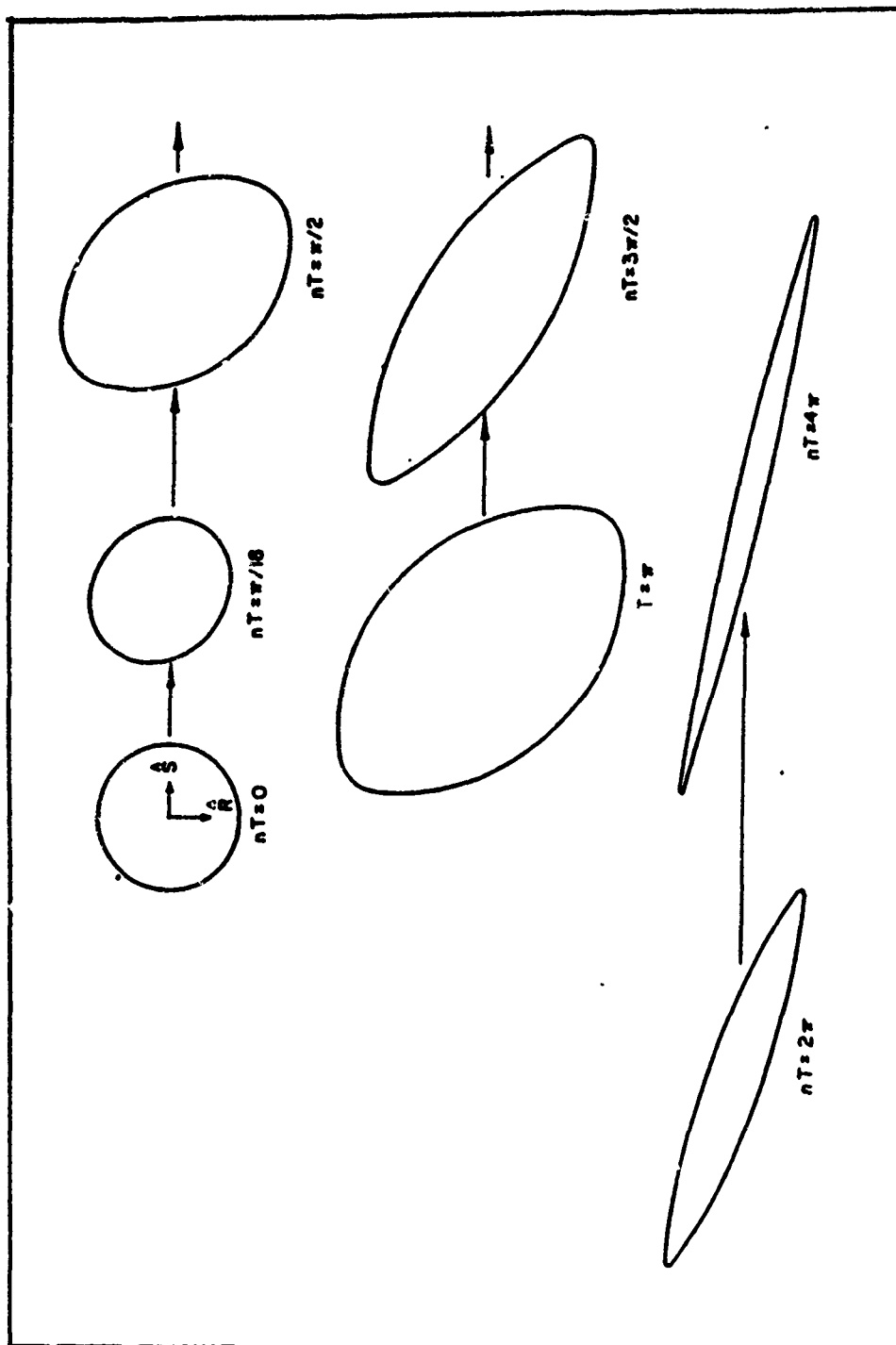


Figure 4. Chaff Cloud Evolution for Case II
(Ross, 1961:82)

With a continually changing orientation of the spin axis relative to the satellite's motion, the velocity components influencing eccentricity and inclination change also. The maximum changes in eccentricity and inclination occur with the spin axis oriented along the path of motion.

When effects of the various changes in period, eccentricity, and inclination are combined with the effects of different velocity magnitudes due to the shrinking size of the dispenser as time progresses, a distribution of particles occurs that has a peak density near the parent orbit. The density rapidly diminishes farther out from the parent satellite.

Shapiro notes an interesting result when the overall cloud is described pictorially. Since the largest change in period occurs only for those particles released when the spin axis is oriented radially from the earth, particles released here will move ahead or lag behind the parent satellite the farthest. Those that lead are in orbits with lower perigee altitudes, and those that lag are in orbits with higher apogee altitudes than the parent satellite.

Assume the spin axis is aligned radially with respect to the earth at $u' = 0$ degrees and $u'' = 180$ degrees as shown in Figure 5. For those particles released at u' , the following situation develops: all particle orbits intersect the parent orbit at this point, with the lagging particles

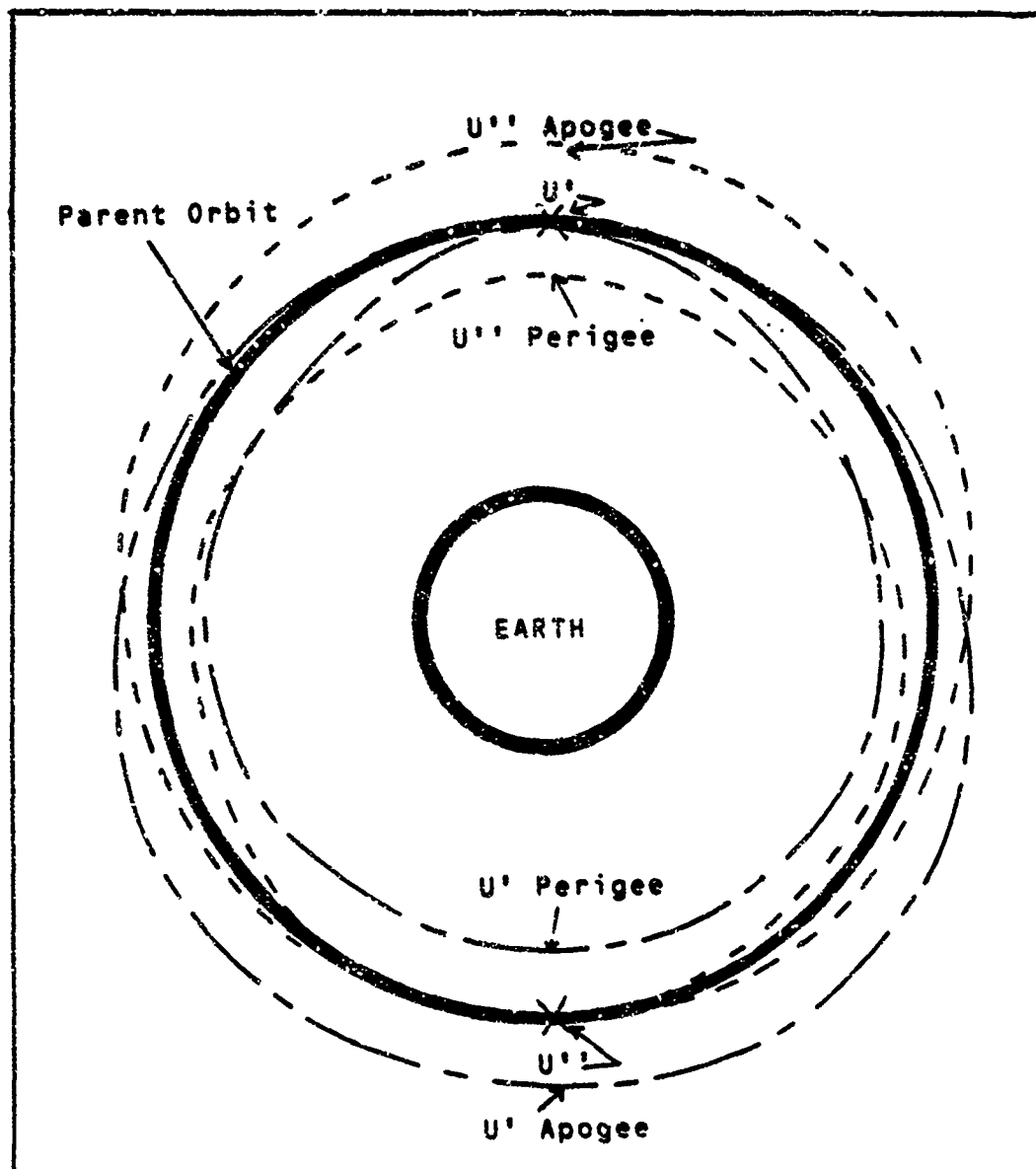


Figure 5. Dispensing Setup for Case III

having perigees and the leading particles having apogees here. For those particles released at u'' , the same thing happens only it is one-half orbit removed. At the u'' point, the particles released at u' are all at either perigee or apogee of their respective orbits and are ahead or behind of the parent satellite, respectively. A similar situation occurs for the particles released at u'' when they reach the u' point in the orbit.

The interesting result is that at both u' and u'' , there are particles that were released at the opposite end of the orbit, some of which are at perigee and some of which are at apogee. Therefore, at u' there are particles leading the parent satellite in a slightly lower orbit (u'' particles at perigee), particles lagging behind the parent satellite in a slightly higher orbit (u'' particles at apogee), and particles leading and lagging the parent satellite at the same altitude (u' particles). A similar result applies to the u'' points. At these points, a four pointed cloud like the one shown in Figure 6 develops. At the points in the orbit where the spin axis is aligned with the direction of satellite motion (90 and 270 degrees), a smooth transition between particle orbits occurs.

According to Shapiro, the overall effect of the particle cloud "can thus be envisioned as a two-headed

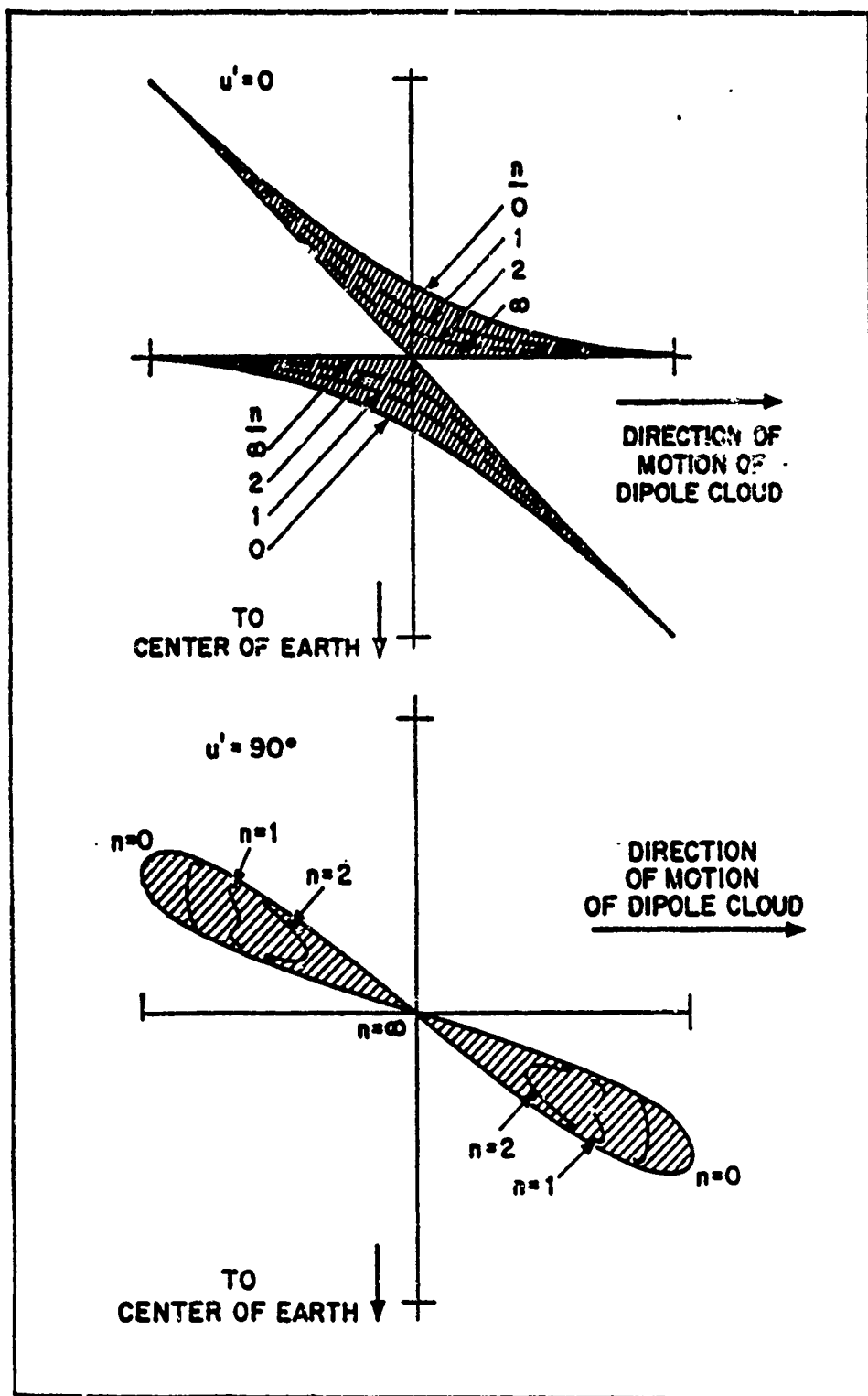


Figure 6. Chaff Cloud Evolution for Case III
(Shapiro, 1964:491)

dragon, snapping its jaws open and closed as it circulates around the earth" (Shapiro and others, 1964:490).

Case IV: Long-Term Dispensing with Inclined Spin Axis.

The only differences between this case and Case II above are that the angle between the spin axis and the orbital plane can be set anywhere between 0 and 90 degrees (instead of being placed rigidly at 90 degrees), and that the dispensing takes place over a long period of time. Shapiro makes some mention of the situation in which the angle is 90 degrees, but the results agree with Case II above, so it will not be discussed here.

For Case III, Shapiro says that the greatest inclination change for the particles occurs at the point along the orbit where the largest velocity component perpendicular to the orbital plane exists. He also says that the greater the angle between the dispenser and the orbital plane, the smaller the spread in the distribution of the inclinations of the particle orbits. This is because at 90 degrees (Case II) no inclination changes occur, and at 0 degrees (Case II') virtually all particles exhibit some inclination changes. Because of these effects, the inclination changes undergone by particles can be kept to within a desired range by changing the angle of tilt of the dispenser relative to the orbital plane.

The effects of inclining the spin axis relative to the orbital plane on the other orbital elements is a combination of all the effects previously mentioned. At an inclined angle of 0 degrees, the distribution of the number of particles with various period changes is the most pronounced, since relatively few particles experience the greatest possible period change. For greater angles of inclination, larger numbers of particles can undergo changes in period, with a maximum number occurring at an inclined angle of 90 degrees (Case II). Thus, Shapiro points out, although the maximum period change can be experienced by particles at any inclined angle (assuming their velocity component is aligned with the direction of motion), the distribution of the number of particles with any given period change is very angle dependent.

Finally, Shapiro says that no matter what the angle of tilt, the resulting distribution of particles is centered about the parent satellite's orbit, with the largest concentration of particles in the vicinity of the parent orbit. The resulting cloud for this case also resembles Figure 6 except for slight differences in both the distribution of the particles and spreads in the inclinations of the particle orbits.

Statistical Mechanics

As mentioned previously, the motivation behind using statistical mechanics to study a collection of particles is that Newton's laws of motion become cumbersome when applied to a large number of particles. Statistical mechanics solves this problem by looking at the collection of particles as a single entity and analyzing its behavior over time.

Several areas of physics routinely utilize statistical mechanics to aid in the solution of problems. Among them are plasma physics and kinetic gas theory. However, since none of these disciplines directly apply to the chaff cloud problem, no further mention of them will be made.

To properly examine the behavior of the particles over time as a group, a distribution function is required. A distribution function describes the location, size and density of the collection of particles as a function of time. Once the distribution function is known and appropriate initial conditions are applied, the time history of the collection of particles can be determined.

An equation commonly used to describe the time evolution of distribution functions is the Boltzmann equation which, according to Chen, is as follows:

$$df/dt + \underline{v} \cdot \nabla f + \underline{F}/m \cdot df/dv = (df/dt)_{coll} \quad (4)$$

Here f represents the function $f(\underline{r}, \underline{v}, t)$ or the number of particles per cm^3 as a function of position (\underline{r}), velocity (\underline{v}), and time (t). df/dt is the derivative of f with respect to time. ∇f represents the gradient in (x, y, z) space so that

$$\underline{v} \cdot \nabla f = \frac{df}{dx} \frac{dx}{dt} + \frac{df}{dy} \frac{dy}{dt} + \frac{df}{dz} \frac{dz}{dt} \quad (5)$$

\underline{F} is the force acting on the particles, m is the mass of the particles, and $df/d\underline{v}$ is the gradient in velocity space so that

$$\underline{F}/m \cdot df/d\underline{v} = \frac{df}{dv_x} \frac{dv_x}{dt} + \frac{df}{dv_y} \frac{dv_y}{dt} + \frac{df}{dv_z} \frac{dv_z}{dt} \quad (6)$$

The term on the right-hand side in Eq (4) describes the time rate of change of f due to collisions between particles (Jen, 1977:206), and will be assumed to be negligible for the remainder of this work.

Orbital Mechanics Via Statistical Mechanics

This section examines the literature which specifically addresses the application of statistical mechanics to problems in orbital mechanics. All the examples addressed here have the common element of a large number of small satellites being released from a parent satellite. Applications of these examples to other problems in orbital

mechanics include examining the behavior of meteor streams coming from a disintegrating comet, expanding star clusters, asteroid belt fragmentations, and exploding earth satellites (Heard, 1977:1025). Due to the similarities between the case of an exploding earth satellite and the expanding chaff cloud, the application of statistical mechanics to the chaff cloud problem is fairly straightforward.

Applications. In their 1987 book Artificial Space Debris, Johnson and McKnight discuss the usefulness of applying statistical mechanics to determine the resulting orbits of the pieces from a satellite breakup. They describe the different particle orbits using an approach outlined by Heard in a paper published in 1978. Heard's work is described in the "General Theory" section below. In addition to outlining Heard's approach to the problem, Johnson and McKnight provide a useful summary of the advantages of using statistical mechanics for analysis of satellite breakups as opposed to using classical mechanics approaches:

First, the statistical approach requires less computational effort and does not require increased effort for larger breakups. It also provides a global definition to a problem which inherently does not lend itself to such an approach. (Johnson and McKnight, 1987:58)

Johnson and McKnight point out, however, that the use of statistical mechanics requires a conversion from basic orbital elements into analytic functions in order to solve the problems. They also mention that the nomenclature particular to statistical mechanics is generally not as well known as that of the classical approaches (Johnson and McKnight, 1987:58).

Heard has authored several articles on the topic of using statistical mechanics to model the propagation of a large number of particles in space over time. He states in his 1976 work that a collection of particles can be studied using either a classical approach or a continuum (statistical mechanics) approach. Like Johnson and McKnight, Heard also emphasizes the increased computational effort required by the former method. He goes on to say that since interactions among the particles are negligible, the solution via statistical mechanics requires nothing more than the application of the theory of linear, partial differential equations (Heard, 1976:63).

In the same paper, Heard also mentions the usefulness of a statistical mechanics approach in the field of astronomy to analyze different systems of particles that move in independent orbits about another body, but whose overall behavior tends to indicate a common origin, such as families of asteroids (Heard, 1976:63). In this paper, he

looks at what he calls the "direct" problem and the "inverse" problem. In the direct problem, the final distribution of a collection of particles is examined beginning with the initial point of dispersion and ending at a future point in time. The inverse problem examines a collection of particles and attempts to recreate the moment of initial dispersion by moving backward in time (Heard, 1976:63-64). Since the current study is concerned only with the future spreading of a chaff cloud and not the origin of an existing chaff cloud, no further mention will be made of the inverse problem.

Heard's paper from 1977 examines the asymptotic (time increasing to infinity) behavior of a collection of particles (Heard, 1977:1025). Like the inverse problem, the final state of the chaff cloud is not important here, since the current study is concerned only with the cloud's spreading up to the point where the desired signal attenuation no longer exists. Therefore, except for the underlying statistical mechanics theory, Heard's 1977 effort is dropped from further discussion here also.

In 1978, Heard published a paper directly applicable to the problem of a satellite breakup which is useful for the current study. In this paper, he again examined the direct, inverse, and asymptotic problems; he also included an analysis of the "continuous source" problem. In the

continuous source problem, the dispersion of particles occurs over time. This is similar to Cases III and IV which were discussed above (Heard, 1978:1-2). Again, the direct problem will be the focus of this effort.

In 1976, Dasenbrock, Kaufman, and Heard co-authored a paper which examined the direct and inverse problems as they apply to satellite breakups and the subsequent debris cloud that develops. The specific stated purpose of this report was to

Study the dynamical characteristics of an evolving fragment cloud in order to yield insight into both its future evolution for purposes of collision probabilities and to determine how the dynamics might be used to obtain the precise origin of the cloud. Specifically, satellite breakups are simulated to study the characteristics of their evolving fragment clouds. These characteristics are then used to determine how the time and place of a satellite explosion might be accurately determined once its fragment cloud has been observed. (Dasenbrock, 1976:2)

The paper, like the works discussed above, goes on to state that a statistical mechanics approach is called for to help ease the computational burden of following the orbital paths of the fragments (Dasenbrock, 1976:2).

Finally, Hameen-Antilla has also applied a statistical mechanics approach in his examination of a system of particles in which collisions between particles occur. In particular, the evolution of the rings of Saturn was discussed. The underlying purpose of the paper was to

improve on a previous work, also by Hameen-Antilla, in which statistical mechanics was used. The differences are that the second work allowed for differences in particle sizes and improved on the statistical orbit model used (Hameen-Antilla, 1976:145).

In each of Heard's three papers discussed above, he used the same basic theory, with slight variations in each work, to arrive at his final results. Aside from Heard's presentations, the only other direct applications to the chaff cloud expansion problem from the above list are the ones found in the Dasenbrock article and Johnson's and McKnight's book. However, the presentation of the theory in the Dasenbrock paper was identical to that in Heard's 1976 paper except for a few minor changes, while Johnson's and McKnight's presentation was taken largely from Heard's 1978 article. Therefore, Heard's method of presentation will be followed closely in the discussion below. Heard's 1978 paper used essentially the same format for presentation as his 1976 work, but in the 1978 work some of the results were presented in a manner more easily understood. Therefore, the theory presentation below will be adapted from both Heard's 1976 and 1978 efforts.

General Theory (Heard, 1976:64-70; Heard, 1978:2-10).

Heard begins by assuming a collection of particles in a common force field with the following equations of motion:

$$\dot{\mathbf{g}} = \mathbf{X}(\mathbf{g}, \mathbf{p}, t), \quad \dot{\mathbf{p}} = \mathbf{Y}(\mathbf{g}, \mathbf{p}, t) \quad (7)$$

where the vectors \mathbf{g} and \mathbf{p} represent the coordinates and momenta of the particles, respectively. The next assumption is that $f(\mathbf{g}, \mathbf{p}, t)$ is the phase-space density function such that a volume contains dN particles with the following relation:

$$dN = f(\mathbf{g}, \mathbf{p}, t) d\mathbf{g} d\mathbf{p} \quad (8)$$

Heard then refers to Chandrasekhar's solution that says the distribution function f follows the relationship

$$df/dt = \sum_{i=1}^n (d/dq_i \cdot (fX_i) + d/dp_i \cdot (fY_i)) = 0 \quad (9)$$

if no source of particles is present. This equation is then rewritten in the following form:

$$Df/Dt = -f\Delta \quad (10)$$

where D/Dt is the "Stokes derivative" ($D/Dt = d/dt + \mathbf{X} \cdot \nabla_{\mathbf{g}} + \mathbf{Y} \cdot \nabla_{\mathbf{p}}$) and $\Delta = \sum_{i=1}^n (dX_i/dq_i + dY_i/dp_i)$.

The next step is to establish the position (\mathbf{g}, \mathbf{p}) of a particle at time $t = 0$. Heard lets $\mathbf{g}_0(\mathbf{g}, \mathbf{p}, t)$, $\mathbf{p}_0(\mathbf{g}, \mathbf{p}, t)$ be

this position. Similarly, $q(g,p,t)$, $p(g,p,t)$ is the particle's position at time t .

Heard now shows the solution of Eq (10), given the initial condition

$$f(g,p,0) = F(g,p) \quad (11)$$

to be

$$f(g,p,t) = F(q_0(g,p,t), p_0(g,p,t)) \exp\{-\Gamma(g,p,t)\} \quad (12)$$

where

$$\Gamma(g,p,t) = \int_0^t \Delta(g(t), p(t), t) dt \quad (13)$$

The integral in Eq (13) is to be evaluated on the trajectory which passes through (g,p) at time t

The spatial density $\rho(g,t)$ is found by integrating f over all momenta as follows:

$$\rho(g,t) = \int f(g,p,t) dp \quad (14)$$

From this equation, the shape and density of the cloud can be found at any time.

Next, Heard finds the solution given dispensing from the initial point g^* . The initial condition

$$F(g,p) = \delta(g - g^*) G(p), \quad (15)$$

applies. Here, $\delta(q - q^*)$ is the Dirac delta-function and $G(p)$ is any function that describes the initial distribution of the particle momenta. Heard next applies theorems relating to the δ -functions to arrive at the following equation to substitute for Eq (14):

$$\rho(q, t) = 1/|J| \times G(p_0(q, p^*, t)) \exp\{-\Gamma(q, p^*, t)\} \quad (16)$$

where p^* is the solution of

$$q_0(q, p^*, t) = q^* \quad (17)$$

and $|J|$ is the Jacobian determinant

$$J = \frac{d(q_{0,1}, \dots, q_{0,n})}{d(p_1, \dots, p_n)} \quad (18)$$

Heard next provides matrix equations to describe the particle motions. When the previous results are combined with the matrix equations, a general solution to the problem can be found.

First, Heard lets q and p represent small deviations from the reference solution of Eq (7). The variational equations of motion for q and p become

$$\begin{pmatrix} \dot{q} \\ \dot{p} \end{pmatrix} = A \begin{pmatrix} q \\ p \end{pmatrix} \quad (19)$$

where A is the matrix

$$A = \begin{pmatrix} A_{11} & A_{12} \\ A_{21} & A_{22} \end{pmatrix}$$

Here $A_{11} = d\bar{x}/dg$, $A_{12} = d\bar{x}/dp$, $A_{21} = d\bar{y}/dg$, and $A_{22} = d\bar{y}/dp$.

All are evaluated on the reference solution. When Heard solves the variational equations, he uses the matrizant

$$\Phi = \begin{pmatrix} U & V \\ W & Y \end{pmatrix} \quad (20)$$

where

$U = dg/dg_0$, $V = dg/dp_0$, $W = dp/dg_0$, and $Y = dp/dp_0$.

The solution then becomes

$$\begin{pmatrix} g \\ p \end{pmatrix} = \Phi \begin{pmatrix} g_0 \\ p_0 \end{pmatrix} \quad (21)$$

where g_0 and p_0 are the initial values.

Heard next adopts the following matrix notation:

$$M_-(t) = M(-t)$$

and notes that for a matrizant the following property holds:

$$\Phi^{-1} = \Phi_- \quad (22)$$

From Eqs (20) and (21) the following holds true:

$$\begin{pmatrix} q_0 \\ p_0 \end{pmatrix} = \Phi_- \begin{pmatrix} q \\ p \end{pmatrix} \quad (23)$$

q_0 , p_0 , and J end up in the following forms:

$$q_0(g, p, t) = U_g + V_p \quad (24)$$

$$p_0(g, p, t) = W_g + Y_p \quad (25)$$

$$J = \det(V_-) \quad (26)$$

Eq (17) now takes on the following form:

$$U_g + V_{p^*} = g^* \quad (27)$$

with a solution of

$$p^* = V_-^{-1}(g^* - U_g) \quad (28)$$

Now, Heard lets $L = \det(\Phi)$ and differentiates L , with the solution being

$$dL/dt = L \sum_{i=1}^n (d\dot{q}_i/dq_i + d\dot{p}_i/dp_i) \quad (29)$$

From this, Heard ultimately obtains the final expression for the exponent term in Eq (16) using

$$dL/dt = L\Delta \quad (30)$$

which becomes

$$d/dt(\ln L) = \Delta \quad (31)$$

to give

$$\exp\left(-\int_0^t \Delta dt\right) = L(0)/L(t) \quad (32)$$

By using Eqs (25), (26), (28), and (32), substituting into Eq (16) and using the fact that $\det(\Phi) = 1$ according to Liouville's Theorem, Heard's solution becomes

$$\rho(g,t) = \{1/|\det(V_-)|\} \{G[(W_- - Y_- V_-^{-1} U_-)g + Y_- V_-^{-1} g^*]\} \quad (33)$$

The last step Heard uses is to apply the previous results to the specific case of a group of particles under the influence of the force of gravity and orbiting about the earth. Heard's solution uses the cylindrical coordinates (\bar{w}, θ, z) and assumes a radially symmetric gravitational potential (v) . The coordinates are set up with $z = 0$ in the equatorial plane, so v becomes a function of only \bar{w} and z . An orbit of radius R can be described in this coordinate system as follows:

$$\bar{w} = R, \quad \theta = \theta_0 + \Omega t, \quad \text{and } z = 0 \quad (34)$$

where $R\Omega^2 = dv/d\bar{w}(R,0)$ and Ω is the angular velocity of the parent satellite. Small changes in the orbit are described by ξ , η , and ζ in the following manner:

$$\bar{w} = R + \xi, \quad \theta = \theta_0 + \Omega t + \eta/R, \quad \text{and } z = \zeta \quad (35)$$

Next, Heard uses the Hamiltonian

$$H = (1/2)(p_1^2 + p_2^2 + p_3^2) - 2\Omega\xi p_2 + (1/2)(n^2\xi^2 + K^2\xi^2) \quad (36)$$

with momenta

$$p_1 = \dot{\xi}, \quad p_2 = \dot{\eta} + 2\Omega\xi, \quad \text{and} \quad p_3 = \dot{\zeta} \quad (37)$$

and where

$$n^2 = 3\Omega^2 - (d^2V/d\bar{w}^2)(R,0) \quad \text{and} \quad K^2 = (d^2V/dz^2)(R,0) \quad (38)$$

In Eqs (36) and (38), n is the epicyclic frequency. Both n^2 and K^2 are assumed to be positive.

Using the following notation:

$$\begin{aligned} \tau &= n t, \quad \tau' = K t, \quad \sigma = 2\Omega/n, \quad s = \sin\tau, \\ c &= \cos\tau, \quad s' = \sin\tau', \quad \text{and} \quad c' = \cos\tau' \end{aligned}$$

Heard then arrives at the fundamental matrices for U , V , W , and Y for use in Eq (33)

$$U = \begin{pmatrix} c & 0 & 0 \\ -\sigma s & 1 & 0 \\ 0 & 0 & c' \end{pmatrix}$$

$$V = \begin{pmatrix} s & (1 - c) & 0 \\ \sigma(c - 1) & (1 - \sigma^2)\tau + \sigma^2 s & 0 \\ 0 & 0 & ns'/K \end{pmatrix}$$

$$W = \begin{pmatrix} -ns & 0 & 0 \\ 0 & 0 & 0 \\ 0 & 0 & -Ks' \end{pmatrix}$$

$$Y = \begin{pmatrix} c & \sigma s & 0 \\ 0 & 1 & 0 \\ 0 & 0 & c' \end{pmatrix}$$

In order to simplify the solution, he also establishes the following convenience:

$$D = [(1 - \sigma^2)s + 2\sigma^2(1-c)] \quad (39)$$

Finally, Heard obtains an equation which describes the density function for the collection of particles using any initial momentum distribution function $G(p_1, p_2, p_3)$. The equation is as follows:

$$\begin{aligned} \rho(\xi, \eta, \zeta, t) = & \{K/s' [(1 - \sigma^2)s\tau + 2\sigma^2(1 - c)]\} \\ & \times G\left(\frac{n}{D} \{[(1 - \sigma^2)\xi + \sigma^2 s]\tau - \sigma(1 - c)\eta\}, \quad (40) \right. \\ & \left. \frac{n}{D} [\sigma(1 - c)\xi + s\eta], \quad [(K/s')\zeta] \right) \end{aligned}$$

where $\sigma = 2$, and $n = K = \Omega = 1$ for Keplerian orbits.

From this equation, the distribution of particles in the chaff cloud at any future point in time can be determined at any point (ξ, η, ζ) with reference to the parent satellite. Since the center of mass of the cloud follows

that of the original orbit and the orbit of the parent satellite is known, the motion of the chaff cloud can be easily determined.

Attenuation Through the Chaff Cloud

The final section of this chapter takes a look at the basic theory describing the attenuation of an electromagnetic signal as it penetrates an absorbing medium such as a chaff cloud. Although the attenuation analysis could be via either wave or particle theory, only particle theory is examined. The primary reason for this one-sided approach is that Brown used particle theory in his work with satisfactory results; an analysis that applied wave theory would be needless duplication of effort.

Chaff Cloud Attenuation Theory. Brown states that a cloud of chaff particles affects an electromagnetic signal by first receiving and absorbing an incident signal and then re-radiating the signal at some later time. This re-radiation can occur in effectively any direction with the overall effect of uniformly scattering over 4π steradians that portion of the signal which was initially absorbed. By placing enough dipoles in random orientations into the path of the incoming signal, the signal can be attenuated

sufficiently to effectively impede transmission through the chaff cloud (Brown, 1987:4-1 to 4-2).

The chance of a dipole interacting with the incoming signal is directly determined by the "effective cross-section" of the dipole. The effective cross-section is a measure of the probability of interaction between a dipole and the signal rather than the true cross-sectional area measurement of the dipole as the name implies. Nonetheless, the effective cross-section is given in units of area (Brown, 1987:4-2).

The effective cross-section is dependent on the frequency of the signal and the length of an individual dipole. A maximum value for effective cross-section occurs when the length of the dipole equals one-half the wavelength of the signal. The value of effective cross-section (σ) for a group of randomly oriented dipoles can be determined from Eq (41) below:

$$\sigma = 0.16 \times \lambda^2 \quad (41)$$

where λ is the wavelength of the signal (Brown, 1987:4-2 to 4-3; Peebles, 1984:128-129).

According to Brown, the effect of a uniform chaff cloud on the entire signal is determined from Eq (42)

$$P_{out}/P_{in} = \exp\{-(\sigma zW/V)\} \quad (42)$$

Here, P_{out}/P_{in} is the decimal fraction of signal power transmitted through the cloud, σ is the effective cross-section from Eq (41), z is the distance the signal travels through the chaff cloud, N is the number of chaff particles in a particular volume of space, and V is the volume in which the cloud is contained (Brown, 1987:4-13 to 4-14). According to Evans, it is essential that the chaff cloud be uniform in order for Eq (42) to provide accurate results (Evans, 1988). Therefore, when the chaff cloud is modeled, it has to be broken down into subvolumes that are small enough for uniform density to be present.

Once the desired degree of signal attenuation is established, the appropriate value for ' zN/V ' to be used in Eq (42) is easily calculated. Since the value for ' z ' through any part of the cloud should be known, the value of ' N/V ' (particle density) required for signal attenuation is also determinable.

The beamwidth of the signal at the altitude of the chaff cloud is also important since any signal which goes around the edges of the cloud is not attenuated. Therefore, the effective attenuation of the signal does not occur until the chaff cloud reaches a size in area at least as large as that of the incident signal (Brown, 1987:4-3 to 4-6). This last statement also assumes enough chaff particles are at the edges of the chaff cloud so that effective attenuation

occurs. In practice, the cloud has to be much greater in size than this minimum so that the number density in the attenuation region is high. This is because of the cloud having a smaller density at its edges and a higher density near the centroid.

Finally, the above values for ' z ', ' N/V ', and signal attenuation are calculated for different points in time after initial deployment of the cloud. These values are used to establish the required dispensing velocity of the particles in order to affect the desired attenuation at any given point in time after deployment. From these values, the period of time before effective attenuation occurs and the period of time over which attenuation takes place are found (Brown, 1987:4-13 to 4-17).

III. Methodology

This chapter outlines the approach followed to complete the chaff cloud study and is designed as only a very basic precursor of what follows in Chapters IV, V, and VI. The chapter is divided into the following sections: application of Heard's results, graphical presentation of new results, and determining the overall effectiveness of the chaff cloud as a communications jamming device.

Applying Heard's Results

The methodology used in the application of Heard's results to the chaff cloud problem can be broken down into five sections. The five sections are 1) a dimensional analysis of Eq (40) to ensure complete understanding, 2) determining the appropriate velocity distribution to be applied to the chaff cloud expansion, 3) determining particle density throughout the chaff cloud using Eq (40), 4) a spreadsheet setup for ease of calculation of results, and 5) attenuation calculations of a signal through the chaff cloud using Brown's thesis as a basis.

Dimensional Analysis. The first thing done with Heard's analysis was to break down Eq (40) into its component parts. These parts were then subjected to a

dimensional analysis to determine the scaling and normalization factors used by Heard in his derivation. The components of the equation were next reassembled and solved using the example velocity distribution function provided by Heard. The values for (ξ, η, ζ, t) obtained in this manner could then be plotted on an η versus ζ graph and compared to η versus ζ plots in Heard's paper to ensure the equation was being solved properly.

Determining the Velocity Distribution Function. Once Eq (40) was fully understood, a solution using a velocity distribution function appropriate to the chaff cloud problem was needed. Since the other portions of this analysis involve a statistical approach rather than strictly numerical solutions, a statistical approach was also applied to the determination of the velocity distribution function. With the distribution of particles being approximately Gaussian, the distribution function arrived at through this approach was Maxwellian.

Determining Particle Density. Eq (40) allows a reference value for particle density to be calculated at any selected point within the chaff cloud. By summing each of these reference values from points throughout the cloud, an aggregate total against which each of the individual values can be compared as a ratio is obtainable. These ratios can

then be multiplied by the number of chaff particles in the entire cloud to convert the ratios into the actual number of chaff particles at each point within the cloud.

The particle density of a particular volume within the cloud can be approximated by the density at the center of the volume if the volume is small enough that major variations across the volume are eliminated. This was accomplished for the chaff cloud by dividing the cloud into small cubic volume elements and then following the ratio procedure from above to determine the number of particles within each volume element.

Spreadsheet Setup. In order to allow the many iterations required for this analysis to be accomplished more easily, a spreadsheet divided into four sections was used to do the calculations. The first section included constants and variables to be used in the later sections with the variables including time and dispensing velocity. The second section consisted of Eq (40) broken up into several parts for ease of calculation. The next section summed up the relative densities mentioned above, determined particles ratios, and calculated the number of particles within volume elements located throughout the cloud. The final section of the spreadsheet contained the calculations for attenuation of the signal through the chaff cloud.

Attenuation of the Incident Signal. Using the number of particles in the volumes along each signal path from above and the values provided by Brown in his thesis for the required size and altitude of the chaff cloud, the values for attenuation of the incident signal at various points across the cloud's cross-section (as seen from the earth) were obtained. These data were compiled for each of several different dispensing velocities and run for the time interval beginning with initial cloud dispensing and ending 12 hours later. The results were then presented in the graphs outlined in the next section to describe the signal attenuation affected by the chaff cloud.

Graphical Presentation

Once results for various dispensing velocities and times after initial dispensing were obtained, it was necessary to present the results in a useful format. It was decided to provide a pictorial representation of the chaff cloud attenuation through plots of dispensing velocity versus signal attenuation. Using different symbols to represent different amounts of time elapsed after cloud dispensing took place, the signal attenuation through the chaff cloud as a function of both time and dispensing velocity was determined.

Several important parameters were obtained from these graphs. First, the amount of time elapsed before effective attenuation occurs could be determined for any given dispensing velocity. Second, the length of the period of effective attenuation for a given dispensing velocity was available. This was possible since the attenuation plots were run past the time at which the attenuation levels drop below effective levels. Finally, a comparison between the various dispensing velocities was made based on specific requirements for signal attenuation. These comparisons were based on the amount of time before effective attenuation, the period of time over which effective attenuation occurs, and the amount of time which elapses before attenuation is no longer effective.

Effectiveness of Attenuation

The final step in the analysis was to determine whether the attenuation levels obtained by the chaff cloud are effective when the following questions were asked:

- 1) Are the attenuation levels attained by the cloud both high enough and maintained long enough for a chaff cloud to be of value?
- 2) How does the fact that the chaff cloud and the satellite to be jammed are moving at different velocities affect signal attenuation?

- 3) Given the initial size, shape, makeup, and weight of the ball of chaff, are the assumptions surrounding the dispensing of the chaff cloud reasonable?
- 4) What are the effects of the chaff cloud on satellites other than the one the chaff cloud is intended to jam?

IV. Application of Heard's Results

This chapter applies the methodology and theory previously outlined to the chaff cloud problem. This allows an overall attenuation picture to be obtained. The chapter is divided into the following sections: 1) dimensional analysis of Heard's final equation, 2) determination of a velocity distribution function, 3) determination of particle densities throughout the chaff cloud, 4) the spreadsheet setup used for analyzing Heard's equation, and 5) a numerical analysis of signal attenuation using Brown's thesis as a basis.

Dimensional Analysis

In order to simplify his calculations, Heard normalized to unity some of the parameters used in his analysis through the use of convenient dimensions. The two major parameters set to unity were the radius of the parent satellite's orbit and the satellite's mean motion.

Satellite Radius. The radius of a satellite's orbit is determined by adding the satellite's altitude above the earth to the earth's radius. Therefore, the parent satellite for the chaff cloud, which is 100 nautical miles (NM) below a geosynchronous satellite, has an orbital radius

of approximately 42,073 kilometers (km) (Brown, 1987:4-4; Illustrated Encyclopedia of Space Technology, 1982:86). Heard normalized the orbital radius of the parent satellite of the chaff cloud to unity using what will be referred to in the remainder of this paper as Radius Units (RU). Therefore, in the case of the parent satellite,

$$1 \text{ RU} = 42073 \text{ km} \quad (43)$$

Mean Motion. A satellite's mean motion describes the time it takes for the satellite to travel through one radian of its orbit. Next, a Satellite Time Unit (STU) is defined so that a Radius Unit per Satellite Time Unit (RU/STU) is the velocity of a satellite. When an RU/STU is set to unity, then the value of 'GM' in Eq (44) below also becomes unity with dimensions of RU^3/STU^2 :

$$V_{cs} = (GM/a)^{1/2} \quad (44)$$

where V_{cs} is the satellite's velocity, and a is the semi-major axis as defined in Chapter II (Bate and others, 1971:34). For the parent satellite, 1 RU/STU has a value of 3078 meters per second (m/s).

Using Eq (45) below, 'n' also acquires a value of unity with units of radians per STU (rad/STU):

$$n = (GM/a^3)^{1/2} \quad (45)$$

(Bate and others, 1971:185).

The conversion between STUs and conventional time units is accomplished by dividing a satellite's orbital period by 2π radians (rad). For the parent satellite, the calculation is as follows:

$$\begin{aligned} 1 \text{ STU} &= 85880 \text{ sec}/2\pi \text{ rad} \\ &= 13670 \text{ sec} \end{aligned} \quad (46)$$

Velocity Distribution Function

The work of Knott, Lewinski, and Hunt suggests that a spherical chaff cloud should have approximately a Gaussian particle distribution (Knott, 1981:3,112). If a Gaussian particle distribution is assumed, the appropriate velocity distribution function should be Maxwellian (Evans, 1988). A Maxwellian distribution function has the following form (Evans, 1987:10)

$$n_v(z,v) = n(z)(2/\pi)^{1/2}(v^2/v_0^3)\exp(-v^2/2v_0^2) \quad (47)$$

where $v^2 = (v_\xi^2 + v_\eta^2 + v_\zeta^2)$, and v_0 represents the "thermal speed" of the particles. The thermal speed of the chaff particles is defined as being equal to the dispensing velocity and is assumed to be known.

A new term, the most probable particle velocity (V_{th}), is now defined by Eq (48)

$$V_{th} = \sqrt{2} v_0 \quad (48)$$

values of V_{th} for several values of V_0 are shown in Table 1.

Table I. Most Probable Particle Speeds
for Various Dispensing Velocities

V_0 (m/s)	V_0 (RU/STU)	V_{th} (RU/STU)	V_{th}^2 (RU ² /STU ²)
0.0050	1.624×10^{-6}	2.297×10^{-6}	5.275×10^{-12}
0.0100	3.249×10^{-6}	4.595×10^{-6}	2.107×10^{-11}
0.0120	3.899×10^{-6}	5.514×10^{-6}	3.040×10^{-11}
0.0130	4.224×10^{-6}	5.973×10^{-6}	3.568×10^{-11}
0.0140	4.548×10^{-6}	6.432×10^{-6}	4.138×10^{-11}
0.0150	4.873×10^{-6}	6.891×10^{-6}	4.749×10^{-11}
0.0200	6.498×10^{-6}	9.190×10^{-6}	8.446×10^{-11}
0.0250	8.122×10^{-6}	1.149×10^{-5}	1.320×10^{-10}
0.0300	9.746×10^{-6}	1.378×10^{-5}	1.899×10^{-10}
0.0350	1.137×10^{-5}	1.608×10^{-5}	2.586×10^{-10}
0.0400	1.300×10^{-5}	1.838×10^{-5}	3.378×10^{-10}
0.0450	1.462×10^{-5}	2.068×10^{-5}	4.277×10^{-10}
0.0500	1.624×10^{-5}	2.297×10^{-5}	5.275×10^{-10}

Now, the momenta are generalized by dividing through by particle mass, and are substituted with Eq (48) into Eq (47). This results in the distribution function shown in Eq (49) below:

$$G(p) \sim \exp(-(p_1^2 + p_2^2 + p_3^2)/V_{th}^2); \quad (49)$$

Determining Particle Density

The distribution function from the previous section is now used in conjunction with Eq (40) to determine a reference value for the number of chaff particles at any given (ξ, η, ζ) coordinates and at any given time after initial cloud dispensing. Once the reference number is known at locations throughout the cloud, the actual number of particles at these same locations is also determinable.

First, the reference values at each location are summed to obtain the reference total. Then, the reference number at each location is divided by the reference total to determine the decimal fraction of the total number of chaff particles at each location. Finally, by multiplying each of these fractions by the total number of chaff particles, the actual number of particles at each location is found.

Since it would be impossible to calculate reference numbers for every location in space, the cloud is broken up into a three-dimensional grid of identically sized cubes

with the centroid (origin) of the innermost cube at the (ξ, η, ξ) coordinate $(0,0,0)$. The grid has a size of seven units on a side with the units for the overall grid being of variable size for the purpose of scaling the model to fit the chaff cloud as it expands over time. The $7 \times 7 \times 7$ grid thus allows for a chaff cloud of size up to plus and minus three and one-half units of the initial dispensing point in each of the three orthogonal directions. The final size of the grid is set at $7 \times 7 \times 7$ because of memory limitations (640 kilobytes of Random Access Memory) in the computer used to run the program. The limitation on the number of grid cubes in which to contain the expanding cloud is counteracted by the scaling capability of the program, however.

With the grid in place, the reference values need to be calculated only at the centroids of each cube. Each of the reference values can now be assumed to represent the reference number of particles within each of these cubic subvolumes of space instead of only at particular coordinates. Therefore, when the actual number of particles at each centroid is determined, the particle densities at the various locations are easily determined by dividing the number of particles by the volume contained in the subvolumes.

One obvious difficulty with the above approach is that to obtain accurate results, the particle density in each

subvolumes must be uniform. In the actual chaff cloud, this clearly might not be the case. However, the use of variable cube sizes for the scaling process also allows for improved internal density resolution of the chaff cloud.

If the uniformity of the particle density in any one cube is suspect, the centroid of the entire grid can be moved from (0,0,0) to the coordinates of the centroid of the appropriate cube. The sizes of the subvolumes within the suspect cube can then be reduced. In this manner, any of the original subvolumes can be "magnified" and subsequently examined for internal particle density uniformity. Figure 7 shows this process pictorially.

Another disadvantage of the grid approach is that while the cloud expands radially to form a sphere and then an ellipsoid, the model employs a cubic grid to examine the cloud. Again, by moving the origin of the entire grid to the various parts of the chaff cloud and using the scaling technique described above, the actual shape of the cloud can be closely approximated at any point in time.

An advantage of the grid approach is that once the number of particles in each grid cube throughout the entire cloud is known, signal attenuation through any particular portion of the cloud can be determined independently of the attenuation through any other portion of the cloud. An example is examining the attenuation of a signal which

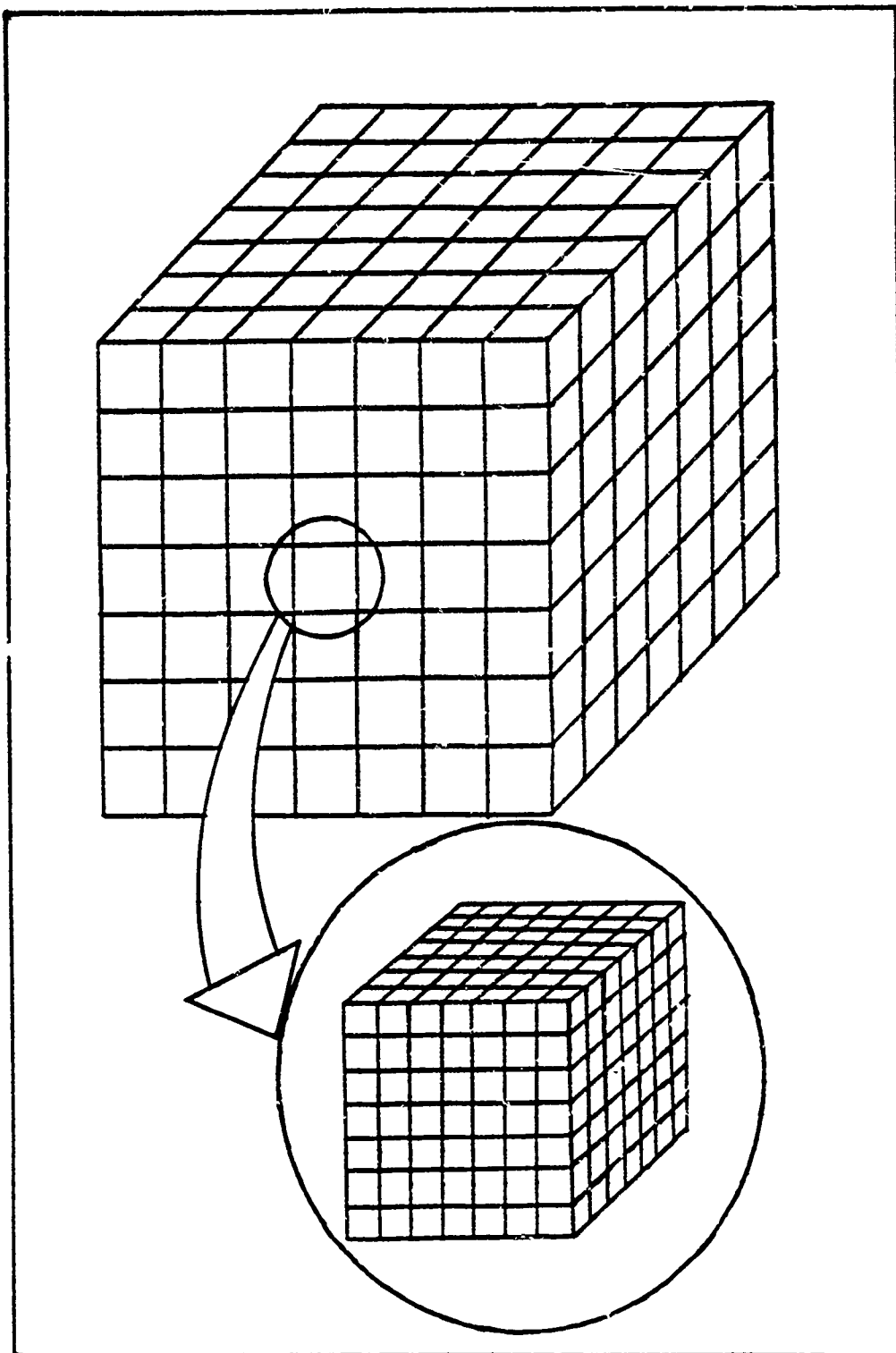


Figure 7. "Magnification of a Subvolume
of the Chaff Cloud

penetrates only through that portion of the cloud within plus or minus one kilometer in the η and ξ directions of the center of the cloud. This advantage will become more evident later in the section concerning Brown's attenuation requirements for a chaff cloud.

Spreadsheet Setup

The attenuation of the electromagnetic signal is calculated using two spreadsheet programs. The first spreadsheet calculates the number density in each cube of the grid. The second calculates the signal attenuation through the cloud starting at subvolumes across the face of the cloud and continues by looking at subvolumes at successive depths (values of ξ) through to the other side. Each run of the spreadsheet programs constitutes one point in time after cloud dispensing began. The spreadsheet programs were devised using Quattro by Borland and are included as Appendices A and B, respectively.

The number density spreadsheet is broken up into three sections. The first provides basic equations and constants, the second calculates reference number densities for the subvolumes in the grid, and the third section calculates actual number densities in each subvolume. A more detailed explanation of the spreadsheet is included as part of Appendix A.

The signal attenuation spreadsheet is divided into two sections. The first is composed of all the values from section three of the number density spreadsheet. In practice, these values are first copied as a block into a separate file and then transported into the signal attenuation spreadsheet. The second section of this spreadsheet uses the values from section one to calculate the attenuation of the incident signal (P_{in}). The attenuation calculations determine the decimal fraction of the signal that penetrates through each of 49 columns of the chaff cloud (P_{out}). The setup and numbering scheme of the 49 columns is shown in Figure 8, with the horizontal and vertical directions corresponding to the η and ξ directions, respectively. For each column, Eq (42) is applied to the number of particles contained within each subvolume; the values at each layer are multiplied together to determine the overall value for ' P_{out} '. Care is taken to ensure the appropriate values are used for ' z ' and ' V ' to compensate for the various magnifications being used in the spreadsheet.

Attenuation Analysis Using Brown's Thesis as a Basis

Brown's thesis shows that the minimum required area of a chaff cloud attempting to jam communications between a DSCS satellite and a circular area the size of Washington

(1,1)	(2,1)	(3,1)	(4,1)	(5,1)	(6,1)	(7,1)
(1,2)	(2,2)	(3,2)	(4,2)	(5,2)	(6,2)	(7,2)
(1,3)	(2,3)	(3,3)	(4,3)	(5,3)	(6,3)	(7,3)
(1,4)	(2,4)	(3,4)	(4,4)	(5,4)	(6,4)	(7,4)
(1,5)	(2,5)	(3,5)	(4,5)	(5,5)	(6,5)	(7,5)
(1,6)	(2,6)	(3,6)	(4,6)	(5,6)	(6,6)	(7,6)
(1,7)	(2,7)	(3,7)	(4,7)	(5,7)	(6,7)	(7,7)

Figure 8. Numbering Scheme for the Subvolumes
Along the Central Column of the Chaff Cloud

D.C. is approximately 97,500 square meters. This assumes that the chaff cloud is located 100 NM (185.2 km) below the DSCS satellite, an 8 Gigahertz (GHz) uplink signal is being jammed, and that the cloud contains 100 billion particles (Brown, 1987:4-3 to 4-5). This equates to a chaff cloud with a required radius of approximately 175 meters (m) and a diameter of 350 m. Brown also states the cloud must reach an attenuation of at least -10 decibels (dB) across the entire area of coverage within one hour of dispensing and must maintain this -10 dB attenuation for at least twelve hours (Brown, 1987:4-14 to 4-17). Stanley's book Electronic Communications Systems provides a good explanation of attenuation calculations using decibels (Stanley, 1982:7-9).

With the area of coverage on the ground for the chaff cloud being circular, the only portion of the chaff cloud important to signal attenuation is the column which runs through the centroid of the cloud. Therefore, only attenuation through this part of the cloud needed to be calculated.

When a circle with a radius of 350 m is inscribed in a cross-section of the spreadsheet model grid with dimensions of 350 m, the squares at the corners of the grid lie entirely outside of the circle. As a result, only 45 of the 49 columns contained within the model needed to be examined for signal attenuation. This is shown in Figure 9.

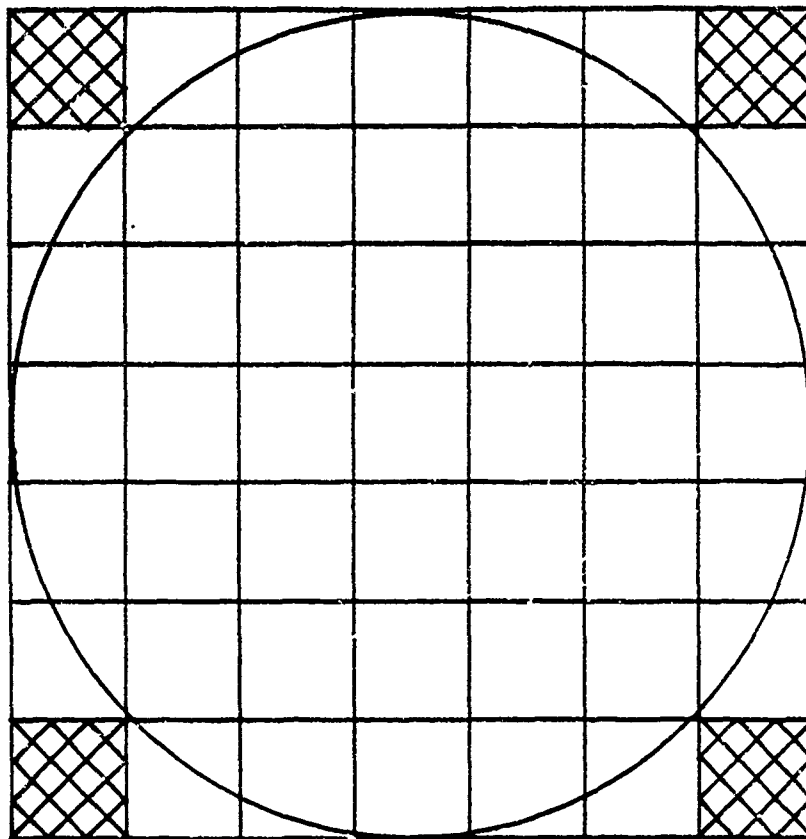


Figure 9. Effect of Inscribing a Circle
Within the Chaff Cloud Model

To determine if Brown's first attenuation requirement is met by a chaff cloud in orbit, the entire cloud is first examined at a time of one hour after dispensing, with the size of the internal grid cubes increased as required to ensure all chaff particles remain within the 7x7x7 model. The number of chaff particles within all of the subvolumes are then recorded. Then, the cloud model is scaled back down a step at a time until grid cubes 50 m on a side are obtained. It is important to assign the proper number of chaff particles to each of the subvolumes and the proper coordinates to the origin of the grid each time the model is scaled up or down. The attenuation of the signal is then determined using the attenuation spreadsheet. By varying the dispensing velocities and repeating the above process, the minimum dispensing velocity which meets the criterion for attenuation within one hour is established.

In order to determine whether a -10 dB attenuation is maintained for a period of twelve hours and, if not, for how long it is maintained, a similar approach is followed. The spreadsheets are run at one hour increments for the following dispensing velocities (all in m/s): 0.01, 0.02, 0.03, 0.04, and 0.05. Again, the entire cloud is kept within the model's grid through appropriate scaling of the spreadsheets for each pair of velocity and time values.

The cloud is then scaled back down as required until the 350 meter diameter cloud is reached. The number of particles within each subvolume are recorded at each step. These values are then used in subsequent steps as the total number of particles contained in the 7x7x7 subscaled grids.

The downscaling process involves first determining the number of particles in each of the seven $(\eta, \xi) = (4, 4)$ subvolumes in the total cloud model. Each of these subvolumes is then run through the density spreadsheet individually. This is accomplished by rescaling the spreadsheet so the outer dimensions of the subvolume exactly fit the 7x7x7 grid, using the coordinates of the subvolume centroids as the origin for the subscaled spreadsheet grid, and ensuring the number of particles within the subvolume is entered into the "constants" section of the spreadsheet. By using this process repetitively, the number of particles in each sub-subvolume is determined until the number of particles within each layer of the central column is determined. Finally, by manually applying Eq (42) through each individual layer of the central column, and multiplying the final results together, the overall attenuation affected by the cloud is obtained.

In order to clarify the above discussion, appendix C describes the procedures followed for one attenuation calculation. The values used in the example for dispensing

velocity and time after dispensing are 0.05 m/s and six hours, respectively.

V. Presentation of Results and Discussion

This chapter presents the results for each of the areas of this research effort and an interpretation of these results. The chapter is divided into the following three sections with interpretations included as a part of each section: physical structure of the chaff cloud over time, signal attenuation one hour after dispensing, and signal attenuation for the first twelve hours after dispensing.

Physical Structure of the Chaff Cloud

As would be expected from the discussion in Chapter II, the chaff cloud's physical structure closely resembles the cloud described for Case II since it is dispensed instantaneously and has velocity components both along the path of motion and radially outward. The only real change should be that some of the chaff particles also have velocity components out of the orbital plane.

The cloud starts out as a sphere and exhibits a gradual spreading out in all directions. The spreading becomes faster for the higher dispensing velocities, but the general shape of the cloud remains similar in each case. Figures 10, 11, 12, and 13 show the cloud evolution over time in the η and ζ directions for a 0.01 m/s dispensing velocity.

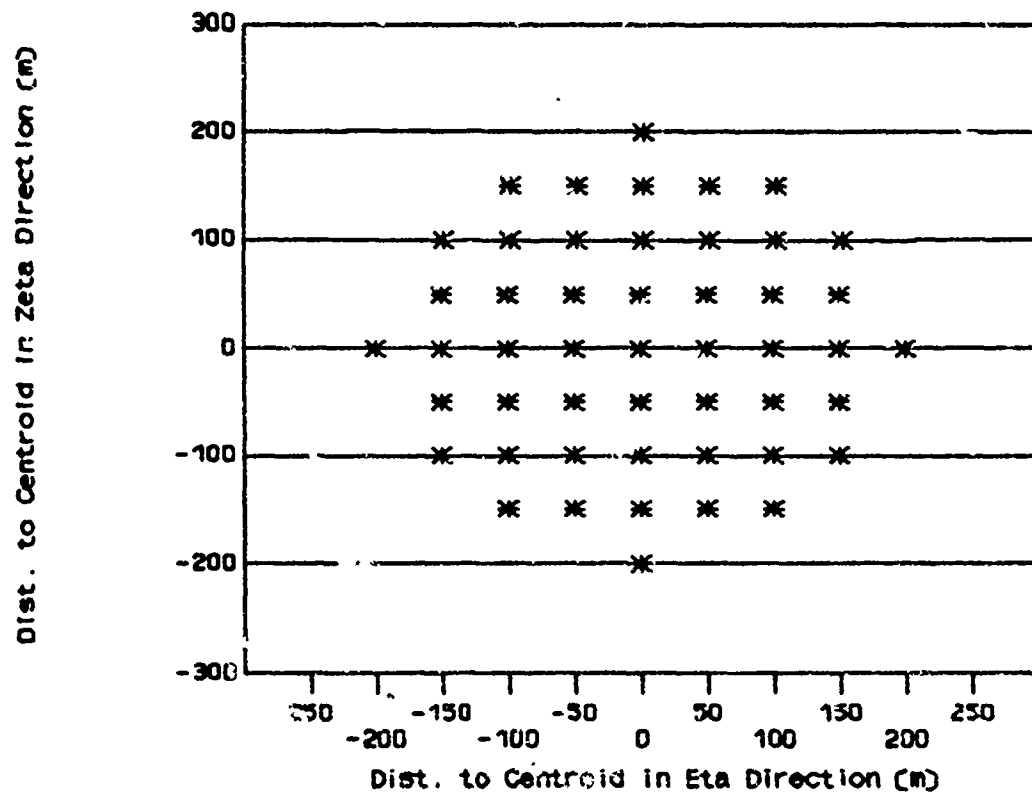


Figure 10. Plume Cloud Evolution for a 0.01 m/s Dispensing Velocity: 3600 Seconds After Dispensing

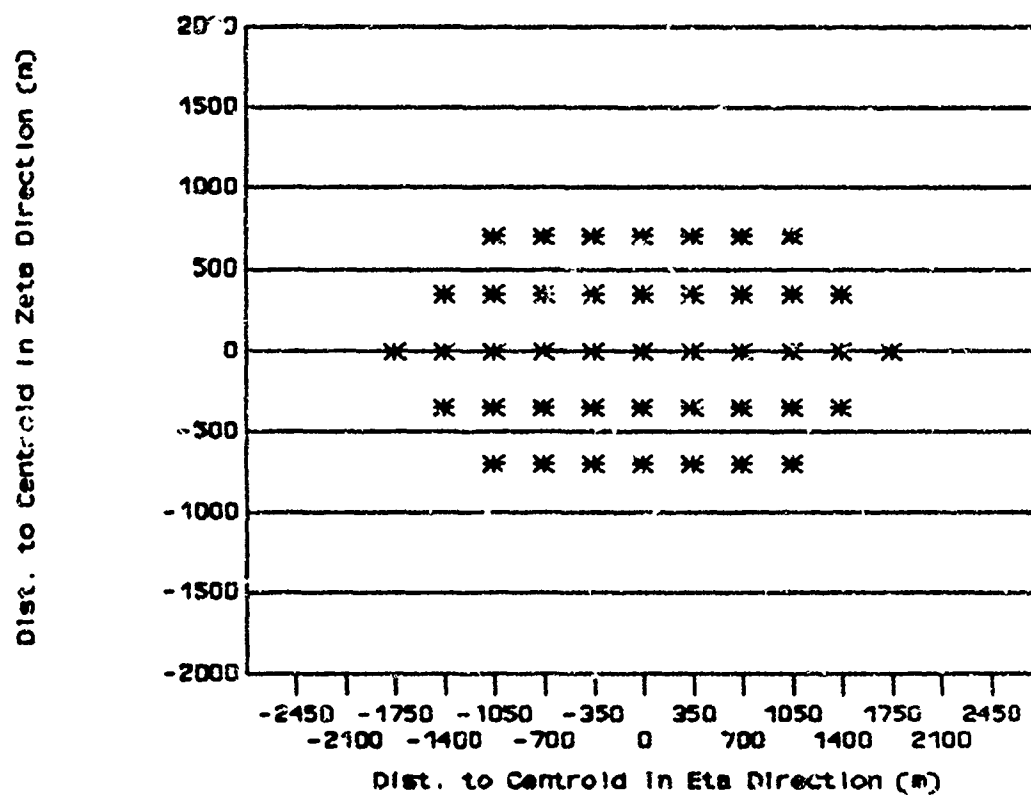


Figure 11. Chaff Cloud Evolution for a 0.01 m/s Dispensing Velocity: 25200 Seconds After Dispensing

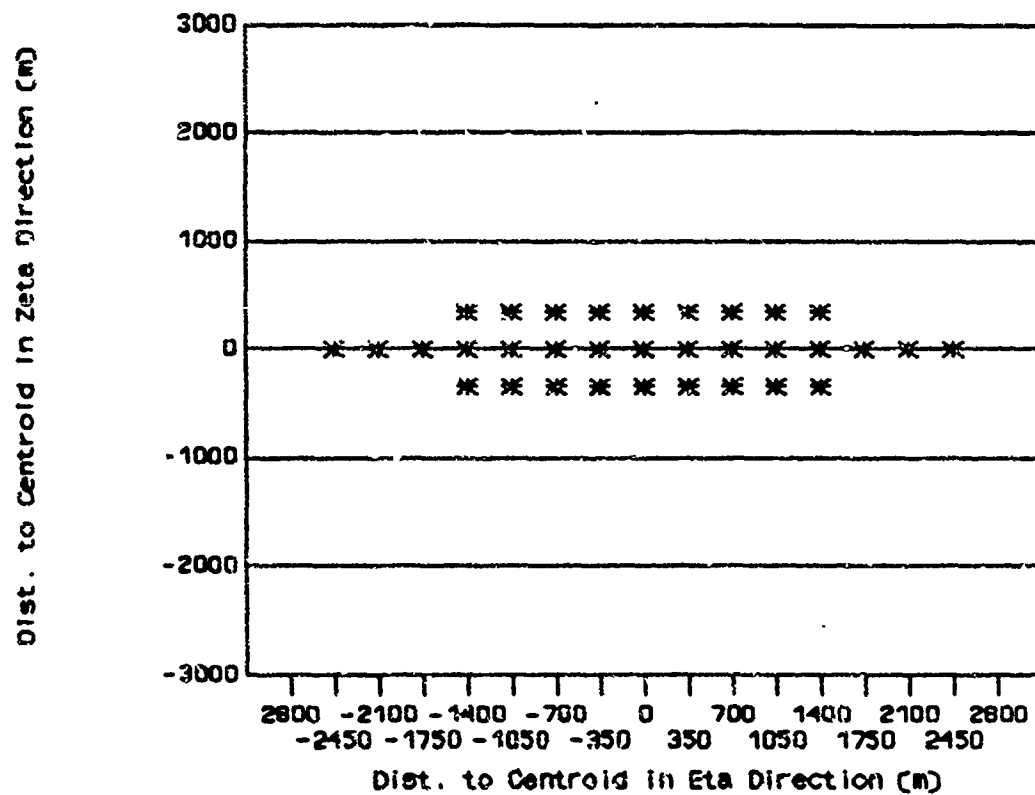


Figure 12. Chaff Cloud Evolution for a 0.01 m/s Dispensing Velocity: 28800 Seconds After Dispensing

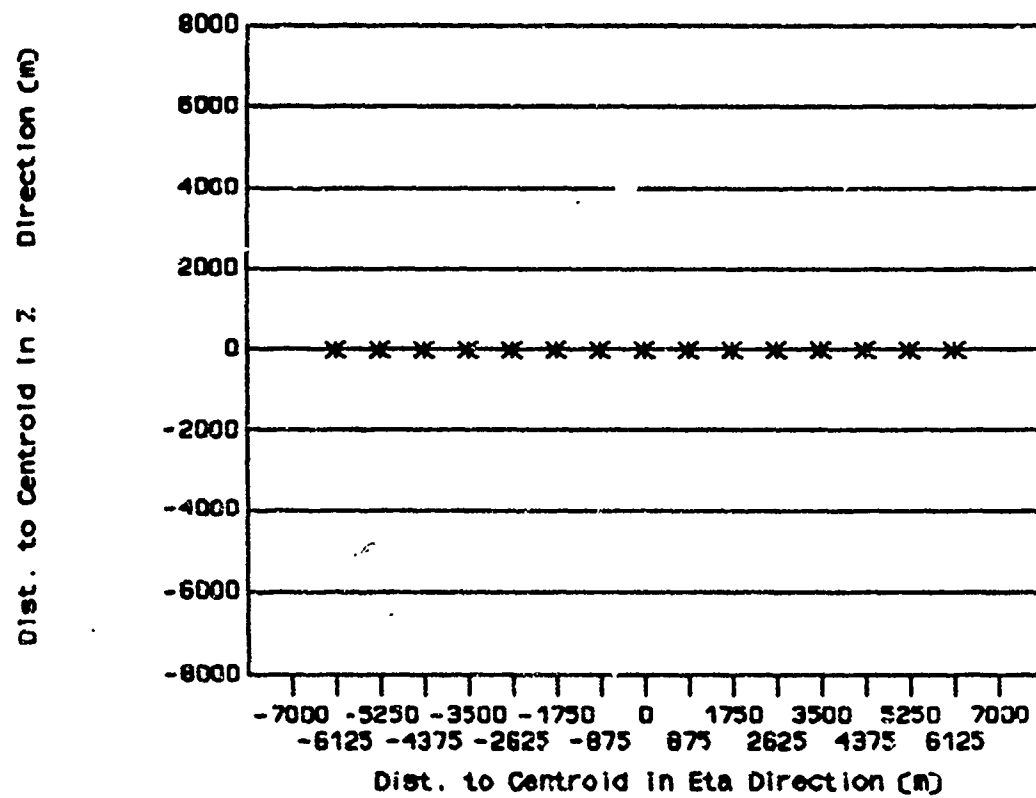


Figure 13. Chaff Cloud Evolution for a 0.01 m/s Dispensing Velocity: 39600 Seconds After Dispensing .

Although not shown in the figure, the spreading in the ξ direction is very nearly circular. To visualize the expansion of the cloud over time in three-dimensions it is probably easiest to imagine a golf ball, an egg, a cucumber, and then a serving platter. Also not shown in the figure is that the cloud eventually expands to form a toroid around the earth.

As mentioned in Chapter II, those particles dispensed along the path of motion of the parent satellite experience changes in their orbital periods and thus, their velocities. These velocity changes cause the chaff particles to continually spread in the η direction as shown in the figures. Not shown in the figures is the appearance of the cloud in the $\xi\eta$ -plane. When viewed from above, the cloud starts out as a circle and then becomes an ellipse. This change in the cloud's shape is caused by the elongation in the η direction.

Also not shown is the displacement in the ξ direction of the "leading" and "trailing" edges of the cloud in relation to its path of motion. In this displacement, the leading edge of the chaff cloud gradually moves farther away from the earth and the trailing edge moves closer. This is caused by the phenomenon noted by Shapiro when he mentioned the "dragon's jaws". Because the eccentricities of the individual chaff particle orbits are disturbed in the

dispensing process, some of the particles necessarily drift away from the parent satellite's position as the cloud approaches the portion of its orbit 180 degrees from the point of dispensing. If the cloud were examined for a longer period of time, it would continue to oscillate slightly up and down in altitude, but the phenomenon would gradually dampen out.

Finally, the reason the cloud becomes "thinner" as it reaches the 12-hour point of its orbit is simply explained by orbital mechanics. As mentioned in Chapter II, the particles displaced out of the orbital plane will return to the plane of the dispenser every one-half revolution as the two planes cross. At an altitude of 42073 km, the parent satellite's orbital period is 23.86 hours. Therefore, at very nearly 12 hours the cloud should pinch down somewhat as shown in Figures 10 through 13.

Figure 14 shows a representative graph of the density profile through the central column of the chaff cloud. The density is shown as a function of percentage of distance travelled through the chaff cloud, with the density being greatest in the center of the cloud. The graph presented is for a dispensing velocity of 0.05 m/s and at a time after dispensing of five hours. Other combinations of dispensing velocity and time after deployment have similar density profiles with profiles of the cloud at earlier times having

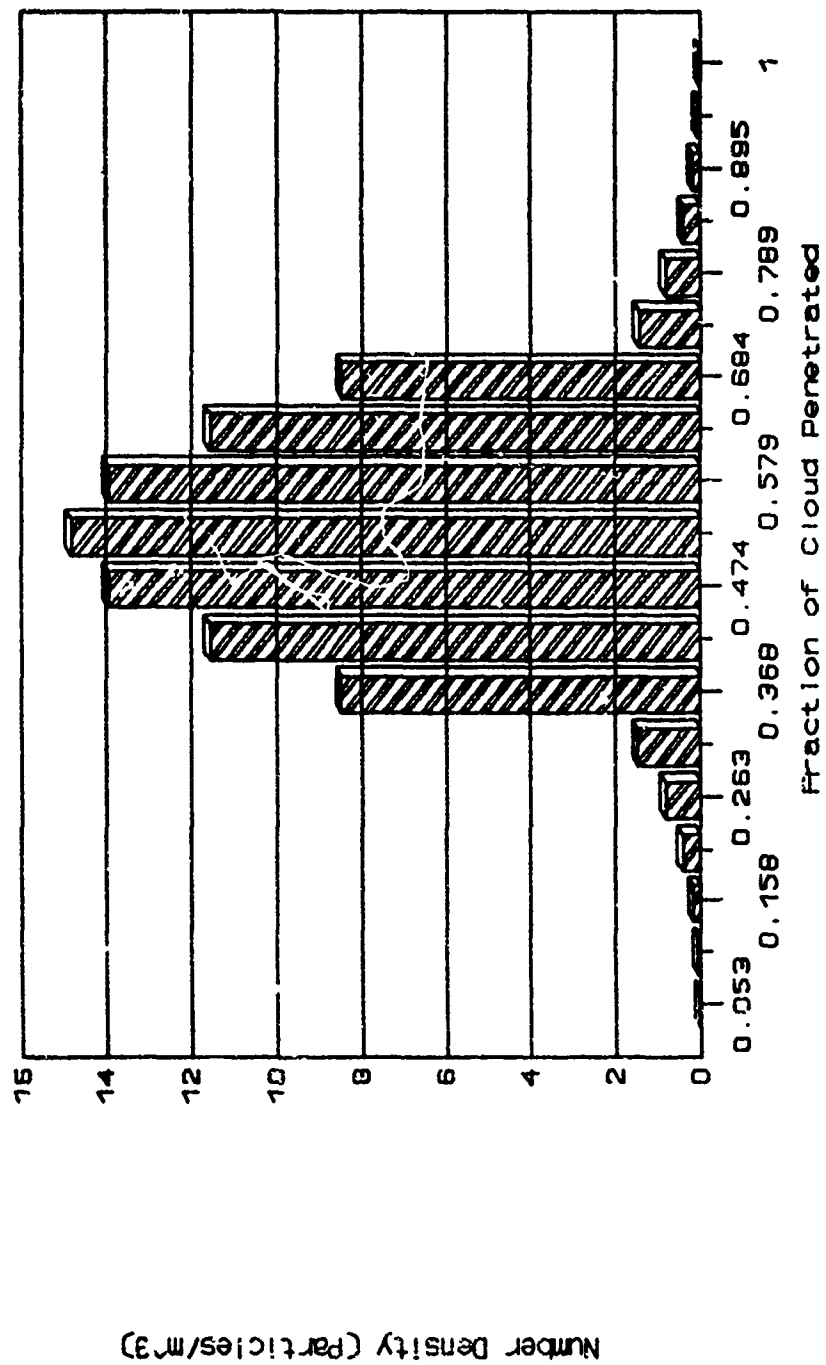


Figure 14. Average Density Through the Centroid of the Chaff Cloud

a higher density at the center and a lower density at the outer edges and with the opposite being true for later times after deployment. For smaller dispensing velocities, the central densities at the same point in time would be higher; for higher velocities they would be lower.

Signal Attenuation After One Hour

This section discusses the amount of signal attenuation affected by the chaff cloud one hour after initial dispensing. Three areas are addressed for various dispensing velocities: attenuation of the signal exactly one hour after dispensing, attenuation of the signal in ten minute increments leading up to one hour after dispensing, and the time it takes for the chaff cloud to achieve a -10 dB attenuation.

Attenuation at One Hour. This section answers the question of whether the chaff cloud can affect at least a -10 dB attenuation of the input signal at a time of one hour after initial dispensing. Since dispensing can occur at virtually any velocity, attenuation is analyzed for dispensing velocities between 0.005 m/s and 0.05 m/s. The reason for limiting the upper velocity at 0.05 m/s will be explained later in the chapter.

Figure 15 shows the attenuation in dB of the signal after it passes through the chaff cloud at a time of one hour for the dispensing velocities of 0.0115 to 0.0155 m/s. As would be expected, the attenuation is greater for the higher dispensing velocities than for the lower velocities. This is because the faster dispensing causes the particles to expand and fill the required cross-sectional area faster than the slower velocities. With more particles within the outer region of the central column, more attenuation is affected. Also, the greater velocity has the effect of making the thickness of the central column increase. With more distance for the signal to traverse, more attenuation is affected.

From the figure, it can also be seen that the attenuation is less than -10 dB for velocities less than approximately 0.014 m/s. Therefore, the dispensing velocity has to be greater than this value for the chaff cloud to be effective.

The range of dispensing velocities examined for this study was expanded in Figure 16 so velocities between 0 and 0.05 m/s could be examined for signal attenuation at a time of one hour after dispensing. As before, the attenuation generally increases with increasing dispensing velocities. However, at a velocity of approximately 0.04 m/s the attenuation level begins to decrease. There are two

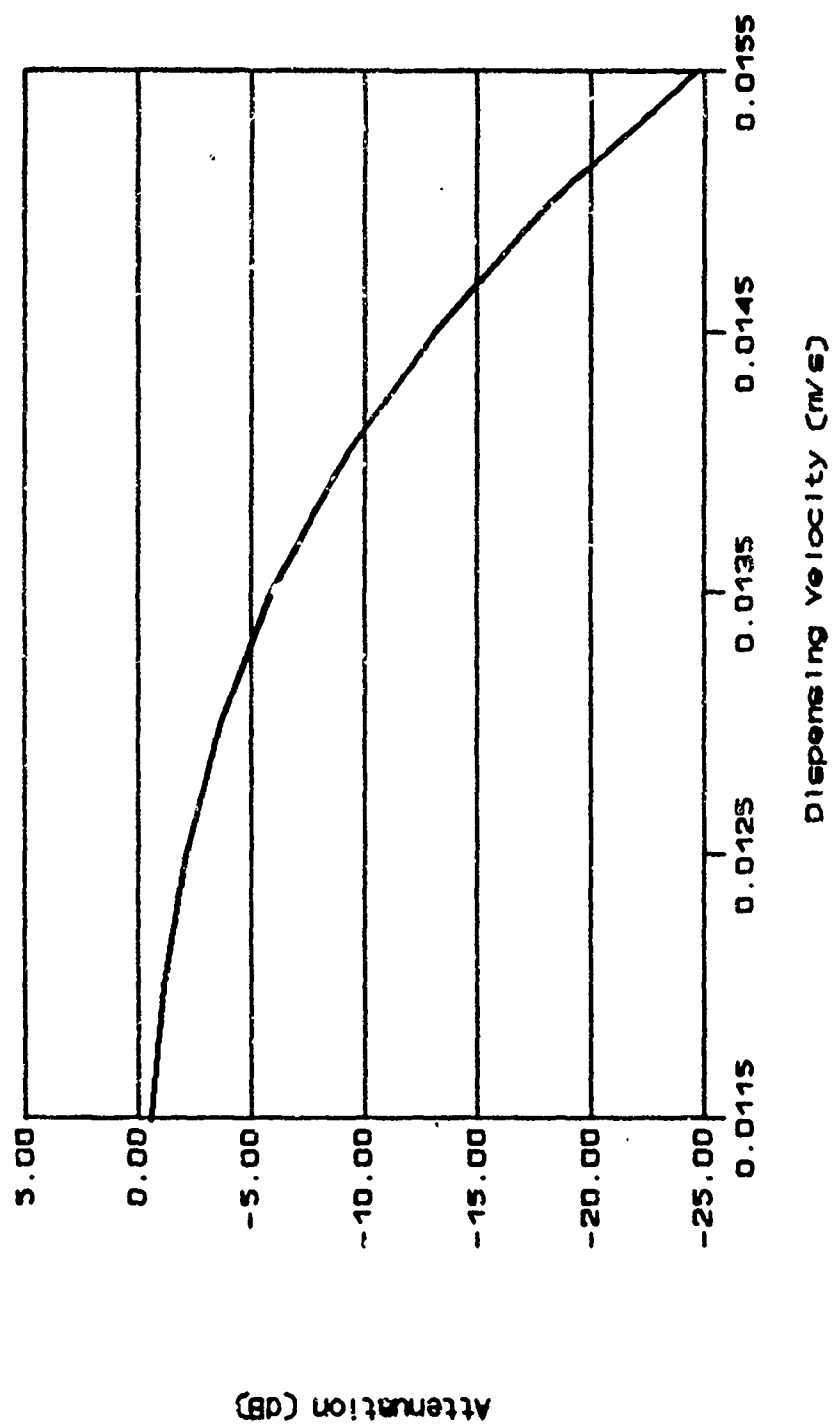


Figure 15. Signal Attenuation at One Hour for Dispensing Velocities Between 0.0115 and 0.0155 m/s

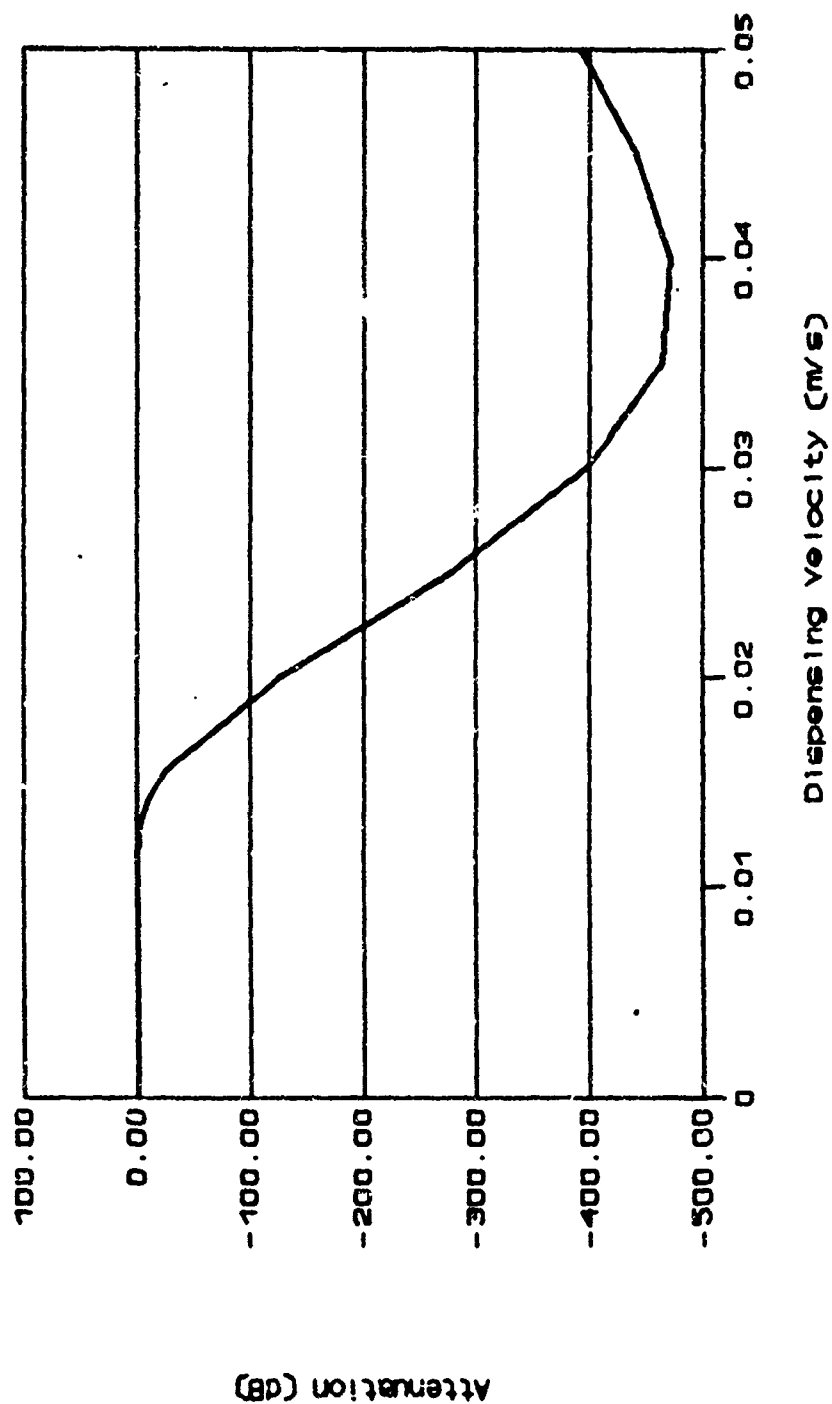


Figure 16. Signal Attenuation at One Hour for Dispensing Velocities Between 0 and 0.05 m/s

phenomena which contribute to the increasing-decreasing attenuation: a decreasing number of particles in the centroid of the chaff cloud and an increasing path length through the chaff cloud.

For velocities less than 0.04 m/s, not enough particles are able to reach the outer edge of the central column to affect a -10 dB attenuation within one hour. For velocities above 0.04 m/s, particles are retreating from the centroid at a rate fast enough that the number left within the centroid decreases below that required for the greatest attenuation. In fact, the maximum attenuation at one hour for the central subvolume occurs for a velocity of about 0.035 m/s. The increasing path length now becomes important to the attenuation of the signal. At dispensing velocities less than 0.04 m/s, the chaff cloud attenuation at the one hour point is accomplished almost entirely by the particles within the subvolume at the centroid of the cloud. At higher velocities, a greater percentage of the signal attenuation is caused by the particles that lie in subvolumes farther from the centroid. It is this combination of attenuation due to the large number of particles in the centroid and attenuation due to the increasing number of particles along the ever increasing path length that cause 0.04 m/s to be the velocity with the highest attenuation. For velocities above 0.04 m/s, the

attenuation in the centroid drops off faster than the surrounding subvolumes can compensate, so the overall attenuation for the chaff cloud gradually begins to decrease.

Attenuation in Ten Minute Increments. Figure 17 shows plots of attenuation versus dispensing velocity for times after dispensing of 10, 20, 30, 40, 50, and 60 minutes. Again as expected, the attenuation is greatest for the highest dispensing velocities for each point in time. From the figure it is clear that at times of 10 and 20 minutes after dispensing, almost none of the dispensing velocities achieve an effective level of attenuation. However, for times greater than 30 minutes after dispensing, the attenuation levels achieved are fairly significant for all dispensing velocities above 0.03 m/s. The decrease in attenuation found in Figure 16 is also apparent in Figure 17.

Time Until -10 dB Attenuation. Although not specifically outlined as a requirement by Brown, it would be nice to know the time it takes for the chaff cloud to achieve a -10 dB attenuation for various dispensing velocities. Figure 18 shows, to an accuracy of plus or minus five minutes, the time it takes the chaff cloud to attain an attenuation level of at least -10 dB. For velocities of 0.03 m/s, effective attenuation is achieved within the first 30 minutes or in

—*	60 minutes
—+	50 minutes
—	40 minutes
—x	30 minutes
—•	20 minutes
—	10 minutes

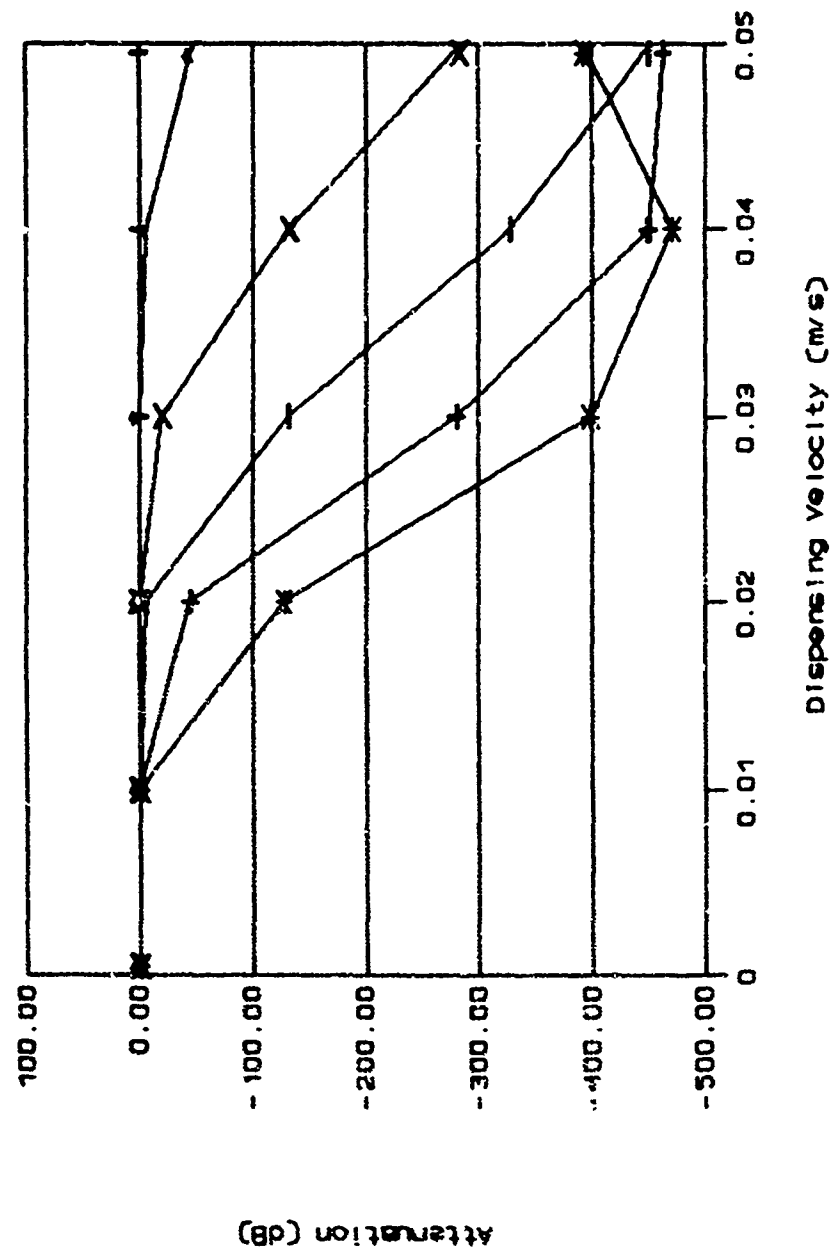


Figure 17. Signal Attenuation in Ten Minute Increments Up to One Hour

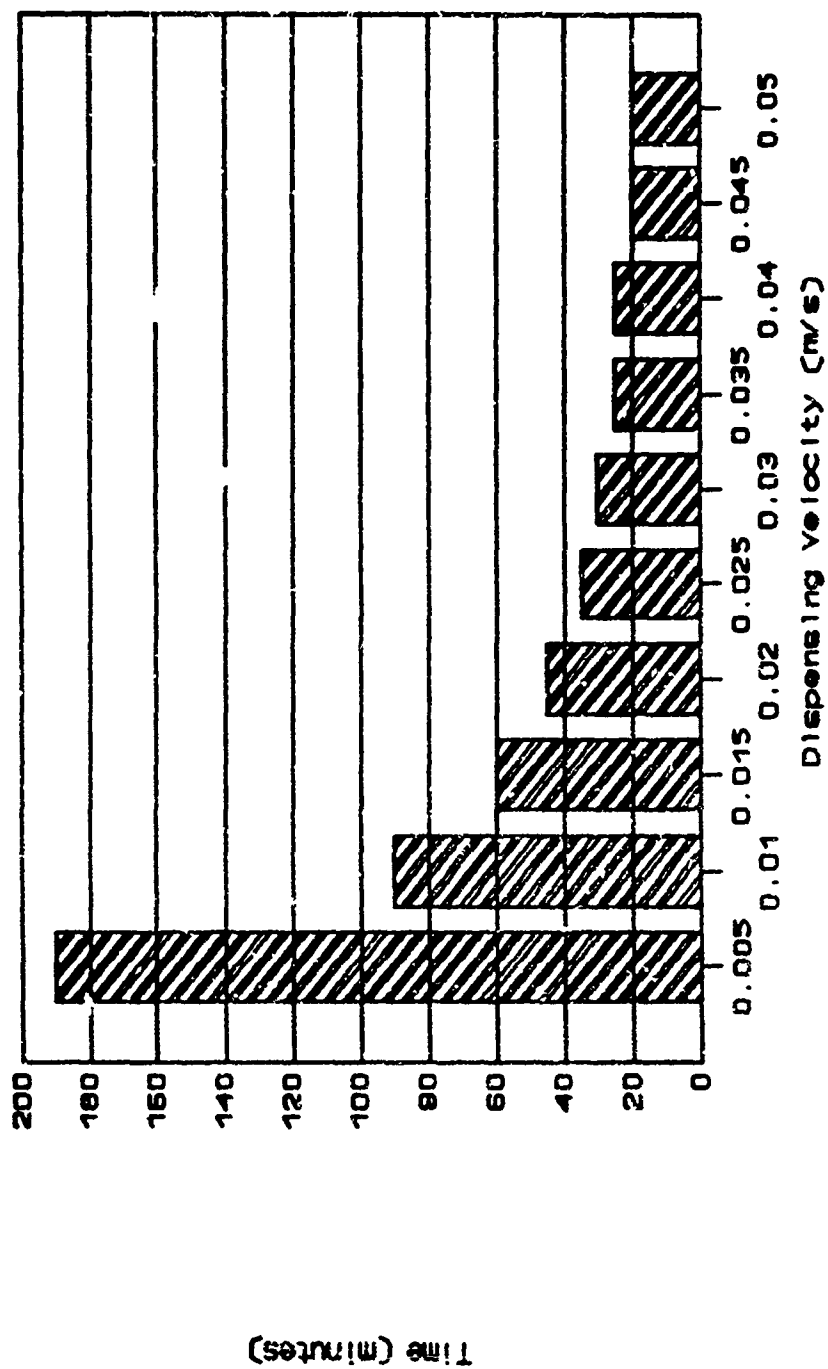


Figure 18. Time Until -10 dB Attenuation

half of the required time. However, for velocities of 0.01 and 0.005 m/s the time before effective attenuation is achieved are 90 and 190 minutes, respectively.

The reason for the great disparity in the time until effective attenuation occurs can be explained by looking at the Maxwellian velocity distribution used for the chaff cloud. The distribution has a negative exponential function which decreases to zero for increasingly large exponents. However, the dispensing velocities are placed in the denominator of the exponent so larger velocities cause the function to increase rather than decrease. The additional effect of squaring the dispensing velocities in the equation causes small changes to have a relatively large effect.

The overall effect of the Maxwellian velocity distribution is that most of the particles will have velocities near the dispensing velocity with a few with much greater velocities as the function decreases in the tail region. Therefore, for a dispensing velocity of 0.005 m/s, not many particles will have velocities even as high as 0.05 m/s and only a very small number will have higher velocities. However, for 0.05 m/s, most particles will have a dispensing velocity of 0.05 m/s with a few having much greater velocities. The result is that the area required of the chaff cloud for attenuation of a signal is covered by

particles at a much faster rate for larger dispensing velocities than for lesser velocities.

Attenuation The First Twelve Hours After Dispensing

This section examines the attenuation affected by the chaff cloud for the first twelve hours after dispensing, since the second requirement for attenuation is that the cloud maintain an attenuation of -10 dB for at least twelve hours. The twelve hour attenuation is examined in two parts. In the first, the attenuation of dispensing velocities between 0.01 m/s and 0.05 m/s will be examined by looking at individual plots of attenuation. In the second, the attenuation levels are examined on a collective plot where all the velocities are represented.

Individual Dispensing Velocities for Twelve Hours.

Figures 19 through 23 show plots of signal attenuation versus time for dispensing velocities of 0.01, 0.02, 0.03, 0.04, and 0.05 m/s respectively. Figure 19 shows the signal attenuation increasing up to the four-hour point at which time it begins to decrease. Figures 20 through 23 show similar occurrences with the maximums being reached at times of two hours, one hour, one hour, and 50 minutes, respectively. These decreases in attenuation are caused by the same phenomena mentioned in the previous section where

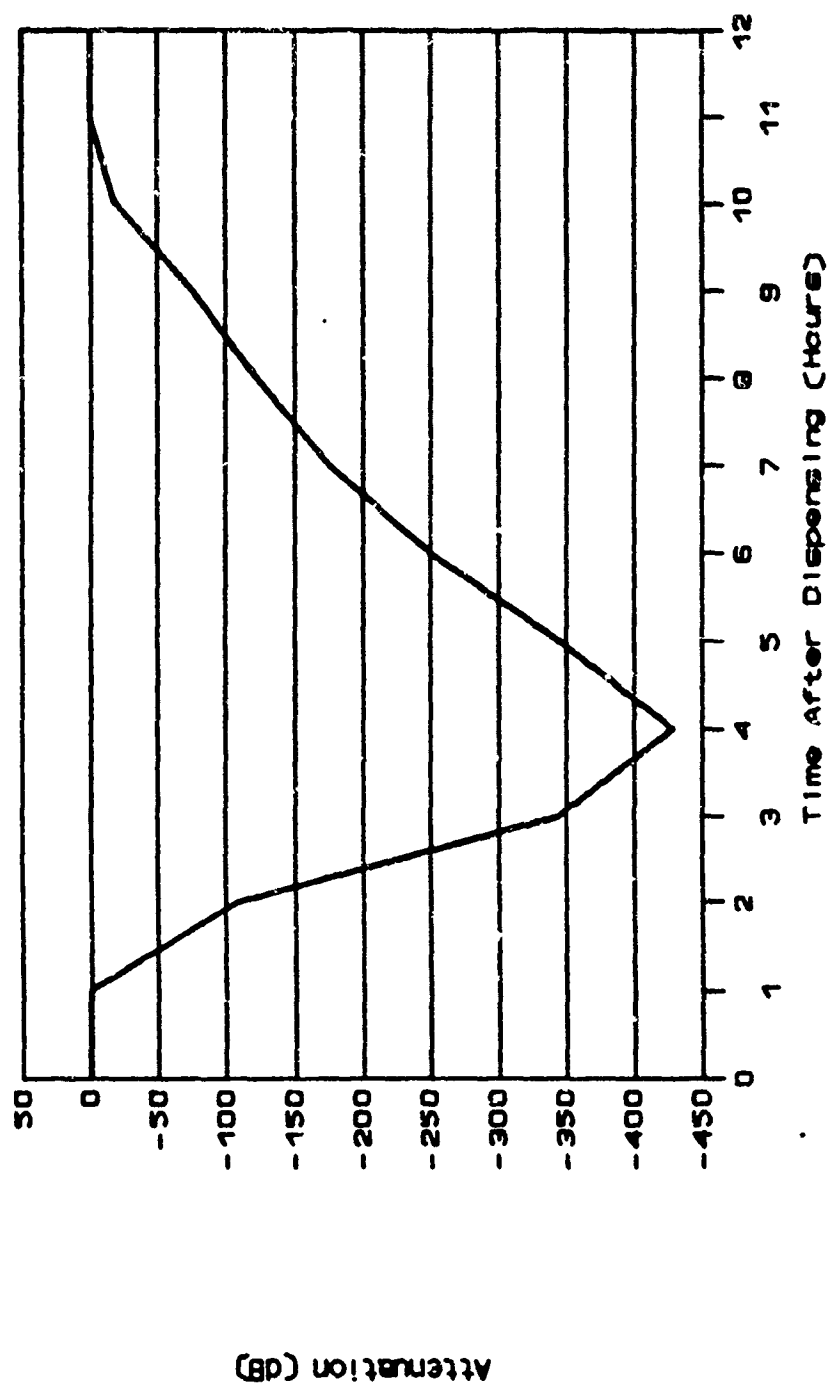


Figure 19. Attenuation for the First Twelve Hours:
0.01 m/s Dispensing Velocity

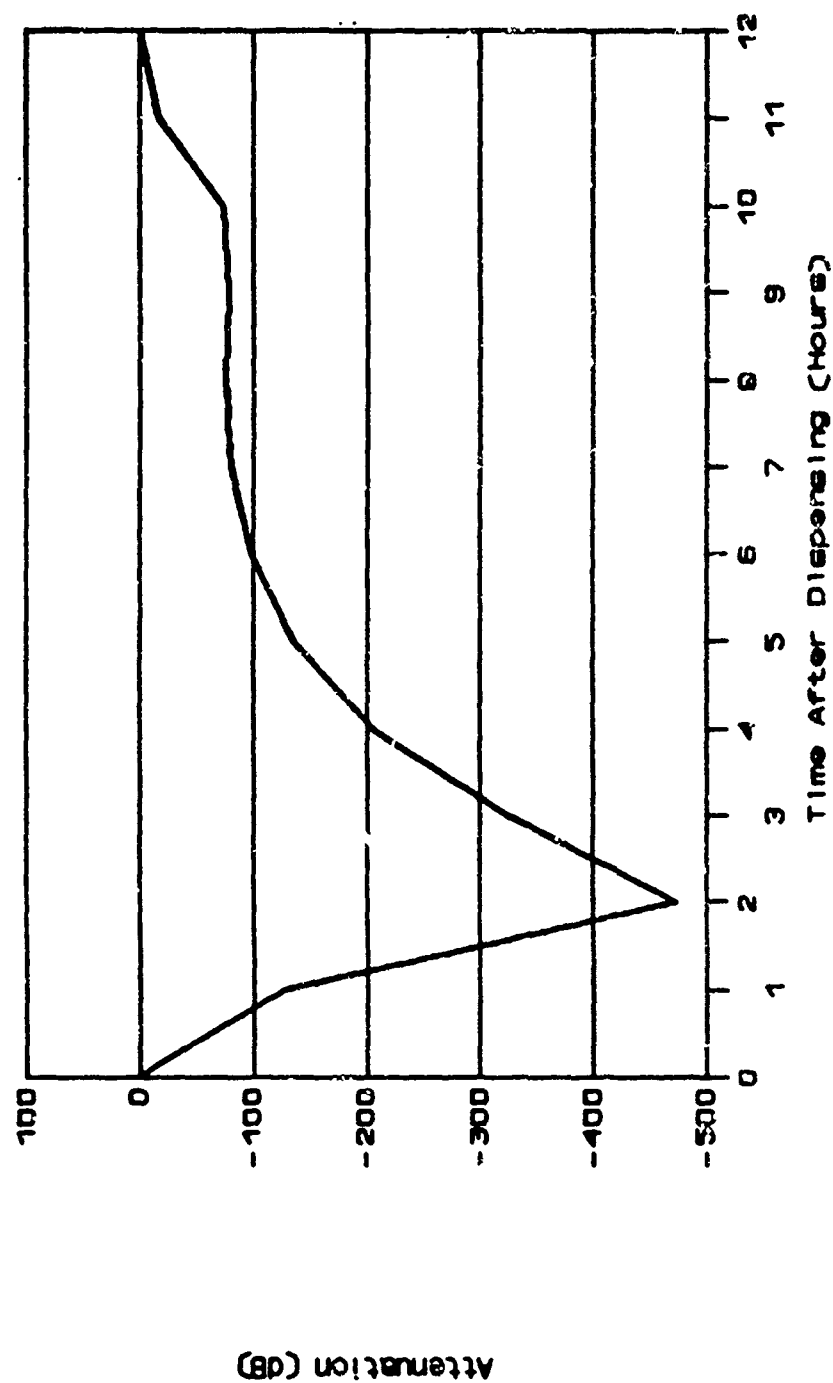


Figure 20. Attenuation for the First Twelve Hours:
0.02 m/s Dispensing Velocity

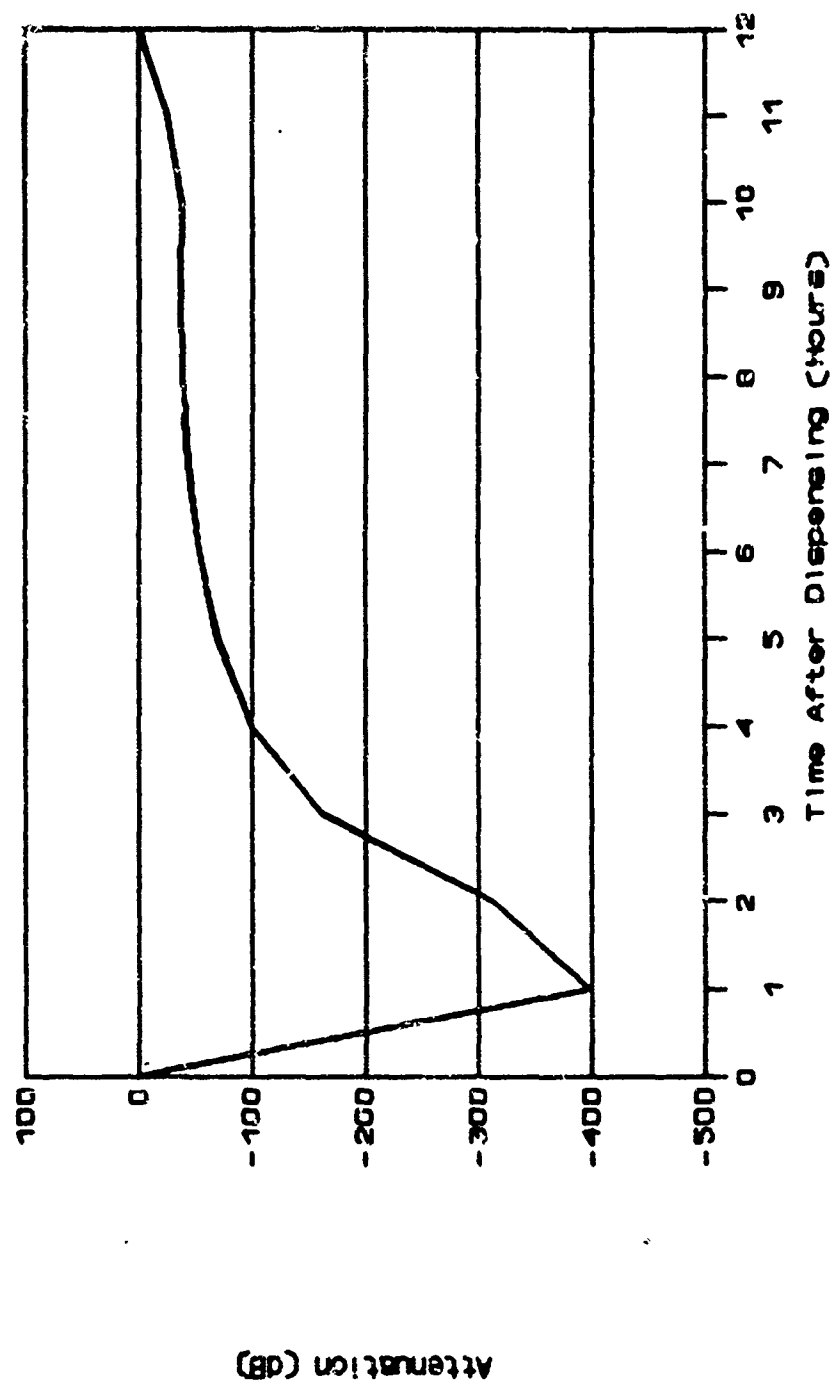


Figure 21. Attenuation for the First Twelve Hours:
0.03 m/s Dispensing Velocity

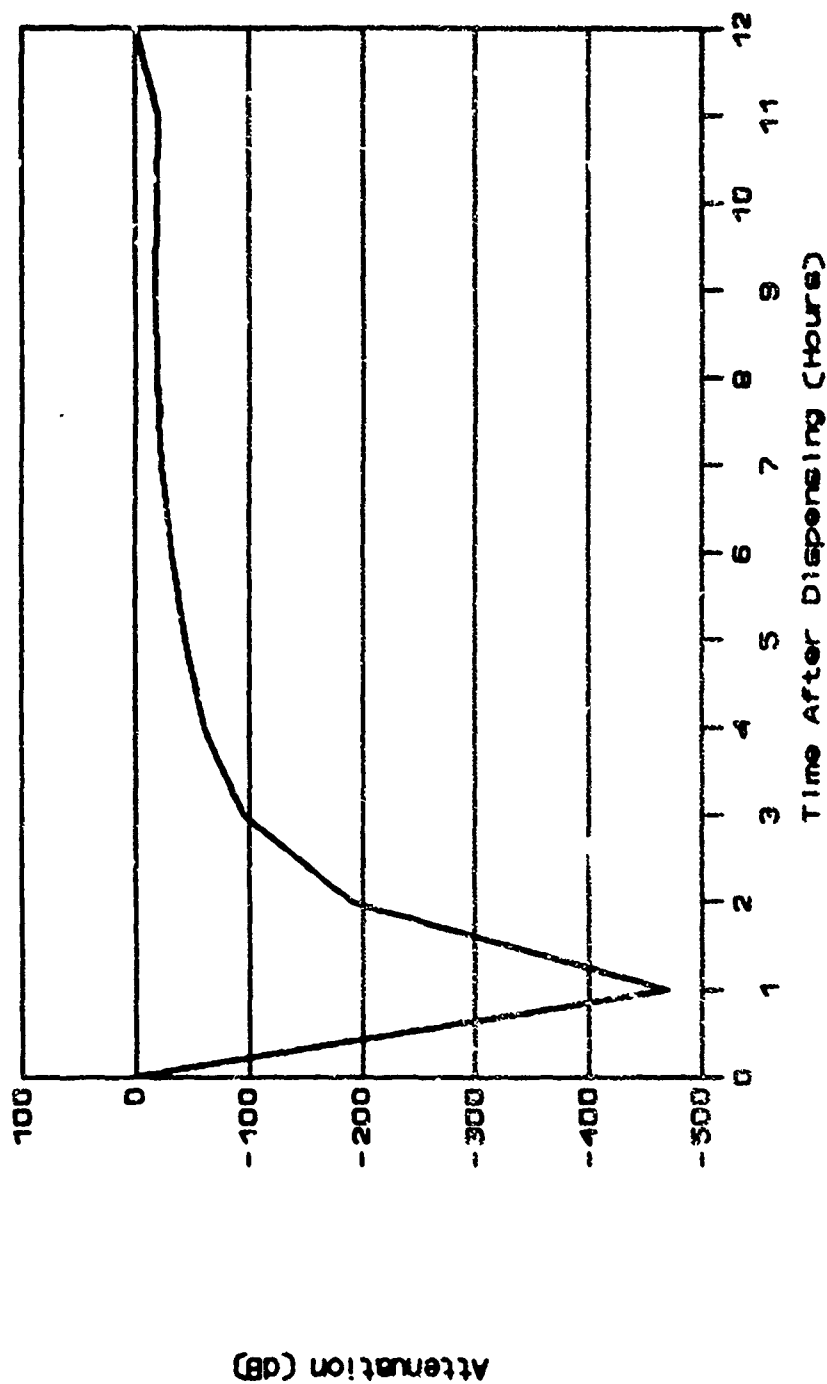


Figure 22. Attenuation for the First Twelve Hours:
0.04 m/s Dispensing Velocity

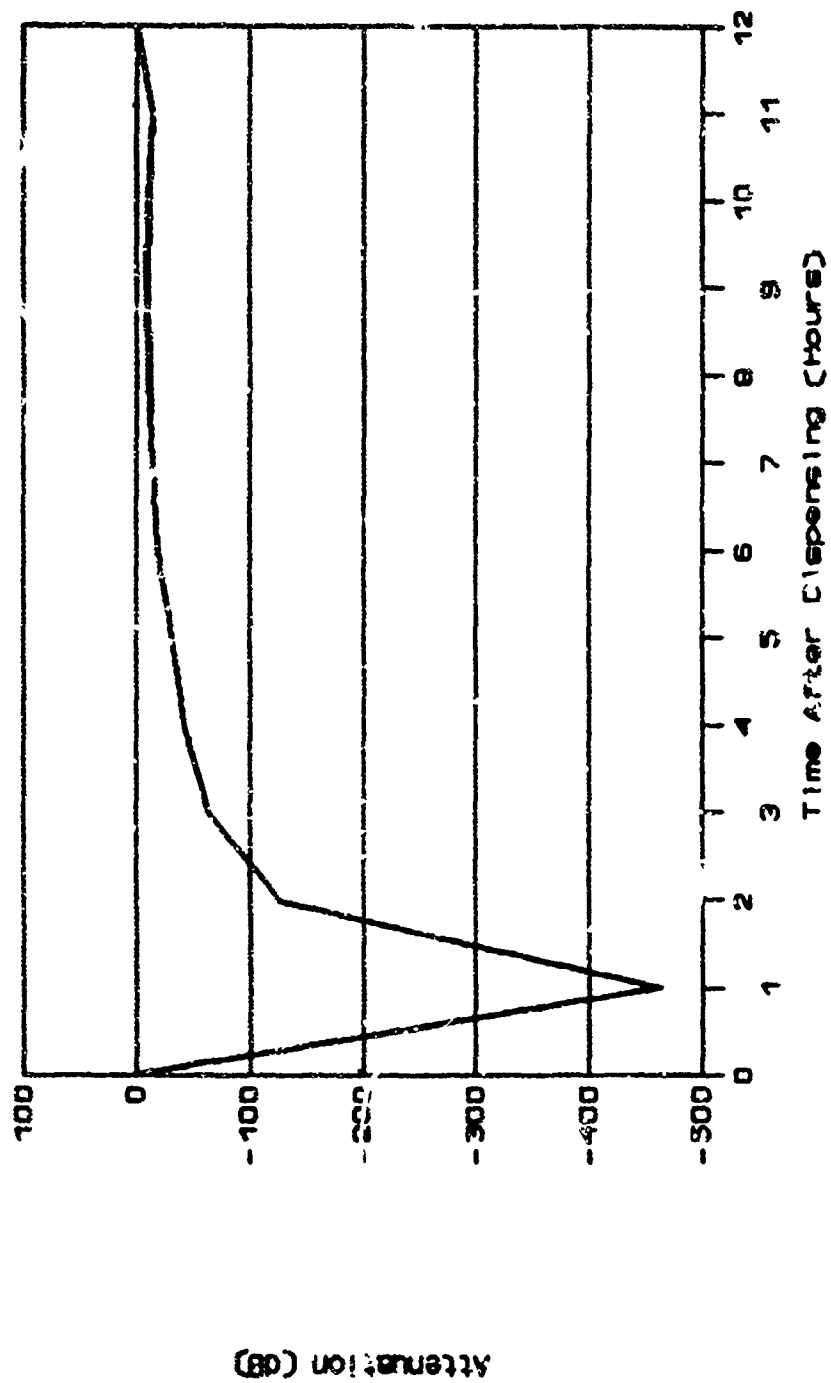


Figure 23. Attenuation for the First Twelve Hours
0.05 m/s Dispensing Velocity

the number of particles left in the centroid of each cloud drops below the number required for maximum attenuation.

Another feature in each of the figures is that the attenuation reaches its maximum value at a faster rate than the attenuation decreases beyond the maximum. Thus, each of the plots take on the shape of "V" with the left leg at a greater angle with respect to the horizontal than the right leg. This feature is most prominent for the higher velocities.

All figures also show the attenuation levels dropping below the -10 dB point before the twelve-hour point is reached. Therefore, none of the clouds meet the second attenuation requirement set by Brown. This problem can be explained by examining the orbital mechanics of the cloud. As mentioned previously, the cloud pinches down as it approaches the twelve-hour point, causing the cloud to become smaller in the ξ direction than that required for proper attenuation across the required cross-sectional area. The only way to get the cloud to pinch down after 12 hours would be to deploy it far enough away from the earth so that its orbital period would be greater than 24 hours. However, since this would cause the cloud to lie outside the orbit of the DSCS satellite it is attempting to jam, the cloud would be rendered useless as a jammer.

Examination of the figures also shows the following interesting feature for all but the 0.01 m/s dispensing velocity: As the time approaches the twelve hour point, the attenuation (which was decreasing) begins to increase again. This can be explained by the fact that the cloud is expanding along the central column in the ξ direction. When a cloud becomes large enough, the fact that attenuation through any one subvolume along the central column does not greatly attenuate the signal is counteracted by the multiplicative effect of the signal passing through more and more subvolumes along the way. For example, if each of 21 subvolumes along the signal's path cut the signal by only 15 percent, the final output signal would be 0.032 of the input signal. This equates to an attenuation of -14.8 dB. The fact that the attenuation again drops off after this portion of the curve for each figure is due to the pinching down of the cloud which was described above.

For most of the dispensing velocities examined, once attenuation of greater than -10 dB is attained, it remains above that level until the pinching of the cloud causes attenuation to decrease again. However, the level of attenuation at which the attenuation stops decreasing and begins to increase again becomes lower for increasing velocities. For example, the attenuation of the 0.02 m/s dispensing velocity cloud began to increase again after

attenuation dropped to about -75 dB. But, for a dispensing velocity of 0.05 m/s, the attenuation did not increase until it was slightly below -10 dB. Therefore, for dispensing velocities greater than 0.05 m/s, the attenuation level would also drop below -10 dB before the attenuation level began to increase again. Since the attenuation of the cloud with a dispensing velocity of 0.05 m/s dropped below -10 dB after only nine hours, higher dispensing velocities would attenuate for even shorter periods of time and, thus, were not examined.

Collective Examination of Dispensing Velocities for Twelve Hours. When Figures 19 through 23 are superimposed upon each other, Figure 24 results. Figure 24 looks pretty much as expected, with the curves for lower dispensing velocities lying below and to the right of the higher dispensing velocities. However, a closer examination shows both the 0.01 and 0.02 m/s curves crossing the other curves beginning at about nine and eleven hours, respectively.

The reason behind this apparent discrepancy with the previous results is once more due to the interaction of the three major functions affecting attenuation: the number of particles within the subvolumes, the size of the chaff cloud, and the pinching of the cloud at the twelve hour point. Since the chaff clouds with higher dispensing

+	.01 m/s
*	.02 m/s
x	.03 m/s
.	.04 m/s
o	.05 m/s

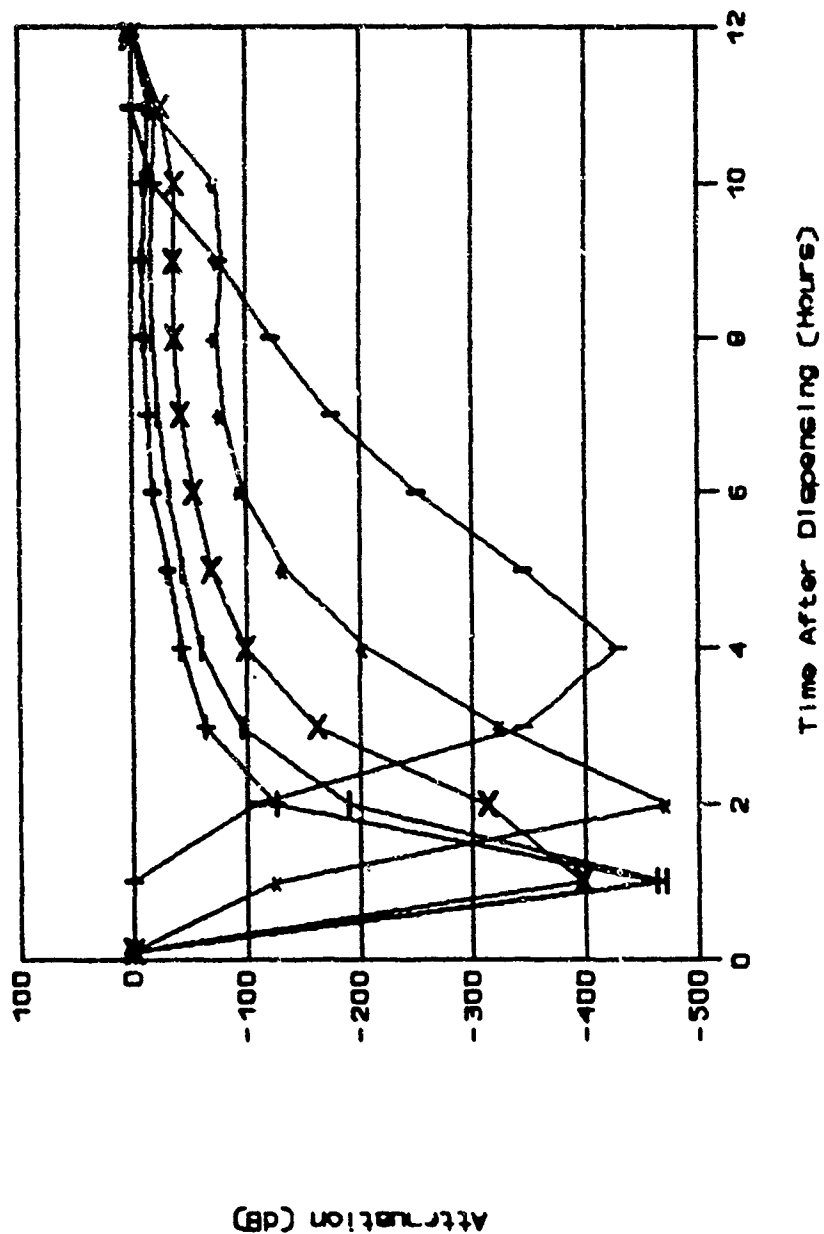


Figure 24. Attenuation for the First Twelve Hours:
0.01, 0.02, 0.03, 0.04, and 0.05 m/s
Dispensing Velocities

velocities expand much more rapidly than the clouds with smaller dispensing velocities, the multiplicative effect of the attenuation through the subvolumes is greater for them than for the clouds with slower dispensing velocities. Thus, despite the fact that the clouds with slower dispensing have more particles contained near their centroids than the clouds with faster dispensing, the small number of subvolumes along the central column becomes an inhibiting factor to overall signal attenuation.

For example, at ten hours, the attenuation through the centroid of the cloud with a 0.01 m/s dispensing velocity is 97.4 percent, while it is only 86.4 percent for the cloud with a 0.05 m/s dispensing velocity. However, with 11 subvolumes 0.35 km on a side along the central column, the cloud with the higher dispensing velocity has an overall attenuation of 99.98 percent. The cloud with a 0.01 m/s dispensing velocity has only five subvolumes along the central column for an attenuation of 98.8 percent. The reason the clouds with 0.03 and 0.04 m/s dispensing velocities do not cross over the other curves is because the pinching effect of the chaff cloud begins to dominate the expansion function for these velocities before the expansion functions show up on the graphs.

VI. Conclusions and Recommendations

This chapter summarizes the research done to study the deployment of a chaff cloud in space. First, it lists and discusses conclusions that can be drawn directly from the results. Then it lists some recommendations for areas of further study and briefly discusses these recommendations.

Conclusions

The results of the previous chapter clearly demonstrate that no dispensing velocity for the chaff cloud allows it to attenuate the incident communications signal for twelve hours because of the laws of orbital mechanics. Also demonstrated was that dispensing velocities less than 0.014 m/s or greater than 0.05 m/s are inadequate, in the first case because the signal is not attenuated quickly enough and in the second case because signal attenuation drops below -10 dB at a time of nine hours after dispensing.

Since none of the dispensing velocities attenuate for a full twelve hours, a compromise with the attenuation requirements set by Brown will have to be reached. It is probably best to choose a dispensing velocity for the chaff cloud that causes attenuation as quickly as possible and that also continues to attenuate for as long as possible.

The early attenuation will help counteract the fact that attenuation does not continue up to the twelve hour point. Dispensing velocities greater than 0.03 m/s seem to be best since they can attenuate the signal within 30 minutes and continue to attenuate the signal up to the point the cloud pinches down near twelve hours. However, the attenuation by the clouds with dispensing velocities of 0.04 and 0.05 m/s drop as low as -17 and -9.8 dB well before the twelve hour point, while the attenuation by the 0.03 m/s velocity cloud drops only as low as -37 dB. For this reason, the dispensing velocity of a chaff cloud in space should be approximately 0.03 m/s to best achieve the attenuation requirements suggested by Brown.

Recommendations

With the feasibility of using a chaff cloud in space as a communications jamming device demonstrated, it is now necessary to ask a few questions regarding the assumptions used in the study and to outline some areas of further research concerning the chaff cloud. This section asks the following four questions:

- 1) Are the attenuation levels achieved by the chaff cloud high enough to make the cloud useful?

- 2) How does relative motion between the centroid of the chaff cloud and the target satellite affect attenuation?
- 3) Are the assumptions regarding the dispensing of the chaff cloud reasonable?, and
- 4) What are the effects of the chaff cloud on other satellites?

Is the Chaff Cloud Useful? Although the chaff cloud does not maintain a significant level of attenuation for a full twelve hours, the fact that it does maintain levels of more than -50 dB for several hours is certainly significant. Therefore, it would be worthwhile to look into the significance to communications of the levels of attenuation attainable by a space-borne chaff cloud. Areas addressed could include: the length of time attenuation needs to be maintained in order for communications to be significantly disrupted; levels of attenuation required to disrupt most satellite communications, and what conditions apply to each level; and what sort of tradeoffs can be made between attenuation levels achieved by a chaff cloud and the periods of time over which the levels are maintained so that the most significant signal disruption occurs. All these questions could be addressed to the various dispensing velocities available for the chaff cloud to help redefine limits for the model.

Another question that needs to be asked is what happens to the signal attenuation after the twelve hour point? Since the cloud will begin to expand again after the twelve hour pinching, perhaps a few more hours of attenuation can be achieved by the cloud after attenuation levels build back up again. The levels of this second period of attenuation need to be examined to see how long they remain significant if, in fact, they are. Maybe the pinching down can be counteracted by another attenuation device until the cloud expands again. Finally, since the chaff cloud is continually expanding and contracting causing periodic signal disturbances, perhaps nothing more needs to be done to significantly disrupt communications.

What is the Effect of Motion Between the Chaff Cloud and the Satellite? As Brown points out in his thesis, the chaff cloud has a motion relative to a geosynchronous satellite of 7 m/s. This is due to the fact that the cloud is in a lower orbit around the earth than the target satellite. Since the chaff cloud is expanding at a much slower rate than this relative motion, the chaff cloud will move out of a position of effective attenuation well before maximum attenuation is reached (Brown, 1987:4-18 to 4-19).

There are several ways of dealing with this problem: deploying the cloud closer to a geosynchronous altitude to

minimize the relative motion; deploying the cloud earlier in time so it drifts across the geosynchronous satellite's field of view after the cloud has grown large enough to effectively attenuate the signal; deploying the chaff cloud from an elliptical orbit and allowing the changing velocity of the chaff cloud, as it follows the elliptical path, to keep the cloud in the geosynchronous satellite's field of view longer; and deploying more than one chaff cloud in orbit, and allowing them to drift past the geosynchronous target in succession.

By deploying the chaff cloud from a higher altitude, the relative motion between it and a geosynchronous target can be reduced substantially. However, if the relative motion was to be reduced to 0.5 m/s, the chaff cloud would be deployed only 13.8 km below geosynchronous altitude. In this case, the relative motion between the two bodies would still be too high as it would take a 2.45 km diameter chaff cloud only a little less than an hour and a half to pass completely in front of a geosynchronous satellite. More importantly, the chaff cloud would be unacceptably close to the target satellite, as expansion of the chaff cloud would eventually cause it to collide with the satellite.

Perhaps the chaff cloud can be dispensed before it is actually needed so that its expansion would be big enough to cause effective attenuation over the required area on the

ground as it drifted past the geosynchronous satellite. This would eliminate the need to wait for the cloud to expand as it drifted out of view of the target satellite. If the timing and direction of motion of the chaff cloud was right, attenuation levels of several hours might be realized, since the chaff cloud expands fastest along its path of motion. For example, the cloud could be dispensed so that just as it reached a length of 2.45 km in the ζ direction, it would begin to cross the path of the uplink signal to the target satellite. By the time the cloud drifted past the geosynchronous satellite, several minutes would have elapsed. This option might also work with the cloud at a higher altitude so the relative velocity between the two bodies is minimized. Both of these options should also be examined in connection with the level of attenuation/time of attenuation calculations mentioned previously, in order to best meet attenuation requirements.

The third option, deploying the chaff cloud in a slightly elliptical orbit such that it slows down as it passes the geosynchronous satellite, was posed by Brown in his thesis. The idea is based on the fact that a satellite travels at a slower velocity at apogee than at perigee. Brown showed that the chaff cloud can be deployed in an orbit with properly chosen apogee and perigee altitudes so that the centroid of the chaff cloud will remain within 42

meters of a point located directly in front of the satellite for twelve hours. This occurs because the satellite catches up to and slightly passes the centroid of the chaff cloud as the cloud approaches its apogee. The satellite then slowly falls behind the chaff cloud as the cloud speeds up on its way to perigee. According to Brown, the orbit for which this will work has a perigee 100 NM below geosynchronous altitude and an apogee at geosynchronous altitude (Brown, 1987:4-19 to 4-22). However, Brown neglects to examine the pinching down of the chaff cloud or the possibility of collisions between the cloud and the geosynchronous satellite in his analysis, so further study in this area is warranted.

Finally, the chaff cloud could be dispensed as a series of clouds along the path of relative motion which exists between the geosynchronous satellite and the chaff cloud. This way, as one cloud passes the field of view of the geosynchronous satellite, another would appear in its place. If enough chaff clouds were dispensed in this manner, the relative motion might no longer pose a problem. Perhaps even the problem of the cloud pinching down could be eliminated by spacing the clouds so that as one cloud began pinching down, another would expand in its place.

Are the Dispensing Assumptions Reasonable? Many assumptions went into the chaff cloud deployment model and while all are reasonable for the first-order calculations of this study, further analyses would require a more critical look in the following areas: weight and volume restrictions on a space-deployed chaff cloud, ability to meet dispensing velocity requirements with a spherical cloud deployment, possibility of birdnesting of chaff particles, and actual velocity distribution of chaff particles.

With 100 billion chaff particles being deployed, the weight and size of the chaff package to be put near geosynchronous altitude could be significant. According to Brown, the volume of a single chaff particle of the size used for this study is $1.47 \times 10^{-12} \text{ m}^3$. The particle density and appropriate packing density for the chaff package are 2550 kg/m^3 and .55, respectively. (Brown, 1987:4-5). Therefore, the particles weigh 375 kg (826 lb) and occupy $2.61 \times 10^{-1} \text{ m}^3$. The volume occupied by the chaff particles is fairly small so the chaff package could probably be easily launched into orbit as a "piggyback" on another satellite. However, the weight is high and would probably require a separate launch to reach orbit. After launch costs are considered, one chaff cloud could easily cost hundreds of thousands of dollars to deploy. If higher attenuation values were desired, the cloud would weigh and

cost even more. One possibility would be to reduce the number of chaff particles. This, of course, would require another attenuation study, but a factor of 10 reduction in the number of particles would result in a more manageable weight of 37.5 kg. If the reduction in attenuation were not too great, the deployment of the cloud might be feasible.

The second dispensing assumption that needs further consideration is the initial spherical dispensing pattern. Although an exploding ball of chaff with a central charge could be constructed, it is not clear if dispensing velocities of less than 0.05 m/s could also be realized. If not, another dispensing mechanism needs to be devised. Additionally, Brown suggests that an explosive charge might damage a large number of the chaff particles (Brown, 1987:4-11). Brown also suggests dispensing the chaff particles using spools of chaff from which the chaff is deployed as the spools rotate. This is how the dipoles were dispensed for Project West Ford. For West Ford, the dipoles were attached to the spools with naphthalene which melted upon exposure to sunlight, thus releasing the dipoles over time. All the spools were initially spun about the axis of minimum moment of inertia so that the release of the dipoles would upset this inherently unstable condition and cause the spools to tumble. Thus, the dipoles were released in all directions (Brown, 1987:4-11 to 4-12). By dispensing the

particles in this manner, however; the model used in this study would be invalidated, since the model used assumed instantaneous dispensing. Maybe a compromise could be reached between dispensing techniques, or Heard's long-term dispensing model could be applied.

Another problem with dispensing chaff particles in space is "birdnesting", the clumping together of particles due to attractive electrical charges on the particles. According to MacLellan, up to 50 percent of the dipoles for project West Ford were involved in birdnesting (MacLellan, 1964:564). This condition would be expected with the dispensing of any lightweight metallic objects in space since there are no aerodynamic forces present to help the particles separate upon deployment. Since all particles in the model were assumed to properly deploy, a correction factor might need to be used to take birdnesting into account, but proper values for the number of particles involved need to be established first.

The final assumption associated with the dispensing process that deserves additional consideration is the velocity distribution function. Although a Maxwellian distribution seems appropriate for the chaff cloud in general, the Maxwellian distribution technically has no upper limit on particle velocity while the chaff particles

definitely have an upper limit on their velocity. This problem becomes important for the chaff cloud because of the large number of particles involved. If only 0.001 percent of the particles had a velocity above a certain value, the number of chaff particles involved would be 1 million. Thus, the model would show a large number of particles located a much greater distance from the centroid of the chaff cloud than there really were. This discrepancy could greatly affect the attenuation calculations, depending on which portion of cloud was being considered and how much time had elapsed since dispensing. Therefore, a new model which properly places an upper bound on dispensing velocity should be looked into if chaff deployment in space is to be further considered.

What Are the Effects of the Chaff on Other Satellites?

Chaff can be expected to have two possible interactions with satellites: attenuation of communication signals and collisions.

Since the chaff cloud is moving with respect to the satellite it is attempting to jam, it has the possibility of drifting in front of other satellites and disrupting their communications. In order to fully assess the impact on communications, the locations and transmitting/receiving frequencies of other nearby satellites would have to be

examined before each chaff cloud deployment. Also, if the frequency the chaff was designed to attenuate was not the same one used by other satellites in the vicinity, even if the chaff cloud passed directly in front of the other satellites, only noise would result. Therefore, even if the chaff cloud did accidentally get in between a satellite and its ground station, the signal might not be attenuated below the level necessary for uninterrupted communication. However, an increase in noise for all satellites the chaff cloud passes in front of can be expected. On the plus side, perhaps the cloud could be deployed to jam more than one satellite for specified periods of time if the satellites were close enough together. Further research into these areas is clearly needed.

Also of major concern should be the possibility of collisions between the chaff particles and other satellites in earth orbit. Fortunately, the chaff cloud as envisioned is well below the altitude of geosynchronous satellites, so impacts with them would not be a problem. However, solar radiation pressure and other perturbative forces will cause the chaff particles to decay into lower orbits, so they could eventually come in contact with satellites nearer to the earth.

Since the chaff particles are so tiny, they at first would not seem to pose much of a threat. However, with the

chaff cloud moving at about 3 km/s, impacts could be devastating. According to Donald J. Kessler, a NASA scientist who studies space debris, objects between 1 mm and 1 cm in size can penetrate spacecraft walls if they are moving at velocities of 10 km/s (Kessler, 1987:587). With the chaff particles being 1.87 cm long (Brown, 1987:4-3), although also being very thin and moving much slower than 10 km/s, impacts might still be a problem.

Even if the chaff particles do not damage the satellites they come into contact with, they could interfere with the satellites' operating functions by sticking to the satellites' surfaces. Since the chaff particles are at least partially composed of metal, the bombardment of the chaff particles by high energy particles from the sun will likely cause the chaff particles to acquire an electric charge. If the charged chaff particles were to fly within close proximity of an oppositely charged satellite surface, they would be drawn to the satellite and stick to the surface. If enough particles stuck to solar panels or antennas, a degradation of satellite operations might result. Therefore, this is another area which warrants further study.

Two suggestions were proposed by Brown to help eliminate the problem of unwanted signal attenuation by and impacts with the chaff cloud: constructing the chaff of

materials so fine they would be broken up and swept away by the solar wind, or using materials for the chaff that deteriorate when exposed to ultraviolet light (Brown, 1987:4-23 to 4-24). Although Brown did not go into much detail on these suggestions, they might deserve further consideration if a chaff cloud is to be deployed in space.

Appendix A: Density Spreadsheet Formulas

This appendix contains a printout of all the formulas used in the density spreadsheet. Each cell of the spreadsheet is listed on a separate line. The cell labels are set up so that letters represent columns and numbers represent rows starting from the upper left corner of the spreadsheet. Therefore, entry "D10" is the fourth entry from the left in the tenth row of the spreadsheet.

In the formula printout, several symbols are used in front of the cell entries. An apostrophe, a set of quotation marks, or a caret symbol (^) indicate that the entry in the cell is a label and not used in any calculations. The symbol "[w10]" is used to represent each new row of the spreadsheet, and the symbol "\-" indicates that the cell is filled with a row of hyphens. All cells without one of these marks are either blank or contain formulas.

Rows 1 through 20 contain constants and variables for use in calculations by the rest of the spreadsheet. The constants are those used by Heard in Eq (40) and the variables are the following: the spreadsheet scaling factor, the square of the thermal velocity of the chaff particles, the time after dispensing, the number of chaff

particles in the spreadsheet grid, the dispensing velocity of the chaff particles, and the displacement coordinates of the centroid of the spreadsheet grid from the centroid of the chaff cloud.

Rows 21 through 78, 80 through 137, 139 through 196, 198 through 255, 257 through 314, 316 through 373, and 375 through 430 calculate the relative number densities for each of the seven values of ξ contained in the spreadsheet model grid. Within each of these sections are subsections which calculate values for P1, P2, and P3; a logic table to help the spreadsheet calculate exponents of negative numbers smaller than negative 200; and calculations of the relative particle densities as solutions for Eq (40).

Finally, Row 433 calculates the sum of the relative number densities and rows 436 through 509 calculate the actual number of particles for each (ξ, η, ζ) coordinate within the 7x7x7 grid modeled by the spreadsheet.

```

A1: [W10] "Eta vs.
B1: "Zeta
C1: "t =
D1: 3600
E1: "sec
F1: "(vch-2 =
G1: 2.107E-11
H1: "RU/STU)
A2: [W10] \-
B2: "-----
C2: "(mult x
D2: 0.05
E2: "
F2: "(VO =
G2: 0.01
H2: "m/s)
A3: [W10] "Constants
B3: "1
C3: "(w Part =
D3: 100000000000
E3: "
F3: "Centroid
G3: "X1
H3: "Eta
A4: [W10] \-
B4: \-
C4: \-
D4: \-
E4: "(In RUs)
F4: 0
G4: 0
H4: 0
A5: [W10] "X
B5: 1
A6: [W10] "n (rad/s)
B6: 7.315288954E-05
A7: [W10] "t
B7: +01
A8: [W10] "Tau
B8: +8E+87
A9: [W10] "s
B9: SIN(88)
A10: [W10] "c
B10: COS(88)
A11: [W10] "1-c
B11: 1-B10
A12: [W10] "sigma
B12: 2
A13: [W10] "sgmsqrd
B13: +B12-2
A14: [W10] "1-sgmsqrd
B14: 1-B13
A15: [W10] "2-sgmsqrd

```

```

B15: 2*813
A16: [W10] "D
B16: (814*89*88)*(815*811)
A17: [W10] "First term
B17: +85/885(89*816)
A18: [W10] \-
B18: \-
C18: \-
D18: \-
E18: \-
A19: [W10] \-
B19: \-
C19: \-
D19: \-
E19: \-
A20: [W10] \-
B20: \-
C20: \-
D20: \-
E20: \-
A21: [W10] "X1(1)
B21: (-7.0992231E-05*DR)*G4
A24: [W10] "P1
A25: [W10] \-
B25: \-
A26: [W10] "P11
B26: ((814*88)+(813*89))*821
A27: [W10] "P1(tot)
B27: (-7.130462718E-05*SD2)*SH54
C27: (-4.753642478E-05*SD2)*SH54
D27: (-2.376821239E-05*SD2)*SH54
E27: (0*SD2)*SH54
F27: (2.376821239E-05*SD2)*SH54
G27: (4.753642478E-05*SD2)*SH54
H27: (7.130463718E-05*SD2)*SH54
B28: \-
C28: \-
D28: \-
E28: \-
F28: \-
G28: \-
H28: \-
B29: (1/8816)*(8826-(8812*8811*8827))
C29: (1/8816)*(8826-(8812*8811*8827))
D29: (1/8816)*(8826-(8812*8811*8827))
E29: (1/8816)*(8826-(8812*8811*8827))
F29: (1/8816)*(8826-(8812*8811*8827))
G29: (1/8816)*(8826-(8812*8811*8827))
H29: (1/8816)*(8826-(8812*8811*8827))
A31: [W10] "P2
A32: [W10] \-
B32: \-
A33: [W10] "P21

```

```

B33: +812*811*821
B35: +8827
C35: +8C27
D35: +8D27
E35: +8E27
F35: +8F27
G35: +8G27
H35: +8H27
B36: -
C36: -
D36: -
E36: -
F36: -
G36: -
H36: -
B37: (1/8816)*(8833+(8889*8835))
C37: (1/8816)*(8833+(8889*8835))
D37: (1/8816)*(8833+(8889*8835))
E37: (1/8816)*(8833+(8889*8835))
F37: (1/8816)*(8833+(8889*8835))
G37: (1/8816)*(8833+(8889*8835))
H37: (1/8816)*(8833+(8889*8835))
A39: CW103 *P3
A40: CW103 -
B40: -
A43: CW103 +8827
B43: (885/889)*8A43
A44: CW103 +8C27
B44: (885/889)*8A44
A45: CW103 +8D27
B45: (885/889)*8A45
A46: CW103 +8E27
B46: (885/889)*8A46
A47: CW103 +8F27
B47: (885/889)*8A47
A48: CW103 +8G27
B48: (885/889)*8A48
A49: CW103 +8H27
B49: (885/889)*8A49
A51: CW103 'Logic table
A52: CW103 -
B52: -
B53: +8827
C53: +8C27
D53: +8D27
E53: +8E27
F53: +8F27
G53: +8G27
H53: +8H27
B54: -
C54: -
D54: -
E54: -
F54: -
G54: -
H54: -
A55: CW103 +8827
B55: 01F((8829-2*8837-2*8843-2)/(8881))>-200,0,1)
C55: 01F((8829-2*8837-2*8843-2)/(8881))>-200,0,1)
D55: 01F((8829-2*8837-2*8843-2)/(8881))>-200,0,1)
E55: 01F((8829-2*8837-2*8843-2)/(8881))>-200,0,1)
F55: 01F((8829-2*8837-2*8843-2)/(8881))>-200,0,1)
G55: 01F((8829-2*8837-2*8843-2)/(8881))>-200,0,1)
H55: 01F((8829-2*8837-2*8843-2)/(8881))>-200,0,1)
A56: CW103 +8C27
B56: 01F((8829-2*8837-2*8844-2)/(8881))>-200,0,1)
C56: 01F((8829-2*8837-2*8844-2)/(8881))>-200,0,1)
D56: 01F((8829-2*8837-2*8844-2)/(8881))>-200,0,1)
E56: 01F((8829-2*8837-2*8844-2)/(8881))>-200,0,1)
F56: 01F((8829-2*8837-2*8844-2)/(8881))>-200,0,1)
G56: 01F((8829-2*8837-2*8844-2)/(8881))>-200,0,1)
H56: 01F((8829-2*8837-2*8844-2)/(8881))>-200,0,1)
A57: CW103 +8D27
B57: 01F((8829-2*8837-2*8845-2)/(8881))>-200,0,1)
C57: 01F((8829-2*8837-2*8845-2)/(8881))>-200,0,1)
D57: 01F((8829-2*8837-2*8845-2)/(8881))>-200,0,1)
E57: 01F((8829-2*8837-2*8845-2)/(8881))>-200,0,1)
F57: 01F((8829-2*8837-2*8845-2)/(8881))>-200,0,1)
G57: 01F((8829-2*8837-2*8845-2)/(8881))>-200,0,1)
H57: 01F((8829-2*8837-2*8845-2)/(8881))>-200,0,1)
A58: CW103 +8E27
B58: 01F((8829-2*8837-2*8846-2)/(8881))>-200,0,1)
C58: 01F((8829-2*8837-2*8846-2)/(8881))>-200,0,1)
D58: 01F((8829-2*8837-2*8846-2)/(8881))>-200,0,1)
E58: 01F((8829-2*8837-2*8846-2)/(8881))>-200,0,1)
F58: 01F((8829-2*8837-2*8846-2)/(8881))>-200,0,1)
G58: 01F((8829-2*8837-2*8846-2)/(8881))>-200,0,1)
H58: 01F((8829-2*8837-2*8846-2)/(8881))>-200,0,1)
A59: CW103 +8F27
B59: 01F((8829-2*8837-2*8847-2)/(8881))>-200,0,1)
C59: 01F((8829-2*8837-2*8847-2)/(8881))>-200,0,1)
D59: 01F((8829-2*8837-2*8847-2)/(8881))>-200,0,1)
E59: 01F((8829-2*8837-2*8847-2)/(8881))>-200,0,1)
F59: 01F((8829-2*8837-2*8847-2)/(8881))>-200,0,1)
G59: 01F((8829-2*8837-2*8847-2)/(8881))>-200,0,1)
H59: 01F((8829-2*8837-2*8847-2)/(8881))>-200,0,1)
A60: CW103 +8G27
B60: 01F((8829-2*8837-2*8848-2)/(8881))>-200,0,1)
C60: 01F((8829-2*8837-2*8848-2)/(8881))>-200,0,1)
D60: 01F((8829-2*8837-2*8848-2)/(8881))>-200,0,1)
E60: 01F((8829-2*8837-2*8848-2)/(8881))>-200,0,1)
F60: 01F((8829-2*8837-2*8848-2)/(8881))>-200,0,1)
G60: 01F((8829-2*8837-2*8848-2)/(8881))>-200,0,1)
H60: 01F((8829-2*8837-2*8848-2)/(8881))>-200,0,1)
A61: CW103 +8H27
B61: 01F((8829-2*8837-2*8849-2)/(8881))>-200,0,1)

```



```

B87: 1-
B87: 1-
D87: 1-
E87: 1-
F87: 1-
G87: 1-
H87: 1-
B88: (1/38316)*(38365-(38312*38311*38366))
C88: (1/38316)*(38365-(38312*38311*38366))
D88: (1/38316)*(38365-(38312*38311*38366))
E88: (1/38316)*(38365-(38312*38311*38366))
F88: (1/38316)*(38365-(38312*38311*38366))
G88: (1/38316)*(38365-(38312*38311*38366))
H88: (1/38316)*(38365-(38312*38311*38366))
A90: CW103 -P2
A91: CW103 1-
A91: 1-
A92: CW103 "P21
B92: +B12*B11*B80
B94: +SB327
C94: +SC327
D94: +SD327
E94: +SE327
F94: +SF327
G94: +SG327
H94: +SH327
B95: 1-
C95: 1-
D95: 1-
E95: 1-
F95: 1-
G95: 1-
H95: 1-
B96: (1/38316)*(38392*(38393*38394))
C96: (1/38316)*(38392*(38393*38394))
D96: (1/38316)*(38392*(38393*38394))
E96: (1/38316)*(38392*(38393*38394))
F96: (1/38316)*(38392*(38393*38394))
G96: (1/38316)*(38392*(38393*38394))
H96: (1/38316)*(38392*(38393*38394))
A98: CW103 -P3
A99: CW103 1-
B99: 1-
A102: CW103 +SB327
B102: (SB35/SB39)*SA102
A103: CW103 +SC327
B103: (SB35/SB39)*SA103
A104: CW103 +SD327
B104: (SB35/SB39)*SA104
A105: CW103 +SE327
B105: (SB35/SB39)*SA105
A106: CW103 +SF327
B106: (SB35/SB39)*SA106

A107: CW103 +SG327
B107: (SB35/SB39)*SA107
A108: CW103 +SH327
B108: (SB35/SB39)*SA108
A110: CW103 'Logic table
A111: CW103 1-
B111: 1-
B112: +SB327
C112: +SC327
D112: +SD327
E112: +SE327
F112: +SF327
G112: +SG327
H112: +SH327
B113: 1-
C113: 1-
D113: 1-
E113: 1-
F113: 1-
G113: 1-
H113: 1-
A114: CW103 +SB327
B114: 01F((C388-2*3896-2*38102-2)/(3831))>-200,0,1)
C114: 01F((C388-2*3896-2*38102-2)/(3831))>-200,0,1)
D114: 01F((C388-2*3896-2*38102-2)/(3831))>-200,0,1)
E114: 01F((C388-2*3896-2*38102-2)/(3831))>-200,0,1)
F114: 01F((C388-2*3896-2*38102-2)/(3831))>-200,0,1)
G114: 01F((C388-2*3896-2*38102-2)/(3831))>-200,0,1)
H114: 01F((C388-2*3896-2*38102-2)/(3831))>-200,0,1)
A115: CW103 +SC327
B115: 01F((C388-2*3896-2*38103-2)/(3831))>-200,0,1)
C115: 01F((C388-2*3896-2*38103-2)/(3831))>-200,0,1)
D115: 01F((C388-2*3896-2*38103-2)/(3831))>-200,0,1)
E115: 01F((C388-2*3896-2*38103-2)/(3831))>-200,0,1)
F115: 01F((C388-2*3896-2*38103-2)/(3831))>-200,0,1)
G115: 01F((C388-2*3896-2*38103-2)/(3831))>-200,0,1)
H115: 01F((C388-2*3896-2*38103-2)/(3831))>-200,0,1)
A116: CW103 +SD327
B116: 01F((C388-2*3896-2*38104-2)/(3831))>-200,0,1)
C116: 01F((C388-2*3896-2*38104-2)/(3831))>-200,0,1)
D116: 01F((C388-2*3896-2*38104-2)/(3831))>-200,0,1)
E116: 01F((C388-2*3896-2*38104-2)/(3831))>-200,0,1)
F116: 01F((C388-2*3896-2*38104-2)/(3831))>-200,0,1)
G116: 01F((C388-2*3896-2*38104-2)/(3831))>-200,0,1)
H116: 01F((C388-2*3896-2*38104-2)/(3831))>-200,0,1)
A117: CW103 +SE327
B117: 01F((C388-2*3896-2*38105-2)/(3831))>-200,0,1)
C117: 01F((C388-2*3896-2*38105-2)/(3831))>-200,0,1)
D117: 01F((C388-2*3896-2*38105-2)/(3831))>-200,0,1)
E117: 01F((C388-2*3896-2*38105-2)/(3831))>-200,0,1)
F117: 01F((C388-2*3896-2*38105-2)/(3831))>-200,0,1)
G117: 01F((C388-2*3896-2*38105-2)/(3831))>-200,0,1)
H117: 01F((C388-2*3896-2*38105-2)/(3831))>-200,0,1)

```

A118: CW103 +SF527
 B118: QIF((B588-2+8596-2+8106-2)/(8581))>>-200,0,1)
 C118: QIF((C588-2+8596-2+8106-2)/(8581))>>-200,0,1)
 D118: QIF((D588-2+8596-2+8106-2)/(8581))>>-200,0,1)
 E118: QIF((E588-2+8596-2+8106-2)/(8581))>>-200,0,1)
 F118: QIF((F588-2+8596-2+8106-2)/(8581))>>-200,0,1)
 G118: QIF((G588-2+8596-2+8106-2)/(8581))>>-200,0,1)
 H118: QIF((H588-2+8596-2+8106-2)/(8581))>>-200,0,1)
 A119: CW103 +SF527
 B119: QIF((B588-2+8596-2+8107-2)/(8581))>>-200,0,1)
 C119: QIF((C588-2+8596-2+8107-2)/(8581))>>-200,0,1)
 D119: QIF((D588-2+8596-2+8107-2)/(8581))>>-200,0,1)
 E119: QIF((E588-2+8596-2+8107-2)/(8581))>>-200,0,1)
 F119: QIF((F588-2+8596-2+8107-2)/(8581))>>-200,0,1)
 G119: QIF((G588-2+8596-2+8107-2)/(8581))>>-200,0,1)
 H119: QIF((H588-2+8596-2+8107-2)/(8581))>>-200,0,1)
 A120: CW103 +SF527
 B120: QIF((B588-2+8596-2+8108-2)/(8581))>>-200,0,1)
 C120: QIF((C588-2+8596-2+8108-2)/(8581))>>-200,0,1)
 D120: QIF((D588-2+8596-2+8108-2)/(8581))>>-200,0,1)
 E120: QIF((E588-2+8596-2+8108-2)/(8581))>>-200,0,1)
 F120: QIF((F588-2+8596-2+8108-2)/(8581))>>-200,0,1)
 G120: QIF((G588-2+8596-2+8108-2)/(8581))>>-200,0,1)
 H120: QIF((H588-2+8596-2+8108-2)/(8581))>>-200,0,1)
 A123: CW103 'Rho
 B124: -
 B125: +SF527
 C125: +SF527
 D125: +SF527
 E125: +SF527
 F125: +SF527
 G125: +SF527
 H125: +SF527
 B126: -
 C126: -
 D126: -
 E126: -
 F126: -
 G126: -
 H126: -
 A127: CW103 +SF527
 B127: QIF(B114-1,85817*QEXP(-(8588-2+8596-2+8102-2)/(8581)),0)
 C127: QIF(C114-1,85817*QEXP(-(8588-2+8596-2+8102-2)/(8581)),0)
 D127: QIF(D114-1,85817*QEXP(-(8588-2+8596-2+8102-2)/(8581)),0)
 E127: QIF(E114-1,85817*QEXP(-(8588-2+8596-2+8102-2)/(8581)),0)
 F127: QIF(F114-1,85817*QEXP(-(8588-2+8596-2+8102-2)/(8581)),0)
 G127: QIF(G114-1,85817*QEXP(-(8588-2+8596-2+8102-2)/(8581)),0)

D131: QIF(D118-1,SB\$17*QEXP(-(DS88-2+DS96-2+SB106-2)/(SG\$1)),0)
 E131: QIF(E118-1,SB\$17*QEXP(-(ES88-2+ES96-2+SB106-2)/(SG\$1)),0)
 F131: QIF(F118-1,SB\$17*QEXP(-(FS88-2+FS96-2+SB106-2)/(SG\$1)),0)
 G131: QIF(G118-1,SB\$17*QEXP(-(GS88-2+GS96-2+SB106-2)/(SG\$1)),0)
 H131: QIF(H118-1,SB\$17*QEXP(-(HS88-2+HS96-2+SB106-2)/(SG\$1)),0)
 A132: [W10] +SG\$27
 B132: QIF(B119-1,SB\$17*QEXP(-(BS88-2+BS96-2+SB107-2)/(SG\$1)),0)
 C132: QIF(C119-1,SB\$17*QEXP(-(CS88-2+CS96-2+SB107-2)/(SG\$1)),0)
 D132: QIF(D119-1,SB\$17*QEXP(-(DS88-2+DS96-2+SB107-2)/(SG\$1)),0)
 E132: QIF(E119-1,SB\$17*QEXP(-(ES88-2+ES96-2+SB107-2)/(SG\$1)),0)
 F132: QIF(F119-1,SB\$17*QEXP(-(FS88-2+FS96-2+SB107-2)/(SG\$1)),0)
 G132: QIF(G119-1,SB\$17*QEXP(-(GS88-2+GS96-2+SB107-2)/(SG\$1)),0)
 H132: QIF(H119-1,SB\$17*QEXP(-(HS88-2+HS96-2+SB107-2)/(SG\$1)),0)
 A133: [W10] +SH\$27
 B133: QIF(B120-1,SB\$17*QEXP(-(BS88-2+BS96-2+SB108-2)/(SG\$1)),0)
 C133: QIF(C120-1,SB\$17*QEXP(-(CS88-2+CS96-2+SB108-2)/(SG\$1)),0)
 D133: QIF(D120-1,SB\$17*QEXP(-(DS88-2+DS96-2+SB108-2)/(SG\$1)),0)
 E133: QIF(E120-1,SB\$17*QEXP(-(ES88-2+ES96-2+SB108-2)/(SG\$1)),0)
 F133: QIF(F120-1,SB\$17*QEXP(-(FS88-2+FS96-2+SB108-2)/(SG\$1)),0)
 G133: QIF(G120-1,SB\$17*QEXP(-(GS88-2+GS96-2+SB108-2)/(SG\$1)),0)
 H133: QIF(H120-1,SB\$17*QEXP(-(HS88-2+HS96-2+SB108-2)/(SG\$1)),0)
 A134: [W10] ^-
 B134: ^-
 C134: ^-
 D134: ^-
 E134: ^-
 F134: ^-
 G134: ^-
 H134: ^-
 A136: [W10] ^--
 B136: ^-
 A137: [W10] ^-
 B137: ^-
 A139: [W10] ^X(3)

B139: (-2.3664077E-05*02)+04
 A142: [W10] ^P1
 A143: [W10] ^-
 B143: ^-
 A144: [W10] ^P11
 B144: (CB14*88)+(B13*89)+B139
 A145: [W10] ^P1(tot)
 B145: +SG\$27
 C145: +SC\$27
 D145: +SD\$27
 E145: +SE\$27
 F145: +SF\$27
 G145: +SG\$27
 H145: +SH\$27
 B146: ^-
 C146: ^-
 D146: ^-
 E146: ^-
 F146: ^-
 G146: ^-
 H146: ^-
 B147: (1/88\$16)*(88\$144-(88\$12*88\$11*88\$145))
 C147: (1/88\$16)*(88\$144-(88\$12*88\$11*88\$145))
 D147: (1/88\$16)*(88\$144-(88\$12*88\$11*88\$145))
 E147: (1/88\$16)*(88\$144-(88\$12*88\$11*88\$145))
 F147: (1/88\$16)*(88\$144-(88\$12*88\$11*88\$145))
 G147: (1/88\$16)*(88\$144-(88\$12*88\$11*88\$145))
 H147: (1/88\$16)*(88\$144-(88\$12*88\$11*88\$145))
 A149: [W10] ^P2
 B150: ^-
 A151: [W10] ^P21
 B151: +B12*811*8139
 C153: +SC\$27
 D153: +SD\$27
 E153: +SE\$27
 F153: +SF\$27
 G153: +SG\$27
 H153: +SH\$27
 B154: ^-
 C154: ^-
 D154: ^-
 E154: ^-
 F154: ^-
 G154: ^-
 H154: ^-
 B155: (1/88\$16)*(88\$151+(88\$9*88\$153))
 C155: (1/88\$16)*(88\$151+(88\$9*88\$153))
 D155: (1/88\$16)*(88\$151+(88\$9*88\$153))
 E155: (1/88\$16)*(88\$151+(88\$9*88\$153))
 F155: (1/88\$16)*(88\$151+(88\$9*88\$153))
 G155: (1/88\$16)*(88\$151+(88\$9*88\$153))

```

H155: (1/$B$16)*($B$151*($B$9*$H$153))
A157: CW10J 'P3
A158: CW10J '-'
B158: '-'
A161: CW10J +$B$27
B161: ($B$5/$B$9)*$A161
A162: CW10J +$C$27
B162: ($B$5/$B$9)*$A162
A163: CW10J +$D$27
B163: ($B$5/$B$9)*$A163
A164: CW10J +$E$27
B164: ($B$5/$B$9)*$A164
A165: CW10J +$F$27
B165: ($B$5/$B$9)*$A165
A166: CW10J +$G$27
B166: ($B$5/$B$9)*$A166
A167: CW10J +$H$27
B167: ($B$5/$B$9)*$A167
A169: CW10J 'Logic table
A170: CW10J '-'
B170: '-'
B171: +$B$27
C171: +$C$27
D171: +$D$27
E171: +$E$27
F171: +$F$27
G171: +$G$27
H171: +$H$27
B172: '-'
C172: '-'
D172: '-'
E172: '-'
F172: '-'
G172: '-'
H172: '-'
A173: CW10J +$B$27
B173: QIF((($B$147*2+$B$155*2+$B$161*2)/($G$1))>-200,0,1)
C173: QIF((($B$147*2+$B$155*2+$B$162*2)/($G$1))>-200,0,1)
D173: QIF((($B$147*2+$B$155*2+$B$163*2)/($G$1))>-200,0,1)
E173: QIF((($B$147*2+$B$155*2+$B$164*2)/($G$1))>-200,0,1)
F173: QIF((($B$147*2+$B$155*2+$B$165*2)/($G$1))>-200,0,1)
G173: QIF((($B$147*2+$B$155*2+$B$166*2)/($G$1))>-200,0,1)
H173: QIF((($B$147*2+$B$155*2+$B$167*2)/($G$1))>-200,0,1)
A174: CW10J +$C$27
B174: QIF((($B$147*2+$B$155*2+$B$162*2)/($G$1))>-200,0,1)
C174: QIF((($B$147*2+$B$155*2+$B$163*2)/($G$1))>-200,0,1)
D174: QIF((($B$147*2+$B$155*2+$B$164*2)/($G$1))>-200,0,1)
E174: QIF((($B$147*2+$B$155*2+$B$165*2)/($G$1))>-200,0,1)
F174: QIF((($B$147*2+$B$155*2+$B$166*2)/($G$1))>-200,0,1)
G174: QIF((($B$147*2+$B$155*2+$B$167*2)/($G$1))>-200,0,1)
H174: QIF((($B$147*2+$B$155*2+$B$168*2)/($G$1))>-200,0,1)
A175: CW10J +$D$27
B175: QIF((($B$147*2+$B$155*2+$B$163*2)/($G$1))>-200,0,1)

```

```

C175: QIF((($B$147*2+$B$155*2+$B$163*2)/($G$1))>-200,0,1)
D175: QIF((($B$147*2+$B$155*2+$B$164*2)/($G$1))>-200,0,1)
E175: QIF((($B$147*2+$B$155*2+$B$165*2)/($G$1))>-200,0,1)
F175: QIF((($B$147*2+$B$155*2+$B$166*2)/($G$1))>-200,0,1)
G175: QIF((($B$147*2+$B$155*2+$B$167*2)/($G$1))>-200,0,1)
H175: QIF((($B$147*2+$B$155*2+$B$168*2)/($G$1))>-200,0,1)
A176: CW10J +$E$27
B176: QIF((($B$147*2+$B$155*2+$B$164*2)/($G$1))>-200,0,1)
C176: QIF((($B$147*2+$B$155*2+$B$165*2)/($G$1))>-200,0,1)
D176: QIF((($B$147*2+$B$155*2+$B$166*2)/($G$1))>-200,0,1)
E176: QIF((($B$147*2+$B$155*2+$B$167*2)/($G$1))>-200,0,1)
F176: QIF((($B$147*2+$B$155*2+$B$168*2)/($G$1))>-200,0,1)
G176: QIF((($B$147*2+$B$155*2+$B$169*2)/($G$1))>-200,0,1)
H176: QIF((($B$147*2+$B$155*2+$B$170*2)/($G$1))>-200,0,1)
A177: CW10J +$F$27
B177: QIF((($B$147*2+$B$155*2+$B$165*2)/($G$1))>-200,0,1)
C177: QIF((($B$147*2+$B$155*2+$B$166*2)/($G$1))>-200,0,1)
D177: QIF((($B$147*2+$B$155*2+$B$167*2)/($G$1))>-200,0,1)
E177: QIF((($B$147*2+$B$155*2+$B$168*2)/($G$1))>-200,0,1)
F177: QIF((($B$147*2+$B$155*2+$B$169*2)/($G$1))>-200,0,1)
G177: QIF((($B$147*2+$B$155*2+$B$170*2)/($G$1))>-200,0,1)
H177: QIF((($B$147*2+$B$155*2+$B$171*2)/($G$1))>-200,0,1)
A178: CW10J +$G$27
B178: QIF((($B$147*2+$B$155*2+$B$166*2)/($G$1))>-200,0,1)
C178: QIF((($B$147*2+$B$155*2+$B$167*2)/($G$1))>-200,0,1)
D178: QIF((($B$147*2+$B$155*2+$B$168*2)/($G$1))>-200,0,1)
E178: QIF((($B$147*2+$B$155*2+$B$169*2)/($G$1))>-200,0,1)
F178: QIF((($B$147*2+$B$155*2+$B$170*2)/($G$1))>-200,0,1)
G178: QIF((($B$147*2+$B$155*2+$B$171*2)/($G$1))>-200,0,1)
H178: QIF((($B$147*2+$B$155*2+$B$172*2)/($G$1))>-200,0,1)
A179: CW10J +$H$27
B179: QIF((($B$147*2+$B$155*2+$B$167*2)/($G$1))>-200,0,1)
C179: QIF((($B$147*2+$B$155*2+$B$168*2)/($G$1))>-200,0,1)
D179: QIF((($B$147*2+$B$155*2+$B$169*2)/($G$1))>-200,0,1)
E179: QIF((($B$147*2+$B$155*2+$B$170*2)/($G$1))>-200,0,1)
F179: QIF((($B$147*2+$B$155*2+$B$171*2)/($G$1))>-200,0,1)
G179: QIF((($B$147*2+$B$155*2+$B$172*2)/($G$1))>-200,0,1)
H179: QIF((($B$147*2+$B$155*2+$B$173*2)/($G$1))>-200,0,1)
A182: CW10J 'Rho
A183: CW10J '-'
B183: '-'
B184: +$B$27
C184: +$C$27
D184: +$D$27
E184: +$E$27
F184: +$F$27
G184: +$G$27
H184: +$H$27
B185: '-'
C185: '-'
D185: '-'
E185: '-'
F185: '-'

```

G185: \-
 H185: \-
 A186: CW10J +S8S27
 B186:
 QIF(B173-1, S8S17*QEXP(-(B8147*2+S8S155*2+S8161*2)/(S8S1)), 0)
 C186:
 QIF(C173-1, S8S17*QEXP(-(C8147*2+C8155*2+S8161*2)/(S8S1)), 0)
 D186:
 QIF(D173-1, S8S17*QEXP(-(D8147*2+D8155*2+S8161*2)/(S8S1)), 0)
 E186:
 QIF(E173-1, S8S17*QEXP(-(E8147*2+E8155*2+S8161*2)/(S8S1)), 0)
 F186:
 QIF(F173-1, S8S17*QEXP(-(F8147*2+F8155*2+S8161*2)/(S8S1)), 0)
 G186:
 QIF(G173-1, S8S17*QEXP(-(G8147*2+G8155*2+S8161*2)/(S8S1)), 0)
 H186:
 QIF(H173-1, S8S17*QEXP(-(H8147*2+H8155*2+S8161*2)/(S8S1)), 0)
 A187: CW10J +S8S27
 B187:
 QIF(B174-1, S8S17*QEXP(-(B8147*2+B8155*2+S8162*2)/(S8S1)), 0)
 C187:
 QIF(C174-1, S8S17*QEXP(-(C8147*2+C8155*2+S8162*2)/(S8S1)), 0)
 D187:
 QIF(D174-1, S8S17*QEXP(-(D8147*2+D8155*2+S8162*2)/(S8S1)), 0)
 E187:
 QIF(E174-1, S8S17*QEXP(-(E8147*2+E8155*2+S8162*2)/(S8S1)), 0)
 F187:
 QIF(F174-1, S8S17*QEXP(-(F8147*2+F8155*2+S8162*2)/(S8S1)), 0)
 G187:
 QIF(G174-1, S8S17*QEXP(-(G8147*2+G8155*2+S8162*2)/(S8S1)), 0)
 H187:
 QIF(H174-1, S8S17*QEXP(-(H8147*2+H8155*2+S8162*2)/(S8S1)), 0)
 A188: CW10J +S8S27
 B188:
 QIF(B175-1, S8S17*QEXP(-(B8147*2+B8155*2+S8163*2)/(S8S1)), 0)
 C188:
 QIF(C175-1, S8S17*QEXP(-(C8147*2+C8155*2+S8163*2)/(S8S1)), 0)
 D188:
 QIF(D175-1, S8S17*QEXP(-(D8147*2+D8155*2+S8163*2)/(S8S1)), 0)
 E188:
 QIF(E175-1, S8S17*QEXP(-(E8147*2+E8155*2+S8163*2)/(S8S1)), 0)
 F188:
 QIF(F175-1, S8S17*QEXP(-(F8147*2+F8155*2+S8163*2)/(S8S1)), 0)
 G188:
 QIF(G175-1, S8S17*QEXP(-(G8147*2+G8155*2+S8163*2)/(S8S1)), 0)
 H188:
 QIF(H175-1, S8S17*QEXP(-(H8147*2+H8155*2+S8163*2)/(S8S1)), 0)
 A189: CW10J +S8S27
 B189:
 QIF(B176-1, S8S17*QEXP(-(B8147*2+B8155*2+S8164*2)/(S8S1)), 0)
 C189:
 QIF(C176-1, S8S17*QEXP(-(C8147*2+C8155*2+S8164*2)/(S8S1)), 0)
 D189:
 QIF(D176-1, S8S17*QEXP(-(D8147*2+D8155*2+S8164*2)/(S8S1)), 0)
 E189:
 QIF(E176-1, S8S17*QEXP(-(E8147*2+E8155*2+S8164*2)/(S8S1)), 0)
 F189:
 QIF(F176-1, S8S17*QEXP(-(F8147*2+F8155*2+S8164*2)/(S8S1)), 0)
 G189:
 QIF(G176-1, S8S17*QEXP(-(G8147*2+G8155*2+S8164*2)/(S8S1)), 0)
 H189:
 QIF(H176-1, S8S17*QEXP(-(H8147*2+H8155*2+S8164*2)/(S8S1)), 0)
 A190: CW10J +S8S27
 B190:
 QIF(B177-1, S8S17*QEXP(-(B8147*2+B8155*2+S8165*2)/(S8S1)), 0)
 C190:
 QIF(C177-1, S8S17*QEXP(-(C8147*2+C8155*2+S8165*2)/(S8S1)), 0)
 D190:
 QIF(D177-1, S8S17*QEXP(-(D8147*2+D8155*2+S8165*2)/(S8S1)), 0)
 E190:
 QIF(E177-1, S8S17*QEXP(-(E8147*2+E8155*2+S8165*2)/(S8S1)), 0)
 F190:
 QIF(F177-1, S8S17*QEXP(-(F8147*2+F8155*2+S8165*2)/(S8S1)), 0)
 G190:
 QIF(G177-1, S8S17*QEXP(-(G8147*2+G8155*2+S8165*2)/(S8S1)), 0)
 H190:
 QIF(H177-1, S8S17*QEXP(-(H8147*2+H8155*2+S8165*2)/(S8S1)), 0)
 A191: CW10J +S8S27
 B191:
 QIF(B178-1, S8S17*QEXP(-(B8147*2+B8155*2+S8166*2)/(S8S1)), 0)
 C191:
 QIF(C178-1, S8S17*QEXP(-(C8147*2+C8155*2+S8166*2)/(S8S1)), 0)
 D191:
 QIF(D178-1, S8S17*QEXP(-(D8147*2+D8155*2+S8166*2)/(S8S1)), 0)
 E191:
 QIF(E178-1, S8S17*QEXP(-(E8147*2+E8155*2+S8166*2)/(S8S1)), 0)
 F191:
 QIF(F178-1, S8S17*QEXP(-(F8147*2+F8155*2+S8166*2)/(S8S1)), 0)
 G191:
 QIF(G178-1, S8S17*QEXP(-(G8147*2+G8155*2+S8166*2)/(S8S1)), 0)
 H191:
 QIF(H178-1, S8S17*QEXP(-(H8147*2+H8155*2+S8166*2)/(S8S1)), 0)
 A192: CW10J +S8S27
 B192:
 QIF(B179-1, S8S17*QEXP(-(B8147*2+B8155*2+S8167*2)/(S8S1)), 0)
 C192:
 QIF(C179-1, S8S17*QEXP(-(C8147*2+C8155*2+S8167*2)/(S8S1)), 0)
 D192:
 QIF(D179-1, S8S17*QEXP(-(D8147*2+D8155*2+S8167*2)/(S8S1)), 0)
 E192:
 QIF(E179-1, S8S17*QEXP(-(E8147*2+E8155*2+S8167*2)/(S8S1)), 0)
 F192:
 QIF(F179-1, S8S17*QEXP(-(F8147*2+F8155*2+S8167*2)/(S8S1)), 0)
 G192:
 QIF(G179-1, S8S17*QEXP(-(G8147*2+G8155*2+S8167*2)/(S8S1)), 0)
 H192:
 QIF(H179-1, S8S17*QEXP(-(H8147*2+H8155*2+S8167*2)/(S8S1)), 0)

@IF(H175=1,\$B\$17*QEXP(-(H\$147^2+H\$155^2+\$B167^2)/((\$G\$1)),0)

A193: C\$10J \-
 B193: \-
 C193: \-
 D193: \-
 E193: \-
 F193: \-
 G193: \-
 H193: \-
 I193: C\$10J \-
 J193: \-
 K193: \-
 L193: \-
 M193: \-
 N193: \-
 O193: \-
 P193: \-
 Q193: \-
 R193: \-
 S193: \-
 T193: \-
 U193: \-
 V193: \-
 W193: \-
 X193: \-
 Y193: \-
 Z193: \-
 A198: C\$10J *X1(4)
 B198: (O*DE)*G4
 A201: C\$10J *P1
 A202: C\$10J \-
 B202: \-
 A203: C\$10J *P11
 B203: (C\$14*88)+(B13*89)*B198
 A204: C\$10J *P1(tot)
 B204: +\$B\$27
 C204: +\$C\$27
 D204: +\$D\$27
 E204: +\$E\$27
 F204: +\$F\$27
 G204: +\$G\$27
 H204: +\$H\$27
 I204: \-
 J204: \-
 K204: \-
 L204: \-
 M204: \-
 N204: \-
 O204: \-
 P204: \-
 Q204: \-
 R204: \-
 S204: \-
 T204: \-
 U204: \-
 V204: \-
 W204: \-
 X204: \-
 Y204: \-
 Z204: \-
 A208: C\$10J *P2
 B208: \-
 C208: \-
 D208: \-
 E208: \-
 F208: \-
 G208: \-
 H208: \-
 I208: \-
 J208: \-
 K208: \-
 L208: \-
 M208: \-
 N208: \-
 O208: \-
 P208: \-
 Q208: \-
 R208: \-
 S208: \-
 T208: \-
 U208: \-
 V208: \-
 W208: \-
 X208: \-
 Y208: \-
 Z208: \-
 A210: C\$10J *P21
 B210: +B12*B11*B198
 C210: \-
 D210: \-
 E210: \-
 F210: \-
 G210: \-
 H210: \-
 I210: \-
 J210: \-
 K210: \-
 L210: \-
 M210: \-
 N210: \-
 O210: \-
 P210: \-
 Q210: \-
 R210: \-
 S210: \-
 T210: \-
 U210: \-
 V210: \-
 W210: \-
 X210: \-
 Y210: \-
 Z210: \-
 A212: +\$C\$27
 B212: +\$D\$27
 C212: +\$E\$27
 D212: +\$F\$27
 E212: +\$G\$27
 F212: +\$H\$27
 G212: +\$I\$27

H212: +\$H\$27
 B213: \-
 C213: \-
 D213: \-
 E213: \-
 F213: \-
 G213: \-
 H213: \-
 I213: \-
 J213: \-
 K213: \-
 L213: \-
 M213: \-
 N213: \-
 O213: \-
 P213: \-
 Q213: \-
 R213: \-
 S213: \-
 T213: \-
 U213: \-
 V213: \-
 W213: \-
 X213: \-
 Y213: \-
 Z213: \-
 A214: (1/\$B\$16)*(\$B\$210+(\$B\$9*\$B\$212))
 B214: (1/\$B\$16)*(\$B\$210+(\$B\$9*\$B\$212))
 C214: (1/\$B\$16)*(\$B\$210+(\$B\$9*\$B\$212))
 D214: (1/\$B\$16)*(\$B\$210+(\$B\$9*\$B\$212))
 E214: (1/\$B\$16)*(\$B\$210+(\$B\$9*\$B\$212))
 F214: (1/\$B\$16)*(\$B\$210+(\$B\$9*\$B\$212))
 G214: (1/\$B\$16)*(\$B\$210+(\$B\$9*\$B\$212))
 H214: (1/\$B\$16)*(\$B\$210+(\$B\$9*\$B\$212))
 I214: (1/\$B\$16)*(\$B\$210+(\$B\$9*\$B\$212))
 J214: (1/\$B\$16)*(\$B\$210+(\$B\$9*\$B\$212))
 K214: (1/\$B\$16)*(\$B\$210+(\$B\$9*\$B\$212))
 L214: (1/\$B\$16)*(\$B\$210+(\$B\$9*\$B\$212))
 M214: (1/\$B\$16)*(\$B\$210+(\$B\$9*\$B\$212))
 N214: (1/\$B\$16)*(\$B\$210+(\$B\$9*\$B\$212))
 O214: (1/\$B\$16)*(\$B\$210+(\$B\$9*\$B\$212))
 P214: (1/\$B\$16)*(\$B\$210+(\$B\$9*\$B\$212))
 Q214: (1/\$B\$16)*(\$B\$210+(\$B\$9*\$B\$212))
 R214: (1/\$B\$16)*(\$B\$210+(\$B\$9*\$B\$212))
 S214: (1/\$B\$16)*(\$B\$210+(\$B\$9*\$B\$212))
 T214: (1/\$B\$16)*(\$B\$210+(\$B\$9*\$B\$212))
 U214: (1/\$B\$16)*(\$B\$210+(\$B\$9*\$B\$212))
 V214: (1/\$B\$16)*(\$B\$210+(\$B\$9*\$B\$212))
 W214: (1/\$B\$16)*(\$B\$210+(\$B\$9*\$B\$212))
 X214: (1/\$B\$16)*(\$B\$210+(\$B\$9*\$B\$212))
 Y214: (1/\$B\$16)*(\$B\$210+(\$B\$9*\$B\$212))
 Z214: (1/\$B\$16)*(\$B\$210+(\$B\$9*\$B\$212))
 A216: C\$10J *P3
 A217: C\$10J \-
 B217: \-
 A220: C\$10J +\$B\$27
 B220: (\$B\$5/\$B\$9)*\$A220
 A221: C\$10J +\$C\$27
 B221: (\$B\$5/\$B\$9)*\$A221
 A222: C\$10J +\$D\$27
 B222: (\$B\$5/\$B\$9)*\$A222
 A223: C\$10J +\$E\$27
 B223: (\$B\$5/\$B\$9)*\$A223
 A224: C\$10J +\$F\$27
 B224: (\$B\$5/\$B\$9)*\$A224
 A225: C\$10J +\$G\$27
 B225: (\$B\$5/\$B\$9)*\$A225
 A226: C\$10J +\$H\$27
 B226: (\$B\$5/\$B\$9)*\$A226
 A228: C\$10J 'Logic table
 A229: C\$10J \-
 B229: \-
 B230: +\$B\$27
 C230: +\$C\$27
 D230: +\$D\$27
 E230: +\$E\$27
 F230: +\$F\$27
 G230: +\$G\$27
 H230: +\$H\$27
 I230: \-
 J230: \-
 K230: \-
 L230: \-
 M230: \-
 N230: \-
 O230: \-
 P230: \-
 Q230: \-
 R230: \-
 S230: \-
 T230: \-
 U230: \-
 V230: \-
 W230: \-
 X230: \-
 Y230: \-
 Z230: \-
 A232: C\$10J +\$B\$27
 B232: @IF(((B\$206^2+\$B\$214^2+\$B\$220^2)/(\$G\$1)))>=200,0,1)
 C232: @IF(((C\$206^2+\$B\$214^2+\$B\$220^2)/(\$G\$1)))>=200,0,1)
 D232: @IF(((D\$206^2+\$B\$214^2+\$B\$220^2)/(\$G\$1)))>=200,0,1)

E232: QIF((E5206-2+5214-2+5220-2)/(SGS1))>-200,0,1)
 F232: QIF((F5206-2+5214-2+5220-2)/(SGS1))>-200,0,1)
 G232: QIF((G5206-2+5214-2+5220-2)/(SGS1))>-200,0,1)
 H232: QIF((H5206-2+5214-2+5220-2)/(SGS1))>-200,0,1)
 A233: CW10J +SC527
 B233: QIF((B5206-2+5214-2+5221-2)/(SGS1))>-200,0,1)
 C233: QIF((C5206-2+5214-2+5221-2)/(SGS1))>-200,0,1)
 D233: QIF((D5206-2+5214-2+5221-2)/(SGS1))>-200,0,1)
 E233: QIF((E5206-2+5214-2+5221-2)/(SGS1))>-200,0,1)
 F233: QIF((F5206-2+5214-2+5221-2)/(SGS1))>-200,0,1)
 G233: QIF((G5206-2+5214-2+5221-2)/(SGS1))>-200,0,1)
 H233: QIF((H5206-2+5214-2+5221-2)/(SGS1))>-200,0,1)
 A234: CW10J +SD527
 B234: QIF((B5206-2+5214-2+5222-2)/(SGS1))>-200,0,1)
 C234: QIF((C5206-2+5214-2+5222-2)/(SGS1))>-200,0,1)
 D234: QIF((D5206-2+5214-2+5222-2)/(SGS1))>-200,0,1)
 E234: QIF((E5206-2+5214-2+5222-2)/(SGS1))>-200,0,1)
 F234: QIF((F5206-2+5214-2+5222-2)/(SGS1))>-200,0,1)
 G234: QIF((G5206-2+5214-2+5222-2)/(SGS1))>-200,0,1)
 H234: QIF((H5206-2+5214-2+5222-2)/(SGS1))>-200,0,1)
 A235: CW10J +SE527
 B235: QIF((B5206-2+5214-2+5223-2)/(SGS1))>-200,0,1)
 C235: QIF((C5206-2+5214-2+5223-2)/(SGS1))>-200,0,1)
 D235: QIF((D5206-2+5214-2+5223-2)/(SGS1))>-200,0,1)
 E235: QIF((E5206-2+5214-2+5223-2)/(SGS1))>-200,0,1)
 F235: QIF((F5206-2+5214-2+5223-2)/(SGS1))>-200,0,1)
 G235: QIF((G5206-2+5214-2+5223-2)/(SGS1))>-200,0,1)
 H235: QIF((H5206-2+5214-2+5223-2)/(SGS1))>-200,0,1)
 A236: CW10J +SF527
 B236: QIF((B5206-2+5214-2+5224-2)/(SGS1))>-200,0,1)
 C236: QIF((C5206-2+5214-2+5224-2)/(SGS1))>-200,0,1)
 D236: QIF((D5206-2+5214-2+5224-2)/(SGS1))>-200,0,1)
 E236: QIF((E5206-2+5214-2+5224-2)/(SGS1))>-200,0,1)
 F236: QIF((F5206-2+5214-2+5224-2)/(SGS1))>-200,0,1)
 G236: QIF((G5206-2+5214-2+5224-2)/(SGS1))>-200,0,1)
 H236: QIF((H5206-2+5214-2+5224-2)/(SGS1))>-200,0,1)
 A237: CW10J +SG527
 B237: QIF((B5206-2+5214-2+5225-2)/(SGS1))>-200,0,1)
 C237: QIF((C5206-2+5214-2+5225-2)/(SGS1))>-200,0,1)
 D237: QIF((D5206-2+5214-2+5225-2)/(SGS1))>-200,0,1)
 E237: QIF((E5206-2+5214-2+5225-2)/(SGS1))>-200,0,1)
 F237: QIF((F5206-2+5214-2+5225-2)/(SGS1))>-200,0,1)
 G237: QIF((G5206-2+5214-2+5225-2)/(SGS1))>-200,0,1)
 H237: QIF((H5206-2+5214-2+5225-2)/(SGS1))>-200,0,1)
 A238: CW10J +SH527
 B238: QIF((B5206-2+5214-2+5226-2)/(SGS1))>-200,0,1)
 C238: QIF((C5206-2+5214-2+5226-2)/(SGS1))>-200,0,1)
 D238: QIF((D5206-2+5214-2+5226-2)/(SGS1))>-200,0,1)
 E238: QIF((E5206-2+5214-2+5226-2)/(SGS1))>-200,0,1)
 F238: QIF((F5206-2+5214-2+5226-2)/(SGS1))>-200,0,1)
 G238: QIF((G5206-2+5214-2+5226-2)/(SGS1))>-200,0,1)
 H238: QIF((H5206-2+5214-2+5226-2)/(SGS1))>-200,0,1)
 A241: CW10J +Rho

A242: CW10J \-
 B242: \-
 B243: +SB527
 C243: +SC527
 D243: +SD527
 E243: +SE527
 F243: +SF527
 G243: +SG527
 H243: +SH527
 B244: \-
 C244: \-
 D244: \-
 E244: \-
 F244: \-
 G244: \-
 H244: \-
 A245: CW10J +SB527
 B245: QIF(B232-1,SB517*QEXP(-(B5206-2+5214-2+5220-2)/(SGS1)),0)
 C245: QIF(C232-1,SB517*QEXP(-(C5206-2+5214-2+5220-2)/(SGS1)),0)
 D245: QIF(D232-1,SB517*QEXP(-(D5206-2+5214-2+5220-2)/(SGS1)),0)
 E245: QIF(E232-1,SB517*QEXP(-(E5206-2+5214-2+5220-2)/(SGS1)),0)
 F245: QIF(F232-1,SB517*QEXP(-(F5206-2+5214-2+5220-2)/(SGS1)),0)
 G245: QIF(G232-1,SB517*QEXP(-(G5206-2+5214-2+5220-2)/(SGS1)),0)
 H245: QIF(H232-1,SB517*QEXP(-(H5206-2+5214-2+5220-2)/(SGS1)),0)
 A246: CW10J +SC527
 B246: QIF(B233-1,SB517*QEXP(-(B5206-2+5214-2+5221-2)/(SGS1)),0)
 C246: QIF(C233-1,SB517*QEXP(-(C5206-2+5214-2+5221-2)/(SGS1)),0)
 D246: QIF(D233-1,SB517*QEXP(-(D5206-2+5214-2+5221-2)/(SGS1)),0)
 E246: QIF(E233-1,SB517*QEXP(-(E5206-2+5214-2+5221-2)/(SGS1)),0)
 F246: QIF(F233-1,SB517*QEXP(-(F5206-2+5214-2+5221-2)/(SGS1)),0)
 G246: QIF(G233-1,SB517*QEXP(-(G5206-2+5214-2+5221-2)/(SGS1)),0)
 H246: QIF(H233-1,SB517*QEXP(-(H5206-2+5214-2+5221-2)/(SGS1)),0)
 A247: CW10J +SD527
 B247: QIF(B234-1,SB517*QEXP(-(B5206-2+5214-2+5222-2)/(SGS1)),0)
 C247: QIF(C234-1,SB517*QEXP(-(C5206-2+5214-2+5222-2)/(SGS1)),0)
 D247: QIF(D234-1,SB517*QEXP(-(D5206-2+5214-2+5222-2)/(SGS1)),0)


```

F265: (1/$B$16)*($B$262-($B$12*$B$11*$F$263))
G265: (1/$B$16)*($B$262-($B$12*$B$11*$F$263))
H265: (1/$B$16)*($B$262-($B$12*$B$11*$F$263))
A267: CW10J *-P2
A268: CW10J \-
B268: \-
A269: CW10J *-P2
B269: +B12*B11*B257
B271: +$B$27
C271: +$C$27
D271: +$D$27
E271: +$E$27
F271: +$F$27
G271: +$G$27
H271: +$H$27
B272: \-
C272: \-
D272: \-
E272: \-
F272: \-
G272: \-
H272: \-
C273: (1/$B$16)*($B$269+($B$9*$B$271))
D273: (1/$B$16)*($B$269+($B$9*$B$271))
E273: (1/$B$16)*($B$269+($B$9*$B$271))
F273: (1/$B$16)*($B$269+($B$9*$B$271))
G273: (1/$B$16)*($B$269+($B$9*$B$271))
H273: (1/$B$16)*($B$269+($B$9*$B$271))
A275: CW10J *-P3
A276: CW10J \-
B276: \-
B279: CW10J +$B$27
B279: ($B$5/$B$9)*$A279
A280: CW10J +$C$27
B280: ($B$5/$B$9)*$A280
B281: CW10J +$D$27
B281: ($B$5/$B$9)*$A281
A282: CW10J +$E$27
B282: ($B$5/$B$9)*$A282
A283: CW10J +$F$27
B283: ($B$5/$B$9)*$A283
A284: CW10J +$G$27
B284: ($B$5/$B$9)*$A284
A285: CW10J +$H$27
B285: ($B$5/$B$9)*$A285
A287: CW10J 'Logic table
A288: CW10J \-
B288: \-
B289: +$B$27
C289: +$C$27
D289: +$D$27
E289: +$E$27
F289: +$F$27
G289: +$G$27
H289: +$H$27
B290: \-
C290: \-
D290: \-
E290: \-
F290: \-
G290: \-
H290: \-
A291: CW10J +$B$27
B291: QIF((($B$265*2+$B$273*2+$B$279*2)/($B$1))>>-200,0,1)
C291: QIF((($B$265*2+$B$273*2+$B$279*2)/($B$1))>>-200,0,1)
D291: QIF((($B$265*2+$B$273*2+$B$279*2)/($B$1))>>-200,0,1)
E291: QIF((($B$265*2+$B$273*2+$B$279*2)/($B$1))>>-200,0,1)
F291: QIF((($B$265*2+$B$273*2+$B$279*2)/($B$1))>>-200,0,1)
G291: QIF((($B$265*2+$B$273*2+$B$279*2)/($B$1))>>-200,0,1)
H291: QIF((($B$265*2+$B$273*2+$B$279*2)/($B$1))>>-200,0,1)
A292: CW10J +$C$27
B292: QIF((($B$265*2+$B$273*2+$B$280*2)/($B$1))>>-200,0,1)
C292: QIF((($B$265*2+$B$273*2+$B$280*2)/($B$1))>>-200,0,1)
D292: QIF((($B$265*2+$B$273*2+$B$280*2)/($B$1))>>-200,0,1)
E292: QIF((($B$265*2+$B$273*2+$B$280*2)/($B$1))>>-200,0,1)
F292: QIF((($B$265*2+$B$273*2+$B$280*2)/($B$1))>>-200,0,1)
G292: QIF((($B$265*2+$B$273*2+$B$280*2)/($B$1))>>-200,0,1)
H292: QIF((($B$265*2+$B$273*2+$B$280*2)/($B$1))>>-200,0,1)
A293: CW10J +$D$27
B293: QIF((($B$265*2+$B$273*2+$B$281*2)/($B$1))>>-200,0,1)
C293: QIF((($B$265*2+$B$273*2+$B$281*2)/($B$1))>>-200,0,1)
D293: QIF((($B$265*2+$B$273*2+$B$281*2)/($B$1))>>-200,0,1)
E293: QIF((($B$265*2+$B$273*2+$B$281*2)/($B$1))>>-200,0,1)
F293: QIF((($B$265*2+$B$273*2+$B$281*2)/($B$1))>>-200,0,1)
G293: QIF((($B$265*2+$B$273*2+$B$281*2)/($B$1))>>-200,0,1)
H293: QIF((($B$265*2+$B$273*2+$B$281*2)/($B$1))>>-200,0,1)
A294: CW10J +$E$27
B294: QIF((($B$265*2+$B$273*2+$B$282*2)/($B$1))>>-200,0,1)
C294: QIF((($B$265*2+$B$273*2+$B$282*2)/($B$1))>>-200,0,1)
D294: QIF((($B$265*2+$B$273*2+$B$282*2)/($B$1))>>-200,0,1)
E294: QIF((($B$265*2+$B$273*2+$B$282*2)/($B$1))>>-200,0,1)
F294: QIF((($B$265*2+$B$273*2+$B$282*2)/($B$1))>>-200,0,1)
G294: QIF((($B$265*2+$B$273*2+$B$282*2)/($B$1))>>-200,0,1)
H294: QIF((($B$265*2+$B$273*2+$B$282*2)/($B$1))>>-200,0,1)
A295: CW10J +$F$27
B295: QIF((($B$265*2+$B$273*2+$B$283*2)/($B$1))>>-200,0,1)
C295: QIF((($B$265*2+$B$273*2+$B$283*2)/($B$1))>>-200,0,1)
D295: QIF((($B$265*2+$B$273*2+$B$283*2)/($B$1))>>-200,0,1)
E295: QIF((($B$265*2+$B$273*2+$B$283*2)/($B$1))>>-200,0,1)
F295: QIF((($B$265*2+$B$273*2+$B$283*2)/($B$1))>>-200,0,1)
G295: QIF((($B$265*2+$B$273*2+$B$283*2)/($B$1))>>-200,0,1)
H295: QIF((($B$265*2+$B$273*2+$B$283*2)/($B$1))>>-200,0,1)
A296: CW10J +$G$27
B296: QIF((($B$265*2+$B$273*2+$B$284*2)/($B$1))>>-200,0,1)
C296: QIF((($B$265*2+$B$273*2+$B$284*2)/($B$1))>>-200,0,1)

```



```

A341: [w10] +$E$27
A341: ($B$5/$B$9)*A341
A342: [w10] +$F$27
A342: ($B$5/$B$9)*A342
A343: [w10] +$G$27
A343: ($B$5/$B$9)*A343
A344: [w10] +$H$27
A344: ($B$5/$B$9)*A344
A345: [w10] 'Logic table
A347: [w10] '-'
A347: '-'
A348: +$E$27
A348: +$E$27
A349: +$F$27
A349: +$F$27
A350: +$G$27
A350: +$G$27
A351: +$H$27
A351: +$H$27
A352: [w10] +$E$27
A352: ($B$5/$B$9)*A352
A353: [w10] +$F$27
A353: ($B$5/$B$9)*A353
A354: [w10] +$G$27
A354: ($B$5/$B$9)*A354
A355: [w10] +$H$27
A355: ($B$5/$B$9)*A355

```

A350: [w10] +\$E\$27

```

E353: 01F((($E$24*2+$E$32*2+$E$34*2)/($G$1))>-200,0,1)
F353: 01F((($E$24*2+$E$32*2+$E$34*2)/($G$1))>-200,0,1)
G353: 01F((($E$24*2+$E$32*2+$E$34*2)/($G$1))>-200,0,1)
H353: 01F((($E$24*2+$E$32*2+$E$34*2)/($G$1))>-200,0,1)
A354: [w10] +$F$27
A354: 01F((($E$24*2+$E$32*2+$E$34*2)/($G$1))>-200,0,1)
C354: 01F((($E$24*2+$E$32*2+$E$34*2)/($G$1))>-200,0,1)
D354: 01F((($E$24*2+$E$32*2+$E$34*2)/($G$1))>-200,0,1)
E354: 01F((($E$24*2+$E$32*2+$E$34*2)/($G$1))>-200,0,1)
F354: 01F((($E$24*2+$E$32*2+$E$34*2)/($G$1))>-200,0,1)
G354: 01F((($E$24*2+$E$32*2+$E$34*2)/($G$1))>-200,0,1)
H354: 01F((($E$24*2+$E$32*2+$E$34*2)/($G$1))>-200,0,1)
A355: [w10] +$G$27
A355: 01F((($E$24*2+$E$32*2+$E$34*2)/($G$1))>-200,0,1)
C355: 01F((($E$24*2+$E$32*2+$E$34*2)/($G$1))>-200,0,1)
D355: 01F((($E$24*2+$E$32*2+$E$34*2)/($G$1))>-200,0,1)
E355: 01F((($E$24*2+$E$32*2+$E$34*2)/($G$1))>-200,0,1)
F355: 01F((($E$24*2+$E$32*2+$E$34*2)/($G$1))>-200,0,1)
G355: 01F((($E$24*2+$E$32*2+$E$34*2)/($G$1))>-200,0,1)
H355: 01F((($E$24*2+$E$32*2+$E$34*2)/($G$1))>-200,0,1)
A356: [w10] +$H$27
A356: 01F((($E$24*2+$E$32*2+$E$34*2)/($G$1))>-200,0,1)
C356: 01F((($E$24*2+$E$32*2+$E$34*2)/($G$1))>-200,0,1)
D356: 01F((($E$24*2+$E$32*2+$E$34*2)/($G$1))>-200,0,1)
E356: 01F((($E$24*2+$E$32*2+$E$34*2)/($G$1))>-200,0,1)
F356: 01F((($E$24*2+$E$32*2+$E$34*2)/($G$1))>-200,0,1)
G356: 01F((($E$24*2+$E$32*2+$E$34*2)/($G$1))>-200,0,1)
H356: 01F((($E$24*2+$E$32*2+$E$34*2)/($G$1))>-200,0,1)
A359: [w10] 'Rho
A359: [w10] '-'
A360: [w10] '-'
A360: [w10] '-'
B361: +$E$27
B361: +$E$27
C361: +$F$27
C361: +$F$27
D361: +$G$27
D361: +$G$27
E361: +$H$27
E361: +$H$27
F361: '-'
F361: '-'
G361: '-'
G361: '-'
H361: '-'
H361: '-'
A362: [w10] +$E$27
A362: ($B$5/$B$9)*A362
A363: [w10] +$F$27
A363: ($B$5/$B$9)*A363
A364: [w10] +$G$27
A364: ($B$5/$B$9)*A364
A365: [w10] +$H$27
A365: ($B$5/$B$9)*A365

```

Q1F(E350-1, \$B\$17*QEXP(-(E\$324*2+E\$332*2+8\$338*2)/(G\$1)), 0)
 F363:
 Q1F(E350-1, \$B\$17*QEXP(-(F\$324*2+F\$332*2+8\$338*2)/(G\$1)), 0)
 G363:
 Q1F(E350-1, \$B\$17*QEXP(-(G\$324*2+G\$332*2+8\$338*2)/(G\$1)), 0)
 H363:
 Q1F(E350-1, \$B\$17*QEXP(-(H\$324*2+H\$332*2+8\$338*2)/(G\$1)), 0)
 A364: [W10] *\$G\$27
 B364:
 Q1F(E351-1, \$B\$17*QEXP(-(B\$324*2+B\$332*2+8\$339*2)/(G\$1)), 0)
 C364:
 Q1F(E351-1, \$B\$17*QEXP(-(C\$324*2+C\$332*2+8\$339*2)/(G\$1)), 0)
 D364:
 Q1F(E351-1, \$B\$17*QEXP(-(D\$324*2+D\$332*2+8\$339*2)/(G\$1)), 0)
 E364:
 Q1F(E351-1, \$B\$17*QEXP(-(E\$324*2+E\$332*2+8\$339*2)/(G\$1)), 0)
 F364:
 Q1F(F351-1, \$B\$17*QEXP(-(F\$324*2+F\$332*2+8\$339*2)/(G\$1)), 0)
 G364:
 Q1F(G351-1, \$B\$17*QEXP(-(G\$324*2+G\$332*2+8\$339*2)/(G\$1)), 0)
 H364:
 Q1F(H351-1, \$B\$17*QEXP(-(H\$324*2+H\$332*2+8\$339*2)/(G\$1)), 0)
 A365: [W10] *\$G\$27
 B365:
 Q1F(E352-1, \$B\$17*QEXP(-(B\$324*2+B\$332*2+8\$340*2)/(G\$1)), 0)
 C365:
 Q1F(E352-1, \$B\$17*QEXP(-(C\$324*2+C\$332*2+8\$340*2)/(G\$1)), 0)
 D365:
 Q1F(D352-1, \$B\$17*QEXP(-(D\$324*2+D\$332*2+8\$340*2)/(G\$1)), 0)
 E365:
 Q1F(E352-1, \$B\$17*QEXP(-(E\$324*2+E\$332*2+8\$340*2)/(G\$1)), 0)
 F365:
 Q1F(F352-1, \$B\$17*QEXP(-(F\$324*2+F\$332*2+8\$340*2)/(G\$1)), 0)
 G365:
 Q1F(G352-1, \$B\$17*QEXP(-(G\$324*2+G\$332*2+8\$340*2)/(G\$1)), 0)
 H365:
 Q1F(H352-1, \$B\$17*QEXP(-(H\$324*2+H\$332*2+8\$340*2)/(G\$1)), 0)
 A366: [W10] *\$G\$27
 B366:
 Q1F(E353-1, \$B\$17*QEXP(-(B\$324*2+B\$332*2+8\$341*2)/(G\$1)), 0)
 C366:
 Q1F(E353-1, \$B\$17*QEXP(-(C\$324*2+C\$332*2+8\$341*2)/(G\$1)), 0)
 D366:
 Q1F(D353-1, \$B\$17*QEXP(-(D\$324*2+D\$332*2+8\$341*2)/(G\$1)), 0)
 E366:
 Q1F(E353-1, \$B\$17*QEXP(-(E\$324*2+E\$332*2+8\$341*2)/(G\$1)), 0)
 F366:
 Q1F(F353-1, \$B\$17*QEXP(-(F\$324*2+F\$332*2+8\$341*2)/(G\$1)), 0)
 G366:
 Q1F(G353-1, \$B\$17*QEXP(-(G\$324*2+G\$332*2+8\$341*2)/(G\$1)), 0)
 H366:
 Q1F(H353-1, \$B\$17*QEXP(-(H\$324*2+H\$332*2+8\$341*2)/(G\$1)), 0)
 A367: [W10] *\$G\$27

B367:
 Q1F(E354-1, \$B\$17*QEXP(-(B\$324*2+B\$332*2+8\$342*2)/(G\$1)), 0)
 C367:
 Q1F(C354-1, \$B\$17*QEXP(-(C\$324*2+C\$332*2+8\$342*2)/(G\$1)), 0)
 D367:
 Q1F(D354-1, \$B\$17*QEXP(-(D\$324*2+D\$332*2+8\$342*2)/(G\$1)), 0)
 E367:
 Q1F(E354-1, \$B\$17*QEXP(-(E\$324*2+E\$332*2+8\$342*2)/(G\$1)), 0)
 F367:
 Q1F(F354-1, \$B\$17*QEXP(-(F\$324*2+F\$332*2+8\$342*2)/(G\$1)), 0)
 G367:
 Q1F(G354-1, \$B\$17*QEXP(-(G\$324*2+G\$332*2+8\$342*2)/(G\$1)), 0)
 H367:
 Q1F(H354-1, \$B\$17*QEXP(-(H\$324*2+H\$332*2+8\$342*2)/(G\$1)), 0)
 A368: [W10] *\$G\$27
 B368:
 Q1F(E355-1, \$B\$17*QEXP(-(B\$324*2+B\$332*2+8\$343*2)/(G\$1)), 0)
 C368:
 Q1F(C355-1, \$B\$17*QEXP(-(C\$324*2+C\$332*2+8\$343*2)/(G\$1)), 0)
 D368:
 Q1F(D355-1, \$B\$17*QEXP(-(D\$324*2+D\$332*2+8\$343*2)/(G\$1)), 0)
 E368:
 Q1F(E355-1, \$B\$17*QEXP(-(E\$324*2+E\$332*2+8\$343*2)/(G\$1)), 0)
 F368:
 Q1F(F355-1, \$B\$17*QEXP(-(F\$324*2+F\$332*2+8\$343*2)/(G\$1)), 0)
 G368:
 Q1F(G355-1, \$B\$17*QEXP(-(G\$324*2+G\$332*2+8\$343*2)/(G\$1)), 0)
 H368:
 Q1F(H355-1, \$B\$17*QEXP(-(H\$324*2+H\$332*2+8\$343*2)/(G\$1)), 0)
 A369: [W10] *\$G\$27
 B369:
 Q1F(E356-1, \$B\$17*QEXP(-(B\$324*2+B\$332*2+8\$344*2)/(G\$1)), 0)
 C369:
 Q1F(C356-1, \$B\$17*QEXP(-(C\$324*2+C\$332*2+8\$344*2)/(G\$1)), 0)
 D369:
 Q1F(D356-1, \$B\$17*QEXP(-(D\$324*2+D\$332*2+8\$344*2)/(G\$1)), 0)
 E369:
 Q1F(E356-1, \$B\$17*QEXP(-(E\$324*2+E\$332*2+8\$344*2)/(G\$1)), 0)
 F369:
 Q1F(F356-1, \$B\$17*QEXP(-(F\$324*2+F\$332*2+8\$344*2)/(G\$1)), 0)
 G369:
 Q1F(G356-1, \$B\$17*QEXP(-(G\$324*2+G\$332*2+8\$344*2)/(G\$1)), 0)
 H369:
 Q1F(H356-1, \$B\$17*QEXP(-(H\$324*2+H\$332*2+8\$344*2)/(G\$1)), 0)
 A370: [W10] *
 B370: *
 C370: *
 D370: *
 E370: *
 F370: *
 G370: *
 H370: *
 A372: [W10] *--

```

B372: \-
A373: [W10] \-
B373: \-
A375: [W10] *X1(7)
B375: (7.099231E-05*02)*G4
A378: [W10] *P1
A379: [W10] \-
B379: \-
A380: [W10] *P11
B380: ((B14*88)+(B13*89))*B375
A381: [W10] *P1(tot)
B381: +S827
C381: +SC27
D381: +SD27
E381: +SE27
F381: +SF27
G381: +SG27
H381: +SH27
B382: \-
C382: \-
D382: \-
E382: \-
F382: \-
G382: \-
H382: \-
B383: (1/$8$16)*($8$380-($8$12*$8$11*$8$381))
C383: (1/$8$16)*($8$380-($8$12*$8$11*$8$381))
D383: (1/$8$16)*($8$380-($8$12*$8$11*$8$381))
E383: (1/$8$16)*($8$380-($8$12*$8$11*$8$381))
F383: (1/$8$16)*($8$380-($8$12*$8$11*$8$381))
G383: (1/$8$16)*($8$380-($8$12*$8$11*$8$381))
H383: (1/$8$16)*($8$380-($8$12*$8$11*$8$381))
A385: [W10] *P2
A385: [W10] \-
B386: \-
A387: [W10] *P21
B387: +B12*811*8375
A389: [W10] *P2(tot)
B389: +S827
C389: +SC27
D389: +SD27
E389: +SE27
F389: +SF27
G389: +SG27
H389: +SH27
B390: \-
C390: \-
D390: \-
E390: \-
F390: \-
G390: \-
H390: \-
B391: (1/$8$16)*($8$387*($8$9*8$388))

C391: (1/$8$16)*($8$387*($8$9*8$388))
D391: (1/$8$16)*($8$387*($8$9*8$388))
E391: (1/$8$16)*($8$387*($8$9*8$388))
F391: (1/$8$16)*($8$387*($8$9*8$388))
G391: (1/$8$16)*($8$387*($8$9*8$388))
H391: (1/$8$16)*($8$387*($8$9*8$388))
A393: [W10] *P3
A393: [W10] \-
B393: \-
A397: [W10] +S827
B397: ($8$5/$8$9)*SA397
A398: [W10] +SC27
B398: ($8$5/$8$9)*SA398
A399: [W10] +SD27
B399: ($8$5/$8$9)*SA399
A400: [W10] +SE27
B400: ($8$5/$8$9)*SA400
A401: [W10] +SF27
B401: ($8$5/$8$9)*SA401
A402: [W10] +SG27
B402: ($8$5/$8$9)*SA402
A403: [W10] +SH27
B403: ($8$5/$8$9)*SA403
A405: [W10] *Logic table
A406: [W10] \-
B406: \-
B407: +S827
C407: +SC27
D407: +SD27
E407: +SE27
F407: +SF27
G407: +SG27
H407: +SH27
B408: \-
C408: \-
D408: \-
E408: \-
F408: \-
G408: \-
H408: \-
A409: [W10] +S827
B409: EIF((($8$383-2+$8$391-2+$8$397-2)/($8$11))>-200,0,1)
C409: EIF((($8$383-2+$8$391-2+$8$397-2)/($8$11))>-200,0,1)
D409: EIF((($8$383-2+$8$391-2+$8$397-2)/($8$11))>-200,0,1)
E409: EIF((($8$383-2+$8$391-2+$8$397-2)/($8$11))>-200,0,1)
F409: EIF((($8$383-2+$8$391-2+$8$397-2)/($8$11))>-200,0,1)
G409: EIF((($8$383-2+$8$391-2+$8$397-2)/($8$11))>-200,0,1)
H409: EIF((($8$383-2+$8$391-2+$8$397-2)/($8$11))>-200,0,1)
A410: [W10] +SC27
B410: EIF((($8$383-2+$8$391-2+$8$397-2)/($8$11))>-200,0,1)
C410: EIF((($8$383-2+$8$391-2+$8$397-2)/($8$11))>-200,0,1)
D410: EIF((($8$383-2+$8$391-2+$8$397-2)/($8$11))>-200,0,1)
E410: EIF((($8$383-2+$8$391-2+$8$397-2)/($8$11))>-200,0,1)

```

F410: QIF((C3383'2+FS391'2+SB398'2)/(SGS1))>-200,0,1)
 G410: QIF((G3383'2+GS391'2+SB398'2)/(SGS1))>-200,0,1)
 H410: QIF((H3383'2+HS391'2+SB398'2)/(SGS1))>-200,0,1)
 A410: CW103 +S0527
 B411: QIF((B3383'2+BS391'2+SB399'2)/(SGS1))>-200,0,1)
 C411: QIF((C3383'2+CS391'2+SB399'2)/(SGS1))>-200,0,1)
 D411: QIF((D3383'2+DS391'2+SB399'2)/(SGS1))>-200,0,1)
 E411: QIF((E3383'2+ES391'2+SB399'2)/(SGS1))>-200,0,1)
 F411: QIF((F3383'2+FS391'2+SB399'2)/(SGS1))>-200,0,1)
 G411: QIF((G3383'2+GS391'2+SB399'2)/(SGS1))>-200,0,1)
 H411: QIF((H3383'2+HS391'2+SB399'2)/(SGS1))>-200,0,1)
 A412: CW103 +S0527
 B412: QIF((B3383'2+BS391'2+SB400'2)/(SGS1))>-200,0,1)
 C412: QIF((C3383'2+CS391'2+SB400'2)/(SGS1))>-200,0,1)
 D412: QIF((D3383'2+DS391'2+SB400'2)/(SGS1))>-200,0,1)
 E412: QIF((E3383'2+ES391'2+SB400'2)/(SGS1))>-200,0,1)
 F412: QIF((F3383'2+FS391'2+SB400'2)/(SGS1))>-200,0,1)
 G412: QIF((G3383'2+GS391'2+SB400'2)/(SGS1))>-200,0,1)
 H412: QIF((H3383'2+HS391'2+SB400'2)/(SGS1))>-200,0,1)
 A413: CW103 +S0527
 B413: QIF((B3383'2+BS391'2+SB401'2)/(SGS1))>-200,0,1)
 C413: QIF((C3383'2+CS391'2+SB401'2)/(SGS1))>-200,0,1)
 D413: QIF((D3383'2+DS391'2+SB401'2)/(SGS1))>-200,0,1)
 E413: QIF((E3383'2+ES391'2+SB401'2)/(SGS1))>-200,0,1)
 F413: QIF((F3383'2+FS391'2+SB401'2)/(SGS1))>-200,0,1)
 G413: QIF((G3383'2+GS391'2+SB401'2)/(SGS1))>-200,0,1)
 H413: QIF((H3383'2+HS391'2+SB401'2)/(SGS1))>-200,0,1)
 A414: CW103 +S0527
 B414: QIF((B3383'2+BS391'2+SB402'2)/(SGS1))>-200,0,1)
 C414: QIF((C3383'2+CS391'2+SB402'2)/(SGS1))>-200,0,1)
 D414: QIF((D3383'2+DS391'2+SB402'2)/(SGS1))>-200,0,1)
 E414: QIF((E3383'2+ES391'2+SB402'2)/(SGS1))>-200,0,1)
 F414: QIF((F3383'2+FS391'2+SB402'2)/(SGS1))>-200,0,1)
 G414: QIF((G3383'2+GS391'2+SB402'2)/(SGS1))>-200,0,1)
 H414: QIF((H3383'2+HS391'2+SB402'2)/(SGS1))>-200,0,1)
 A415: CW103 +S0527
 B415: QIF((B3383'2+BS391'2+SB403'2)/(SGS1))>-200,0,1)
 C415: QIF((C3383'2+CS391'2+SB403'2)/(SGS1))>-200,0,1)
 D415: QIF((D3383'2+DS391'2+SB403'2)/(SGS1))>-200,0,1)
 E415: QIF((E3383'2+ES391'2+SB403'2)/(SGS1))>-200,0,1)
 F415: QIF((F3383'2+FS391'2+SB403'2)/(SGS1))>-200,0,1)
 G415: QIF((G3383'2+GS391'2+SB403'2)/(SGS1))>-200,0,1)
 H415: QIF((H3383'2+HS391'2+SB403'2)/(SGS1))>-200,0,1)
 A418: CW103 'rho
 A419: CW103 \-
 B419: \-
 C420: +S0527
 D420: +S0527
 F420: +S0527
 G420: +S0527
 H420: +S0527

B421: \-
 C421: \-
 D421: \-
 E421: \-
 F421: \-
 G421: \-
 H421: \-
 A422: CW103 +S0527
 B422: QIF(B409-1,SB517*QEXP(-(BS383'2+BS391'2+SB397'2)/(SGS1)),0)
 C422: QIF(C409-1,SB517*QEXP(-(CS383'2+CS391'2+SB397'2)/(SGS1)),0)
 D422: QIF(D409-1,SB517*QEXP(-(DS383'2+DS391'2+SB397'2)/(SGS1)),0)
 E422: QIF(E409-1,SB517*QEXP(-(ES383'2+ES391'2+SB397'2)/(SGS1)),0)
 F422: QIF(F409-1,SB517*QEXP(-(FS383'2+FS391'2+SB397'2)/(SGS1)),0)
 G422: QIF(G409-1,SB517*QEXP(-(GS383'2+GS391'2+SB397'2)/(SGS1)),0)
 H422: QIF(H409-1,SB517*QEXP(-(HS383'2+HS391'2+SB397'2)/(SGS1)),0)
 A423: CW103 +S0527
 B423: QIF(B410-1,SB517*QEXP(-(BS383'2+BS391'2+SB398'2)/(SGS1)),0)
 C423: QIF(C410-1,SB517*QEXP(-(CS383'2+CS391'2+SB398'2)/(SGS1)),0)
 D423: QIF(D410-1,SB517*QEXP(-(DS383'2+DS391'2+SB398'2)/(SGS1)),0)
 E423: QIF(E410-1,SB517*QEXP(-(ES383'2+ES391'2+SB398'2)/(SGS1)),0)
 F423: QIF(F410-1,SB517*QEXP(-(FS383'2+FS391'2+SB398'2)/(SGS1)),0)
 G423: QIF(G410-1,SB517*QEXP(-(GS383'2+GS391'2+SB398'2)/(SGS1)),0)
 H423: QIF(H410-1,SB517*QEXP(-(HS383'2+HS391'2+SB398'2)/(SGS1)),0)
 A424: CW103 +S0527
 B424: QIF(B411-1,SB517*QEXP(-(BS383'2+BS391'2+SB399'2)/(SGS1)),0)
 C424: QIF(C411-1,SB517*QEXP(-(CS383'2+CS391'2+SB399'2)/(SGS1)),0)
 D424: QIF(D411-1,SB517*QEXP(-(DS383'2+DS391'2+SB399'2)/(SGS1)),0)
 E424: QIF(E411-1,SB517*QEXP(-(ES383'2+ES391'2+SB399'2)/(SGS1)),0)
 F424: QIF(F411-1,SB517*QEXP(-(FS383'2+FS391'2+SB399'2)/(SGS1)),0)
 G424: QIF(G411-1,SB517*QEXP(-(GS383'2+GS391'2+SB399'2)/(SGS1)),0)
 H424: QIF(H411-1,SB517*QEXP(-(HS383'2+HS391'2+SB399'2)/(SGS1)),0)
 A425: CW103 +S0527


```

F428:
G428:
G429:
G430:
G431:
G432:
G433:
G434:
G435:
G436:
G437:
G438:
G439:
G440:
G441:
G442:
G443:
G444:
G445:
G446:
G447:
G448:
G449:
G450:
G451:
G452:
G453:
G454:
G455:
G456:
G457:
G458:
G459:
G460:
G461:
G462:
G463:
G464:
G465:
G466:
G467:
G468:
G469:
G470:
G471:
G472:
G473:
G474:
G475:
G476:
G477:
G478:
G479:
G480:
G481:
G482:
G483:
G484:
G485:
G486:
G487:
G488:
G489:
G490:
G491:
G492:
G493:
G494:
G495:
G496:
G497:
G498:
G499:
G500:
G501:
G502:
G503:
G504:
G505:
G506:
G507:
G508:
G509:
G510:
G511:
G512:
G513:
G514:
G515:
G516:
G517:
G518:
G519:
G520:
G521:
G522:
G523:
G524:
G525:
G526:
G527:
G528:
G529:
G530:
G531:
G532:
G533:
G534:
G535:
G536:
G537:
G538:
G539:
G540:
G541:
G542:
G543:
G544:
G545:
G546:
G547:
G548:
G549:
G550:
G551:
G552:
G553:
G554:
G555:
G556:
G557:
G558:
G559:
G560:
G561:
G562:
G563:
G564:
G565:
G566:
G567:
G568:
G569:
G570:
G571:
G572:
G573:
G574:
G575:
G576:
G577:
G578:
G579:
G580:
G581:
G582:
G583:
G584:
G585:
G586:
G587:
G588:
G589:
G590:
G591:
G592:
G593:
G594:
G595:
G596:
G597:
G598:
G599:
G600:
G601:
G602:
G603:
G604:
G605:
G606:
G607:
G608:
G609:
G610:
G611:
G612:
G613:
G614:
G615:
G616:
G617:
G618:
G619:
G620:
G621:
G622:
G623:
G624:
G625:
G626:
G627:
G628:
G629:
G630:
G631:
G632:
G633:
G634:
G635:
G636:
G637:
G638:
G639:
G640:
G641:
G642:
G643:
G644:
G645:
G646:
G647:
G648:
G649:
G650:
G651:
G652:
G653:
G654:
G655:
G656:
G657:
G658:
G659:
G660:
G661:
G662:
G663:
G664:
G665:
G666:
G667:
G668:
G669:
G670:
G671:
G672:
G673:
G674:
G675:
G676:
G677:
G678:
G679:
G680:
G681:
G682:
G683:
G684:
G685:
G686:
G687:
G688:
G689:
G690:
G691:
G692:
G693:
G694:
G695:
G696:
G697:
G698:
G699:
G700:
G701:
G702:
G703:
G704:
G705:
G706:
G707:
G708:
G709:
G710:
G711:
G712:
G713:
G714:
G715:
G716:
G717:
G718:
G719:
G720:
G721:
G722:
G723:
G724:
G725:
G726:
G727:
G728:
G729:
G730:
G731:
G732:
G733:
G734:
G735:
G736:
G737:
G738:
G739:
G740:
G741:
G742:
G743:
G744:
G745:
G746:
G747:
G748:
G749:
G750:
G751:
G752:
G753:
G754:
G755:
G756:
G757:
G758:
G759:
G760:
G761:
G762:
G763:
G764:
G765:
G766:
G767:
G768:
G769:
G770:
G771:
G772:
G773:
G774:
G775:
G776:
G777:
G778:
G779:
G780:
G781:
G782:
G783:
G784:
G785:
G786:
G787:
G788:
G789:
G790:
G791:
G792:
G793:
G794:
G795:
G796:
G797:
G798:
G799:
G800:
G801:
G802:
G803:
G804:
G805:
G806:
G807:
G808:
G809:
G810:
G811:
G812:
G813:
G814:
G815:
G816:
G817:
G818:
G819:
G820:
G821:
G822:
G823:
G824:
G825:
G826:
G827:
G828:
G829:
G830:
G831:
G832:
G833:
G834:
G835:
G836:
G837:
G838:
G839:
G840:
G841:
G842:
G843:
G844:
G845:
G846:
G847:
G848:
G849:
G850:
G851:
G852:
G853:
G854:
G855:
G856:
G857:
G858:
G859:
G860:
G861:
G862:
G863:
G864:
G865:
G866:
G867:
G868:
G869:
G870:
G871:
G872:
G873:
G874:
G875:
G876:
G877:
G878:
G879:
G880:
G881:
G882:
G883:
G884:
G885:
G886:
G887:
G888:
G889:
G890:
G891:
G892:
G893:
G894:
G895:
G896:
G897:
G898:
G899:
G900:
G901:
G902:
G903:
G904:
G905:
G906:
G907:
G908:
G909:
G910:
G911:
G912:
G913:
G914:
G915:
G916:
G917:
G918:
G919:
G920:
G921:
G922:
G923:
G924:
G925:
G926:
G927:
G928:
G929:
G930:
G931:
G932:
G933:
G934:
G935:
G936:
G937:
G938:
G939:
G940:
G941:
G942:
G943:
G944:
G945:
G946:
G947:
G948:
G949:
G950:
G951:
G952:
G953:
G954:
G955:
G956:
G957:
G958:
G959:
G960:
G961:
G962:
G963:
G964:
G965:
G966:
G967:
G968:
G969:
G970:
G971:
G972:
G973:
G974:
G975:
G976:
G977:
G978:
G979:
G980:
G981:
G982:
G983:
G984:
G985:
G986:
G987:
G988:
G989:
G990:
G991:
G992:
G993:
G994:
G995:
G996:
G997:
G998:
G999:

```

C457: QINT((C131/SAS434)*SD53)
 D457: QINT((C131/SAS434)*SD53)
 F457: QINT((C131/SAS434)*SD53)
 G457: QINT((C131/SAS434)*SD53)
 H457: QINT((C131/SAS434)*SD53)
 C458: QINT((C132/SAS434)*SD53)
 D458: QINT((C132/SAS434)*SD53)
 F458: QINT((C132/SAS434)*SD53)
 G458: QINT((C132/SAS434)*SD53)
 H458: QINT((C132/SAS434)*SD53)
 C459: QINT((C133/SAS434)*SD53)
 D459: QINT((C133/SAS434)*SD53)
 F459: QINT((C133/SAS434)*SD53)
 G459: QINT((C133/SAS434)*SD53)
 H459: QINT((C133/SAS434)*SD53)
 A461: CW101 'Part XI(3)
 A462: CW101 '-
 B463: QINT((C186/SAS434)*SD53)
 C463: QINT((C186/SAS434)*SD53)
 D463: QINT((C186/SAS434)*SD53)
 F463: QINT((C186/SAS434)*SD53)
 G463: QINT((C186/SAS434)*SD53)
 H463: QINT((C186/SAS434)*SD53)
 C464: QINT((C187/SAS434)*SD53)
 D464: QINT((C187/SAS434)*SD53)
 F464: QINT((C187/SAS434)*SD53)
 G464: QINT((C187/SAS434)*SD53)
 H464: QINT((C187/SAS434)*SD53)
 C465: QINT((C188/SAS434)*SD53)
 D465: QINT((C188/SAS434)*SD53)
 F465: QINT((C188/SAS434)*SD53)
 G465: QINT((C188/SAS434)*SD53)
 H465: QINT((C188/SAS434)*SD53)
 C466: QINT((C189/SAS434)*SD53)
 D466: QINT((C189/SAS434)*SD53)
 F466: QINT((C189/SAS434)*SD53)
 G466: QINT((C189/SAS434)*SD53)
 H466: QINT((C189/SAS434)*SD53)
 C467: QINT((C190/SAS434)*SD53)
 D467: QINT((C190/SAS434)*SD53)
 F467: QINT((C190/SAS434)*SD53)
 G467: QINT((C190/SAS434)*SD53)
 H467: QINT((C190/SAS434)*SD53)
 A468: QINT((C190/SAS434)*SD53)
 B468: QINT((C190/SAS434)*SD53)
 C468: QINT((C190/SAS434)*SD53)
 D468: QINT((C190/SAS434)*SD53)
 F468: QINT((C190/SAS434)*SD53)
 G468: QINT((C190/SAS434)*SD53)
 H468: QINT((C190/SAS434)*SD53)
 A469: QINT((C190/SAS434)*SD53)
 B469: QINT((C190/SAS434)*SD53)
 C469: QINT((C190/SAS434)*SD53)
 D469: QINT((C190/SAS434)*SD53)
 F469: QINT((C190/SAS434)*SD53)
 G469: QINT((C190/SAS434)*SD53)
 H469: QINT((C190/SAS434)*SD53)
 A470: QINT((C190/SAS434)*SD53)
 B470: QINT((C190/SAS434)*SD53)
 C470: QINT((C190/SAS434)*SD53)
 D470: QINT((C190/SAS434)*SD53)
 F470: QINT((C190/SAS434)*SD53)
 G470: QINT((C190/SAS434)*SD53)
 H470: QINT((C190/SAS434)*SD53)

H446: QINT((H71/SAS434)*SD53)
 B447: QINT((B72/SAS434)*SD53)
 C447: QINT((C72/SAS434)*SD53)
 D447: QINT((D72/SAS434)*SD53)
 F447: QINT((F72/SAS434)*SD53)
 G447: QINT((G72/SAS434)*SD53)
 H447: QINT((H72/SAS434)*SD53)
 B448: QINT((B73/SAS434)*SD53)
 C448: QINT((C73/SAS434)*SD53)
 D448: QINT((D73/SAS434)*SD53)
 F448: QINT((F73/SAS434)*SD53)
 G448: QINT((G73/SAS434)*SD53)
 H448: QINT((H73/SAS434)*SD53)
 B449: QINT((B74/SAS434)*SD53)
 C449: QINT((C74/SAS434)*SD53)
 D449: QINT((D74/SAS434)*SD53)
 F449: QINT((F74/SAS434)*SD53)
 G449: QINT((G74/SAS434)*SD53)
 H449: QINT((H74/SAS434)*SD53)
 A451: CW101 'Part XI(2)
 A452: CW101 '-
 B453: QINT((B127/SAS434)*SD53)
 C453: QINT((C127/SAS434)*SD53)
 D453: QINT((D127/SAS434)*SD53)
 F453: QINT((F127/SAS434)*SD53)
 G453: QINT((G127/SAS434)*SD53)
 H453: QINT((H127/SAS434)*SD53)
 B454: QINT((B128/SAS434)*SD53)
 C454: QINT((C128/SAS434)*SD53)
 D454: QINT((D128/SAS434)*SD53)
 F454: QINT((F128/SAS434)*SD53)
 G454: QINT((G128/SAS434)*SD53)
 H454: QINT((H128/SAS434)*SD53)
 B455: QINT((B129/SAS434)*SD53)
 C455: QINT((C129/SAS434)*SD53)
 D455: QINT((D129/SAS434)*SD53)
 F455: QINT((F129/SAS434)*SD53)
 G455: QINT((G129/SAS434)*SD53)
 H455: QINT((H129/SAS434)*SD53)
 B456: QINT((B130/SAS434)*SD53)
 C456: QINT((C130/SAS434)*SD53)
 D456: QINT((D130/SAS434)*SD53)
 F456: QINT((F130/SAS434)*SD53)
 G456: QINT((G130/SAS434)*SD53)
 H456: QINT((H130/SAS434)*SD53)
 B457: QINT((B131/SAS434)*SD53)

G477: QINT((G249/SAS434)*S053)
 H477: QINT((H249/SAS434)*S053)
 B478: QINT((B250/SAS434)*S053)
 C478: QINT((C250/SAS434)*S053)
 D478: QINT((D250/SAS434)*S053)
 F478: QINT((F250/SAS434)*S053)
 F478: QINT((F250/SAS434)*S053)
 G478: QINT((G250/SAS434)*S053)
 H478: QINT((H250/SAS434)*S053)
 B479: QINT((B251/SAS434)*S053)
 C479: QINT((C251/SAS434)*S053)
 D479: QINT((D251/SAS434)*S053)
 F479: QINT((F251/SAS434)*S053)
 F479: QINT((F251/SAS434)*S053)
 G479: QINT((G251/SAS434)*S053)
 H479: QINT((H251/SAS434)*S053)
 A481: CW103 'Part X1(S)
 A482: CW103 '-
 B483: QINT((B304/SAS434)*S053)
 C483: QINT((C304/SAS434)*S053)
 D483: QINT((D304/SAS434)*S053)
 F483: QINT((F304/SAS434)*S053)
 F483: QINT((F304/SAS434)*S053)
 H483: QINT((H304/SAS434)*S053)
 H483: QINT((H304/SAS434)*S053)
 B484: QINT((B305/SAS434)*S053)
 C484: QINT((C305/SAS434)*S053)
 D484: QINT((D305/SAS434)*S053)
 F484: QINT((F305/SAS434)*S053)
 F484: QINT((F305/SAS434)*S053)
 G484: QINT((G305/SAS434)*S053)
 H484: QINT((H305/SAS434)*S053)
 B485: QINT((B306/SAS434)*S053)
 C485: QINT((C306/SAS434)*S053)
 D485: QINT((D306/SAS434)*S053)
 F485: QINT((F306/SAS434)*S053)
 F485: QINT((F306/SAS434)*S053)
 G485: QINT((G306/SAS434)*S053)
 H485: QINT((H306/SAS434)*S053)
 B486: QINT((B307/SAS434)*S053)
 C486: QINT((C307/SAS434)*S053)
 D486: QINT((D307/SAS434)*S053)
 F486: QINT((F307/SAS434)*S053)
 F486: QINT((F307/SAS434)*S053)
 G486: QINT((G307/SAS434)*S053)
 H486: QINT((H307/SAS434)*S053)
 B487: QINT((B308/SAS434)*S053)
 C487: QINT((C308/SAS434)*S053)
 D487: QINT((D308/SAS434)*S053)
 F487: QINT((F308/SAS434)*S053)
 F487: QINT((F308/SAS434)*S053)
 G487: QINT((G308/SAS434)*S053)
 H487: QINT((H308/SAS434)*S053)

E467: QINT((E190/SAS434)*S053)
 F467: QINT((F190/SAS434)*S053)
 G467: QINT((G190/SAS434)*S053)
 H467: QINT((H190/SAS434)*S053)
 B468: QINT((B191/SAS434)*S053)
 C468: QINT((C191/SAS434)*S053)
 D468: QINT((D191/SAS434)*S053)
 F468: QINT((F191/SAS434)*S053)
 F468: QINT((F191/SAS434)*S053)
 G468: QINT((G191/SAS434)*S053)
 H468: QINT((H191/SAS434)*S053)
 B469: QINT((B192/SAS434)*S053)
 C469: QINT((C192/SAS434)*S053)
 D469: QINT((D192/SAS434)*S053)
 F469: QINT((F192/SAS434)*S053)
 F469: QINT((F192/SAS434)*S053)
 G469: QINT((G192/SAS434)*S053)
 H469: QINT((H192/SAS434)*S053)
 A471: CW103 'Part X1(S)
 A472: CW103 '-
 B473: QINT((B245/SAS434)*S053)
 C473: QINT((C245/SAS434)*S053)
 D473: QINT((D245/SAS434)*S053)
 F473: QINT((F245/SAS434)*S053)
 F473: QINT((F245/SAS434)*S053)
 H473: QINT((H245/SAS434)*S053)
 H473: QINT((H245/SAS434)*S053)
 B474: QINT((B246/SAS434)*S053)
 C474: QINT((C246/SAS434)*S053)
 D474: QINT((D246/SAS434)*S053)
 F474: QINT((F246/SAS434)*S053)
 F474: QINT((F246/SAS434)*S053)
 G474: QINT((G246/SAS434)*S053)
 H474: QINT((H246/SAS434)*S053)
 B475: QINT((B247/SAS434)*S053)
 C475: QINT((C247/SAS434)*S053)
 D475: QINT((D247/SAS434)*S053)
 F475: QINT((F247/SAS434)*S053)
 F475: QINT((F247/SAS434)*S053)
 G475: QINT((G247/SAS434)*S053)
 H475: QINT((H247/SAS434)*S053)
 B476: QINT((B248/SAS434)*S053)
 C476: QINT((C248/SAS434)*S053)
 D476: QINT((D248/SAS434)*S053)
 F476: QINT((F248/SAS434)*S053)
 F476: QINT((F248/SAS434)*S053)
 G476: QINT((G248/SAS434)*S053)
 H476: QINT((H248/SAS434)*S053)
 B477: QINT((B249/SAS434)*S053)
 C477: QINT((C249/SAS434)*S053)
 D477: QINT((D249/SAS434)*S053)
 F477: QINT((F249/SAS434)*S053)
 F477: QINT((F249/SAS434)*S053)

F508: @INT((F427/SAS434)*SD33)
G508: @INT((H427/SAS434)*SD33)
H508: @INT((H427/SAS434)*SD33)
B509: @INT((B428/SAS434)*SD33)
C509: @INT((C428/SAS434)*SD33)
D509: @INT((D428/SAS434)*SD33)
E509: @INT((E428/SAS434)*SD33)
F509: @INT((F428/SAS434)*SD33)
G509: @INT((G428/SAS434)*SD33)
H509: @INT((H428/SAS434)*SD33)

Appendix B: Attenuation Spreadsheet Formulas

This appendix contains a printout of all the formulas used in the attenuation spreadsheet. As in Appendix A, each cell of the spreadsheet is listed on a separate line and the cell labels are set up so that letters represent columns and numbers represent rows starting from the upper left corner of the spreadsheet. The symbols used in front of the cell entries are the same as in Appendix A also.

The first row contains variables used for the calculations in the rest of the spreadsheet. The variables are the time after dispensing and the cloud scaling size. The second row calculates the ' z/V ' term from Eq (42).

Rows 4 through 70 of the spreadsheet are reserved for the values in rows 443 through 509 of the density spreadsheet. In practice, the entries are transferred by first copying the values from the density spreadsheet into a separate file and then transporting them to this spreadsheet. The cells in the printout contain only zeros since until the data transferral occurs, the cells in this spreadsheet are empty.

The remainder of the spreadsheet calculates values for signal attenuation through the central column of the chaff cloud. Each of the 49 subsections in this portion of the

spreadsheet calculates the decimal fraction of the incident signal which penetrates through sections of the cloud corresponding to those in Figure 8.

A1: "t -
 B1: 3600
 C1: "sec
 D1: 0.05
 E1: "(2 ln K*)
 A2: 1/(0.1)^2
 B2: "(2/Vol)
 D2: 0.01
 E2: "m/s
 A4: 0
 S4: 10
 C4: 214
 D4: 605
 E4: 237
 F4: 12
 G4: 0
 A5: 10
 B5: 1479
 C5: 30141
 D5: 85178
 E5: 33382
 F5: 1814
 G5: 13
 A6: 195
 B6: 28759
 C6: 586030
 D6: 1656092
 E6: 649037
 F6: 35275
 G6: 265
 A7: 526
 B7: 77332
 C7: 1575812
 D7: 4453162
 E7: 1745235
 F7: 94855
 G7: 714
 A8: 195
 B8: 28759
 C8: 586030
 D8: 1656092
 E8: 649037
 F8: 35275
 G8: 265
 A9: 1C
 B9: 1479
 C9: 30141
 D9: 85178
 E9: 33382
 F9: 1814
 G9: 13
 A10: 0
 B10: 10

C10: 214
 D10: 605
 E10: 237
 F10: 12
 G10: 0
 A14: 7
 B14: 1063
 C14: 21298
 D14: 59172
 E14: 22798
 F14: 1218
 G14: 9
 A15: 1034
 B15: 149456
 C15: 2994101
 D15: 8318384
 E15: 3205035
 F15: 171256
 G15: 1269
 A16: 20115
 B16: 2905812
 C16: 58212812
 D16: 161730160
 E16: 62313854
 F16: 3329662
 G16: 24673
 A17: 34090
 B17: 7813607
 C17: 156531801
 D17: 434885594
 E17: 167559439
 F17: 8953322
 G17: 68346
 A18: 20115
 B18: 2905812
 C18: 58212812
 D18: 161730160
 E18: 62313854
 F18: 3329662
 G18: 24673
 A19: 1034
 B19: 149456
 C19: 2994101
 D19: 8318384
 E19: 3205035
 F19: 171256
 G19: 1269
 A20: 7
 B20: 1063
 C20: 21298
 D20: 59172
 E20: 22798
 F20: 1218

G20: 9
 A24: 121
 B24: 17187
 C24: 338502
 D24: 924576
 E24: 350223
 F24: 18397
 G24: 134
 A25: 17013
 B25: 2416142
 C25: 47586309
 D25: 129375915
 E25: 49234007
 F25: 2586359
 G25: 18842
 A26: 340778
 B26: 46975847
 C26: 925186524
 D26: 2527056187
 E26: 957231974
 F26: 50285287
 G26: 366341
 A27: 889448
 B27: 126316075
 C27: 2487814782
 D27: 6795147724
 E27: 2573956489
 F27: 135215021
 G27: 985076
 A28: 340778
 B28: 46975847
 C28: 925186524
 D28: 2527056167
 E28: 957231974
 F28: 50285287
 G28: 366341
 A29: 17013
 B29: 2416142
 C29: 47586309
 D29: 129375915
 E29: 49234007
 F29: 2586359
 G29: 18842
 A30: 121
 B30: 17187
 C30: 338502
 D30: 924576
 E30: 350223
 F30: 18397
 G30: 134
 A31: 318
 B31: 44455
 C31: 860785

D31: 2311448
 E31: 860785
 F31: 44455
 G31: 318
 A35: 44761
 B35: 6249525
 C35: 121008227
 D35: 324940750
 E35: 121008227
 F35: 6249525
 G35: 44761
 A36: 870267
 B36: 121506377
 C36: 2352701946
 D36: 6317659159
 E36: 2352701946
 F36: 121506377
 G36: 870267
 A37: 2340112
 B37: 326725533
 C37: 6326316511
 D37: 16387919575
 E37: 6326316511
 F37: 326725533
 G37: 2340112
 A38: 870267
 B38: 121506377
 C38: 2352701946
 D38: 6317659159
 E38: 2352701946
 F38: 121506377
 G38: 870267
 A39: 44761
 B39: 6249525
 C39: 121008227
 D39: 324940750
 E39: 121008227
 F39: 6249525
 G39: 44761
 A40: 318
 B40: 44455
 C40: 860785
 D40: 2311448
 E40: 860785
 F40: 44455
 G40: 318
 A41: 134
 B41: 18397
 C41: 350223
 D41: 924576
 E41: 338502
 F41: 17187
 G41: 121

A15	18842	E55:	2994101
B45	2586359	F55:	149456
C45:	49234007	G55:	1034
D45:	129975915	A56:	24673
E45:	47586309	B56:	3329662
F45:	2416142	C56:	62313634
G45:	17013	D56:	161730160
A46:	368341	E56:	58212812
B46:	50285287	F56:	2905812
C46:	957231974	G56:	20115
D46:	2527058187	A57:	66346
E46:	92515224	B57:	8953322
F46:	46975847	C57:	167559435
G46:	330778	D57:	434885394
A47:	985076	E57:	156531801
B47:	135215021	F57:	7813607
C47:	2573956489	G57:	54090
D47:	6705147724	A58:	24673
E47:	2487814782	B58:	3329662
F47:	126316075	C58:	62313634
G47:	889448	D58:	161730160
A48:	366341	E58:	58212812
B48:	50285287	F58:	2905812
C48:	957231374	G58:	20115
D48:	2527058187	A59:	1269
E48:	92515224	B59:	171256
F48:	46975847	C59:	3205035
G48:	330778	D59:	8318384
A49:	18842	E59:	2994101
B49:	2586359	F59:	149456
C49:	49234007	G59:	1034
D49:	129975915	A60:	9
E49:	47586309	B60:	1218
F49:	2416142	C60:	22798
G49:	17013	D60:	59172
A50:	134	E60:	21298
B50:	18347	F60:	1063
C50:	350223	G60:	7
D50:	924576	A64:	0
E50:	338502	B64:	12
F50:	17187	C64:	237
G50:	121	D64:	605
A54:	0	E64:	214
B54:	1218	F64:	10
C54:	22798	G64:	0
D54:	59172	A65:	13
E54:	21248	B65:	1814
F54:	1063	C65:	33382
G54:	7	D65:	85178
A55:	1269	E65:	30141
B55:	171256	F65:	1479
C55:	3205035	G65:	10
D55:	8318384	A66:	265

B76: (QEXP(-\$A6*2.25E-10*\$A\$2))
 C76: (QEXP(-\$A16*2.25E-10*\$A\$2))
 D76: (QEXP(-\$A26*2.25E-10*\$A\$2))
 E76: (QEXP(-\$A36*2.25E-10*\$A\$2))
 F76: (QEXP(-\$A46*2.25E-10*\$A\$2))
 G76: (QEXP(-\$A56*2.25E-10*\$A\$2))
 H76: (QEXP(-\$A66*2.25E-10*\$A\$2))
 A77: 'Pout(1,4)
 B77: (QEXP(-\$A7*2.25E-10*\$A\$2))
 C77: (QEXP(-\$A17*2.25E-10*\$A\$2))
 D77: (QEXP(-\$A27*2.25E-10*\$A\$2))
 E77: (QEXP(-\$A37*2.25E-10*\$A\$2))
 F77: (QEXP(-\$A47*2.25E-10*\$A\$2))
 G77: (QEXP(-\$A57*2.25E-10*\$A\$2))
 H77: (QEXP(-\$A67*2.25E-10*\$A\$2))
 A78: 'Pout(1,5)
 B78: (QEXP(-\$A8*2.25E-10*\$A\$2))
 C78: (QEXP(-\$A18*2.25E-10*\$A\$2))
 D78: (QEXP(-\$A28*2.25E-10*\$A\$2))
 E78: (QEXP(-\$A38*2.25E-10*\$A\$2))
 F78: (QEXP(-\$A48*2.25E-10*\$A\$2))
 G78: (QEXP(-\$A58*2.25E-10*\$A\$2))
 H78: (QEXP(-\$A68*2.25E-10*\$A\$2))
 A79: 'Pout(1,6)
 B79: (QEXP(-\$A9*2.25E-10*\$A\$2))
 C79: (QEXP(-\$A19*2.25E-10*\$A\$2))
 D79: (QEXP(-\$A29*2.25E-10*\$A\$2))
 E79: (QEXP(-\$A39*2.25E-10*\$A\$2))
 F79: (QEXP(-\$A49*2.25E-10*\$A\$2))
 G79: (QEXP(-\$A59*2.25E-10*\$A\$2))
 H79: (QEXP(-\$A69*2.25E-10*\$A\$2))
 A80: 'Pout(1,7)
 B80: (QEXP(-\$A10*2.25E-10*\$A\$2))
 C80: (QEXP(-\$A20*2.25E-10*\$A\$2))
 D80: (QEXP(-\$A30*2.25E-10*\$A\$2))
 E80: (QEXP(-\$A40*2.25E-10*\$A\$2))
 F80: (QEXP(-\$A50*2.25E-10*\$A\$2))
 G80: (QEXP(-\$A60*2.25E-10*\$A\$2))
 H80: (QEXP(-\$A70*2.25E-10*\$A\$2))
 A82: 'Pout(2,1)
 B82: (QEXP(-\$B4*2.25E-10*\$A\$2))
 C82: (QEXP(-\$B14*2.25E-10*\$A\$2))
 D82: (QEXP(-\$B24*2.25E-10*\$A\$2))
 E82: (QEXP(-\$B34*2.25E-10*\$A\$2))
 F82: (QEXP(-\$B44*2.25E-10*\$A\$2))
 G82: (QEXP(-\$B54*2.25E-10*\$A\$2))
 H82: (QEXP(-\$B64*2.25E-10*\$A\$2))
 A83: 'Pout(2,2)
 B83: (QEXP(-\$B5*2.25E-10*\$A\$2))
 C83: (QEXP(-\$B15*2.25E-10*\$A\$2))
 D83: (QEXP(-\$B25*2.25E-10*\$A\$2))
 E83: (QEXP(-\$B35*2.25E-10*\$A\$2))
 F83: (QEXP(-\$B45*2.25E-10*\$A\$2))
 G83: (QEXP(-\$B55*2.25E-10*\$A\$2))
 H83: (QEXP(-\$B65*2.25E-10*\$A\$2))

B66: 35275
 C66: 649037
 D66: 1656092
 E66: 506030
 F66: 28759
 G66: 195
 A67: 714
 B67: 94855
 C67: 1745235
 D67: 4453162
 E67: 1575812
 F67: 77332
 G67: 526
 A68: 265
 B68: 35275
 C68: 649037
 D68: 1656092
 E68: 506030
 F68: 28759
 G68: 195
 A69: 13
 B69: 1814
 C69: 33382
 D69: 85178
 E69: 30141
 F69: 1479
 G69: 10
 A70: 0
 B70: 12
 C70: 237
 D70: 505
 E70: 214
 F70: 10
 G70: 0
 A72: 'CALCULATIONS
 B72: 'Pout(1,1)
 A74: (QEXP(-\$A4*2.25E-10*\$A\$2))
 B74: (QEXP(-\$A14*2.25E-10*\$A\$2))
 C74: (QEXP(-\$A24*2.25E-10*\$A\$2))
 D74: (QEXP(-\$A34*2.25E-10*\$A\$2))
 E74: (QEXP(-\$A44*2.25E-10*\$A\$2))
 F74: (QEXP(-\$A54*2.25E-10*\$A\$2))
 G74: (QEXP(-\$A64*2.25E-10*\$A\$2))
 A75: 'Pout(1,2)
 B75: (QEXP(-\$A5*2.25E-10*\$A\$2))
 C75: (QEXP(-\$A15*2.25E-10*\$A\$2))
 D75: (QEXP(-\$A25*2.25E-10*\$A\$2))
 E75: (QEXP(-\$A35*2.25E-10*\$A\$2))
 F75: (QEXP(-\$A45*2.25E-10*\$A\$2))
 G75: (QEXP(-\$A55*2.25E-10*\$A\$2))
 H75: (QEXP(-\$A65*2.25E-10*\$A\$2))
 A76: 'Pout(1,3)

G83: (QEXP(-\$B55*2.25E-10*\$A32))*F83
 H83: (QEXP(-\$B65*2.25E-10*\$A32))*G83
 A84: 'Pout(2,3)
 B84: (QEXP(-\$B6*2.25E-10*\$A32))
 C84: (QEXP(-\$B16*2.25E-10*\$A32))*B84
 D84: (QEXP(-\$B26*2.25E-10*\$A32))*C84
 E84: (QEXP(-\$B36*2.25E-10*\$A32))*D84
 F84: (QEXP(-\$B46*2.25E-10*\$A32))*E84
 G84: (QEXP(-\$B56*2.25E-10*\$A32))*F84
 H84: (QEXP(-\$B66*2.25E-10*\$A32))*G84
 A85: 'Pout(2,4)
 B85: (QEXP(-\$B7*2.25E-10*\$A32))
 C85: (QEXP(-\$B17*2.25E-10*\$A32))*B85
 D85: (QEXP(-\$B27*2.25E-10*\$A32))*C85
 E85: (QEXP(-\$B37*2.25E-10*\$A32))*D85
 F85: (QEXP(-\$B47*2.25E-10*\$A32))*E85
 G85: (QEXP(-\$B57*2.25E-10*\$A32))*F85
 H85: (QEXP(-\$B67*2.25E-10*\$A32))*G85
 A86: 'Pout(2,5)
 B86: (QEXP(-\$B8*2.25E-10*\$A32))
 C86: (QEXP(-\$B18*2.25E-10*\$A32))*B86
 D86: (QEXP(-\$B28*2.25E-10*\$A32))*C86
 E86: (QEXP(-\$B38*2.25E-10*\$A32))*D86
 F86: (QEXP(-\$B48*2.25E-10*\$A32))*E86
 G86: (QEXP(-\$B58*2.25E-10*\$A32))*F86
 H86: (QEXP(-\$B68*2.25E-10*\$A32))*G86
 A87: 'Pout(2,6)
 B87: (QEXP(-\$B9*2.25E-10*\$A32))
 C87: (QEXP(-\$B19*2.25E-10*\$A32))*B87
 D87: (QEXP(-\$B29*2.25E-10*\$A32))*C87
 E87: (QEXP(-\$B39*2.25E-10*\$A32))*D87
 F87: (QEXP(-\$B49*2.25E-10*\$A32))*E87
 G87: (QEXP(-\$B59*2.25E-10*\$A32))*F87
 H87: (QEXP(-\$B69*2.25E-10*\$A32))*G87
 A88: 'Pout(2,7)
 B88: (QEXP(-\$B10*2.25E-10*\$A32))
 C88: (QEXP(-\$B20*2.25E-10*\$A32))*B88
 D88: (QEXP(-\$B30*2.25E-10*\$A32))*C88
 E88: (QEXP(-\$B40*2.25E-10*\$A32))*D88
 F88: (QEXP(-\$B50*2.25E-10*\$A32))*E88
 G88: (QEXP(-\$B60*2.25E-10*\$A32))*F88
 H88: (QEXP(-\$B70*2.25E-10*\$A32))*G88
 A89: 'Pout(3,1)
 B89: (QEXP(-\$C4*2.25E-10*\$A32))
 C90: (QEXP(-\$C14*2.25E-10*\$A32))*B89
 D90: (QEXP(-\$C24*2.25E-10*\$A32))*C90
 E90: (QEXP(-\$C34*2.25E-10*\$A32))*D90
 F90: (QEXP(-\$C44*2.25E-10*\$A32))*E90
 G90: (QEXP(-\$C54*2.25E-10*\$A32))*F90
 H90: (QEXP(-\$C64*2.25E-10*\$A32))*G90
 A91: 'Pout(3,2)
 B91: (QEXP(-\$C5*2.25E-10*\$A32))
 C91: (QEXP(-\$C15*2.25E-10*\$A32))*B91
 D91: (QEXP(-\$C25*2.25E-10*\$A32))*C91
 E91: (QEXP(-\$C35*2.25E-10*\$A32))*D91
 F91: (QEXP(-\$C45*2.25E-10*\$A32))*E91
 G91: (QEXP(-\$C55*2.25E-10*\$A32))*F91
 H91: (QEXP(-\$C65*2.25E-10*\$A32))*G91
 A92: 'Pout(3,3)
 B92: (QEXP(-\$C6*2.25E-10*\$A32))
 C92: (QEXP(-\$C16*2.25E-10*\$A32))*B92
 D92: (QEXP(-\$C26*2.25E-10*\$A32))*C92
 E92: (QEXP(-\$C36*2.25E-10*\$A32))*D92
 F92: (QEXP(-\$C46*2.25E-10*\$A32))*E92
 G92: (QEXP(-\$C56*2.25E-10*\$A32))*F92
 H92: (QEXP(-\$C66*2.25E-10*\$A32))*G92
 A93: 'Pout(3,4)
 B93: (QEXP(-\$C7*2.25E-10*\$A32))
 C93: (QEXP(-\$C17*2.25E-10*\$A32))*B93
 D93: (QEXP(-\$C27*2.25E-10*\$A32))*C93
 E93: (QEXP(-\$C37*2.25E-10*\$A32))*D93
 F93: (QEXP(-\$C47*2.25E-10*\$A32))*E93
 G93: (QEXP(-\$C57*2.25E-10*\$A32))*F93
 H93: (QEXP(-\$C67*2.25E-10*\$A32))*G93
 A94: 'Pout(3,5)
 B94: (QEXP(-\$C8*2.25E-10*\$A32))
 C94: (QEXP(-\$C18*2.25E-10*\$A32))*B94
 D94: (QEXP(-\$C28*2.25E-10*\$A32))*C94
 E94: (QEXP(-\$C38*2.25E-10*\$A32))*D94
 F94: (QEXP(-\$C48*2.25E-10*\$A32))*E94
 G94: (QEXP(-\$C58*2.25E-10*\$A32))*F94
 H94: (QEXP(-\$C68*2.25E-10*\$A32))*G94
 A95: 'Pout(3,6)
 B95: (QEXP(-\$C9*2.25E-10*\$A32))
 C95: (QEXP(-\$C19*2.25E-10*\$A32))*B95
 D95: (QEXP(-\$C29*2.25E-10*\$A32))*C95
 E95: (QEXP(-\$C39*2.25E-10*\$A32))*D95
 F95: (QEXP(-\$C49*2.25E-10*\$A32))*E95
 G95: (QEXP(-\$C59*2.25E-10*\$A32))*F95
 H95: (QEXP(-\$C69*2.25E-10*\$A32))*G95
 A96: 'Pout(3,7)
 B96: (QEXP(-\$C10*2.25E-10*\$A32))
 C96: (QEXP(-\$C20*2.25E-10*\$A32))*B96
 D96: (QEXP(-\$C30*2.25E-10*\$A32))*C96
 E96: (QEXP(-\$C40*2.25E-10*\$A32))*D96
 F96: (QEXP(-\$C50*2.25E-10*\$A32))*E96
 G96: (QEXP(-\$C60*2.25E-10*\$A32))*F96
 H96: (QEXP(-\$C70*2.25E-10*\$A32))*G96
 A98: 'Pout(4,1)
 B98: (QEXP(-\$D4*2.25E-10*\$A32))
 C98: (QEXP(-\$D14*2.25E-10*\$A32))*B98
 D98: (QEXP(-\$D24*2.25E-10*\$A32))*C98
 E98: (QEXP(-\$D34*2.25E-10*\$A32))*D98
 F98: (QEXP(-\$D44*2.25E-10*\$A32))*E98
 G98: (QEXP(-\$D54*2.25E-10*\$A32))*F98
 H98: (QEXP(-\$D64*2.25E-10*\$A32))*G98

F106: (QEXP(-SE44*2.25E-10*SA32))•E106
 G106: (QEXP(-SE54*2.25E-10*SA32))•F106
 H106: (QEXP(-SE64*2.25E-10*SA32))•G106
 A107: 'Pout(5,2)
 B107: QEXP(-SE5*2.25E-10*SA32)
 C107: (QEXP(-SE15*2.25E-10*SA32))•B107
 D107: (QEXP(-SE25*2.25E-10*SA32))•C107
 E107: (QEXP(-SE35*2.25E-10*SA32))•D107
 F107: (QEXP(-SE45*2.25E-10*SA32))•E107
 G107: (QEXP(-SE55*2.25E-10*SA32))•F107
 H107: (QEXP(-SE65*2.25E-10*SA32))•G107
 A108: 'Pout(5,3)
 B108: QEXP(-SE6*2.25E-10*SA32)
 C108: (QEXP(-SE16*2.25E-10*SA32))•B108
 D108: (QEXP(-SE26*2.25E-10*SA32))•C108
 E108: (QEXP(-SE36*2.25E-10*SA32))•D108
 F108: (QEXP(-SE46*2.25E-10*SA32))•E108
 G108: (QEXP(-SE56*2.25E-10*SA32))•F108
 H108: (QEXP(-SE66*2.25E-10*SA32))•G108
 A109: 'Pout(5,4)
 B109: QEXP(-SE7*2.25E-10*SA32)
 C109: (QEXP(-SE17*2.25E-10*SA32))•B109
 D109: (QEXP(-SE27*2.25E-10*SA32))•C109
 E109: (QEXP(-SE37*2.25E-10*SA32))•D109
 F109: (QEXP(-SE47*2.25E-10*SA32))•E109
 G109: (QEXP(-SE57*2.25E-10*SA32))•F109
 H109: (QEXP(-SE67*2.25E-10*SA32))•G109
 A110: 'Pout(5,5)
 B110: QEXP(-SE8*2.25E-10*SA32)
 C110: (QEXP(-SE18*2.25E-10*SA32))•B110
 D110: (QEXP(-SE28*2.25E-10*SA32))•C110
 E110: (QEXP(-SE38*2.25E-10*SA32))•D110
 F110: (QEXP(-SE48*2.25E-10*SA32))•E110
 G110: (QEXP(-SE58*2.25E-10*SA32))•F110
 H110: (QEXP(-SE68*2.25E-10*SA32))•G110
 A111: 'Pout(5,6)
 B111: QEXP(-SE9*2.25E-10*SA32)
 C111: (QEXP(-SE19*2.25E-10*SA32))•B111
 D111: (QEXP(-SE29*2.25E-10*SA32))•C111
 E111: (QEXP(-SE39*2.25E-10*SA32))•D111
 F111: (QEXP(-SE49*2.25E-10*SA32))•E111
 G111: (QEXP(-SE59*2.25E-10*SA32))•F111
 H111: (QEXP(-SE69*2.25E-10*SA32))•G111
 A112: 'Pout(5,7)
 B112: QEXP(-SE10*2.25E-10*SA32)
 C112: (QEXP(-SE20*2.25E-10*SA32))•B112
 D112: (QEXP(-SE30*2.25E-10*SA32))•C112
 E112: (QEXP(-SE40*2.25E-10*SA32))•D112
 F112: (QEXP(-SE50*2.25E-10*SA32))•E112
 G112: (QEXP(-SE60*2.25E-10*SA32))•F112
 H112: (QEXP(-SE70*2.25E-10*SA32))•G112
 A114: 'Pout(6,1)
 B114: QEXP(-SF4*2.25E-10*SA32)

A99: 'Pout(4,2)
 B99: QEXP(-SD5*2.25E-10*SA32)
 C99: (QEXP(-SD15*2.25E-10*SA32))•B99
 D99: (QEXP(-SD25*2.25E-10*SA32))•C99
 E99: (QEXP(-SD35*2.25E-10*SA32))•D99
 F99: (QEXP(-SD45*2.25E-10*SA32))•E99
 G99: (QEXP(-SD55*2.25E-10*SA32))•F99
 H99: (QEXP(-SD65*2.25E-10*SA32))•G99
 A100: 'Pout(4,3)
 B100: QEXP(-SD6*2.25E-10*SA32)
 C100: (QEXP(-SD16*2.25E-10*SA32))•B100
 D100: (QEXP(-SD26*2.25E-10*SA32))•C100
 E100: (QEXP(-SD36*2.25E-10*SA32))•D100
 F100: (QEXP(-SD46*2.25E-10*SA32))•E100
 G100: (QEXP(-SD56*2.25E-10*SA32))•F100
 H100: (QEXP(-SD66*2.25E-10*SA32))•G100
 A101: 'Pout(4,4)
 B101: QEXP(-SD7*2.25E-10*SA32)
 C101: (QEXP(-SD17*2.25E-10*SA32))•B101
 D101: (QEXP(-SD27*2.25E-10*SA32))•C101
 E101: (QEXP(-SD37*2.25E-10*SA32))•D101
 F101: (QEXP(-SD47*2.25E-10*SA32))•E101
 G101: (QEXP(-SD57*2.25E-10*SA32))•F101
 H101: (QEXP(-SD67*2.25E-10*SA32))•G101
 A102: 'Pout(4,5)
 B102: QEXP(-SD8*2.25E-10*SA32)
 C102: (QEXP(-SD18*2.25E-10*SA32))•B102
 D102: (QEXP(-SD28*2.25E-10*SA32))•C102
 E102: (QEXP(-SD38*2.25E-10*SA32))•D102
 F102: (QEXP(-SD48*2.25E-10*SA32))•E102
 G102: (QEXP(-SD58*2.25E-10*SA32))•F102
 H102: (QEXP(-SD68*2.25E-10*SA32))•G102
 A103: 'Pout(4,6)
 B103: QEXP(-SD9*2.25E-10*SA32)
 C103: (QEXP(-SD19*2.25E-10*SA32))•B103
 D103: (QEXP(-SD29*2.25E-10*SA32))•C103
 E103: (QEXP(-SD39*2.25E-10*SA32))•D103
 F103: (QEXP(-SD49*2.25E-10*SA32))•E103
 G103: (QEXP(-SD59*2.25E-10*SA32))•F103
 H103: (QEXP(-SD69*2.25E-10*SA32))•G103
 A104: 'Pout(4,7)
 B104: QEXP(-SD10*2.25E-10*SA32)
 C104: (QEXP(-SD20*2.25E-10*SA32))•B104
 D104: (QEXP(-SD30*2.25E-10*SA32))•C104
 E104: (QEXP(-SD40*2.25E-10*SA32))•D104
 F104: (QEXP(-SD50*2.25E-10*SA32))•E104
 G104: (QEXP(-SD60*2.25E-10*SA32))•F104
 H104: (QEXP(-SD70*2.25E-10*SA32))•G104
 A106: 'Pout(5,1)
 B106: QEXP(-SE4*2.25E-10*SA32)
 C106: (QEXP(-SE14*2.25E-10*SA32))•B106
 D106: (QEXP(-SE24*2.25E-10*SA32))•C106
 E106: (QEXP(-SE34*2.25E-10*SA32))•D106

C114: (QEXP(-\$F14*2.25E-10*SA\$2))\$B114
 D114: (QEXP(-\$F24*2.25E-10*SA\$2))\$C114
 E114: (QEXP(-\$F34*2.25E-10*SA\$2))\$D114
 F114: (QEXP(-\$F44*2.25E-10*SA\$2))\$E114
 G114: (QEXP(-\$F54*2.25E-10*SA\$2))\$F114
 H114: (QEXP(-\$F64*2.25E-10*SA\$2))\$G114
 A115: 'Pout(6,2)
 B115: QEXP(-\$F5*2.25E-10*SA\$2)
 C115: (QEXP(-\$F15*2.25E-10*SA\$2))\$B115
 D115: (QEXP(-\$F25*2.25E-10*SA\$2))\$C115
 E115: (QEXP(-\$F35*2.25E-10*SA\$2))\$D115
 F115: (QEXP(-\$F45*2.25E-10*SA\$2))\$E115
 G115: (QEXP(-\$F55*2.25E-10*SA\$2))\$F115
 H115: (QEXP(-\$F65*2.25E-10*SA\$2))\$G115
 A116: 'Pout(6,3)
 B116: QEXP(-\$F6*2.25E-10*SA\$2)
 C116: (QEXP(-\$F16*2.25E-10*SA\$2))\$B116
 D116: (QEXP(-\$F26*2.25E-10*SA\$2))\$C116
 E116: (QEXP(-\$F36*2.25E-10*SA\$2))\$D116
 F116: (QEXP(-\$F46*2.25E-10*SA\$2))\$E116
 G116: (QEXP(-\$F56*2.25E-10*SA\$2))\$F116
 H116: (QEXP(-\$F66*2.25E-10*SA\$2))\$G116
 A117: 'Pout(6,4)
 B117: QEXP(-\$F7*2.25E-10*SA\$2)
 C117: (QEXP(-\$F17*2.25E-10*SA\$2))\$B117
 D117: (QEXP(-\$F27*2.25E-10*SA\$2))\$C117
 E117: (QEXP(-\$F37*2.25E-10*SA\$2))\$D117
 F117: (QEXP(-\$F47*2.25E-10*SA\$2))\$E117
 G117: (QEXP(-\$F57*2.25E-10*SA\$2))\$F117
 H117: (QEXP(-\$F67*2.25E-10*SA\$2))\$G117
 A118: 'Pout(6,5)
 B118: QEXP(-\$F8*2.25E-10*SA\$2)
 C118: (QEXP(-\$F18*2.25E-10*SA\$2))\$B118
 D118: (QEXP(-\$F28*2.25E-10*SA\$2))\$C118
 E118: (QEXP(-\$F38*2.25E-10*SA\$2))\$D118
 F118: (QEXP(-\$F48*2.25E-10*SA\$2))\$E118
 G118: (QEXP(-\$F58*2.25E-10*SA\$2))\$F118
 H118: (QEXP(-\$F68*2.25E-10*SA\$2))\$G118
 A119: 'Pout(6,6)
 B119: QEXP(-\$F9*2.25E-10*SA\$2)
 C119: (QEXP(-\$F19*2.25E-10*SA\$2))\$B119
 D119: (QEXP(-\$F29*2.25E-10*SA\$2))\$C119
 E119: (QEXP(-\$F39*2.25E-10*SA\$2))\$D119
 F119: (QEXP(-\$F49*2.25E-10*SA\$2))\$E119
 G119: (QEXP(-\$F59*2.25E-10*SA\$2))\$F119
 H119: (QEXP(-\$F69*2.25E-10*SA\$2))\$G119
 A120: 'Pout(6,7)
 B120: QEXP(-\$F10*2.25E-10*SA\$2)
 C120: (QEXP(-\$F20*2.25E-10*SA\$2))\$B120
 D120: (QEXP(-\$F30*2.25E-10*SA\$2))\$C120
 E120: (QEXP(-\$F40*2.25E-10*SA\$2))\$D120
 F120: (QEXP(-\$F50*2.25E-10*SA\$2))\$E120
 G120: (QEXP(-\$F60*2.25E-10*SA\$2))\$F120

H120: (QEXP(-\$F70*2.25E-10*SA\$2))\$G120
 A122: 'Pout(7,1)
 B122: QEXP(-\$94*2.25E-10*SA\$2)
 C122: (QEXP(-\$G14*2.25E-10*SA\$2))\$B122
 D122: (QEXP(-\$G24*2.25E-10*SA\$2))\$C122
 E122: (QEXP(-\$G34*2.25E-10*SA\$2))\$D122
 F122: (QEXP(-\$G44*2.25E-10*SA\$2))\$E122
 G122: (QEXP(-\$G54*2.25E-10*SA\$2))\$F122
 H122: (QEXP(-\$G64*2.25E-10*SA\$2))\$G122
 A123: 'Pout(7,2)
 B123: QEXP(-\$95*2.25E-10*SA\$2)
 C123: (QEXP(-\$G15*2.25E-10*SA\$2))\$B123
 D123: (QEXP(-\$G25*2.25E-10*SA\$2))\$C123
 E123: (QEXP(-\$G35*2.25E-10*SA\$2))\$D123
 F123: (QEXP(-\$G45*2.25E-10*SA\$2))\$E123
 G123: (QEXP(-\$G55*2.25E-10*SA\$2))\$F123
 H123: (QEXP(-\$G65*2.25E-10*SA\$2))\$G123
 A124: 'Pout(7,3)
 B124: QEXP(-\$96*2.25E-10*SA\$2)
 C124: (QEXP(-\$G16*2.25E-10*SA\$2))\$B124
 D124: (QEXP(-\$G26*2.25E-10*SA\$2))\$C124
 E124: (QEXP(-\$G36*2.25E-10*SA\$2))\$D124
 F124: (QEXP(-\$G46*2.25E-10*SA\$2))\$E124
 G124: (QEXP(-\$G56*2.25E-10*SA\$2))\$F124
 H124: (QEXP(-\$G66*2.25E-10*SA\$2))\$G124
 A125: 'Pout(7,4)
 B125: QEXP(-\$97*2.25E-10*SA\$2)
 C125: (QEXP(-\$G17*2.25E-10*SA\$2))\$B125
 D125: (QEXP(-\$G27*2.25E-10*SA\$2))\$C125
 E125: (QEXP(-\$G37*2.25E-10*SA\$2))\$D125
 F125: (QEXP(-\$G47*2.25E-10*SA\$2))\$E125
 G125: (QEXP(-\$G57*2.25E-10*SA\$2))\$F125
 H125: (QEXP(-\$G67*2.25E-10*SA\$2))\$G125
 A126: 'Pout(7,5)
 B126: QEXP(-\$98*2.25E-10*SA\$2)
 C126: (QEXP(-\$G18*2.25E-10*SA\$2))\$B126
 D126: (QEXP(-\$G28*2.25E-10*SA\$2))\$C126
 E126: (QEXP(-\$G38*2.25E-10*SA\$2))\$D126
 F126: (QEXP(-\$G48*2.25E-10*SA\$2))\$E126
 G126: (QEXP(-\$G58*2.25E-10*SA\$2))\$F126
 H126: (QEXP(-\$G68*2.25E-10*SA\$2))\$G126
 A127: 'Pout(7,6)
 B127: QEXP(-\$99*2.25E-10*SA\$2)
 C127: (QEXP(-\$G19*2.25E-10*SA\$2))\$B127
 D127: (QEXP(-\$G29*2.25E-10*SA\$2))\$C127
 E127: (QEXP(-\$G39*2.25E-10*SA\$2))\$D127
 F127: (QEXP(-\$G49*2.25E-10*SA\$2))\$E127
 G127: (QEXP(-\$G59*2.25E-10*SA\$2))\$F127
 H127: (QEXP(-\$G69*2.25E-10*SA\$2))\$G127
 A128: 'Pout(7,7)
 B128: QEXP(-\$G10*2.25E-10*SA\$2)
 C128: (QEXP(-\$G20*2.25E-10*SA\$2))\$B128
 D128: (QEXP(-\$G30*2.25E-10*SA\$2))\$C128

E128: (QEXP(-9840*2.25E-10*9AS2))*D128
F128: (QEXP(-9650*2.25E-10*9AS2))*E12
G128: (QEXP(-9660*2.25E-10*9AS2))*F128
H128: (QEXP(-9670*2.25E-10*9AS2))*G128

Appendix C: An Example Calculation

To help clarify the description provided in Chapter IV of the procedures for determining signal attenuation, an example describing the calculation of signal attenuation achieved by the chaff cloud is provided below. For this example, the dispensing velocity was 0.05 m/s and the time after initial dispensing was six hours.

First, the cloud model using the density spreadsheet was scaled up by factors of seven (for ease of subsequent calculations, and rescaling) until all of the chaff particles were contained within the subvolume at the origin of the grid. The size of this cube (cube A) was 120.05 km on a side with the subvolume (cube B) 17.15 km on a side. This is shown in Figure C1. The grid could now be downscaled by a factor of seven and still contain all the chaff particles inside.

Next, the density spreadsheet was rerun for subvolumes 2.45 km on a side to determine the extent of the cloud in the ξ direction within cube B. Using this procedure, the cloud was found to extend into (but not completely through) one subvolume on each side of the central subvolume of cube B (cubes D and E). Thus, the cloud was only 7.35 km thick in the ξ direction at this point in time. This is shown in

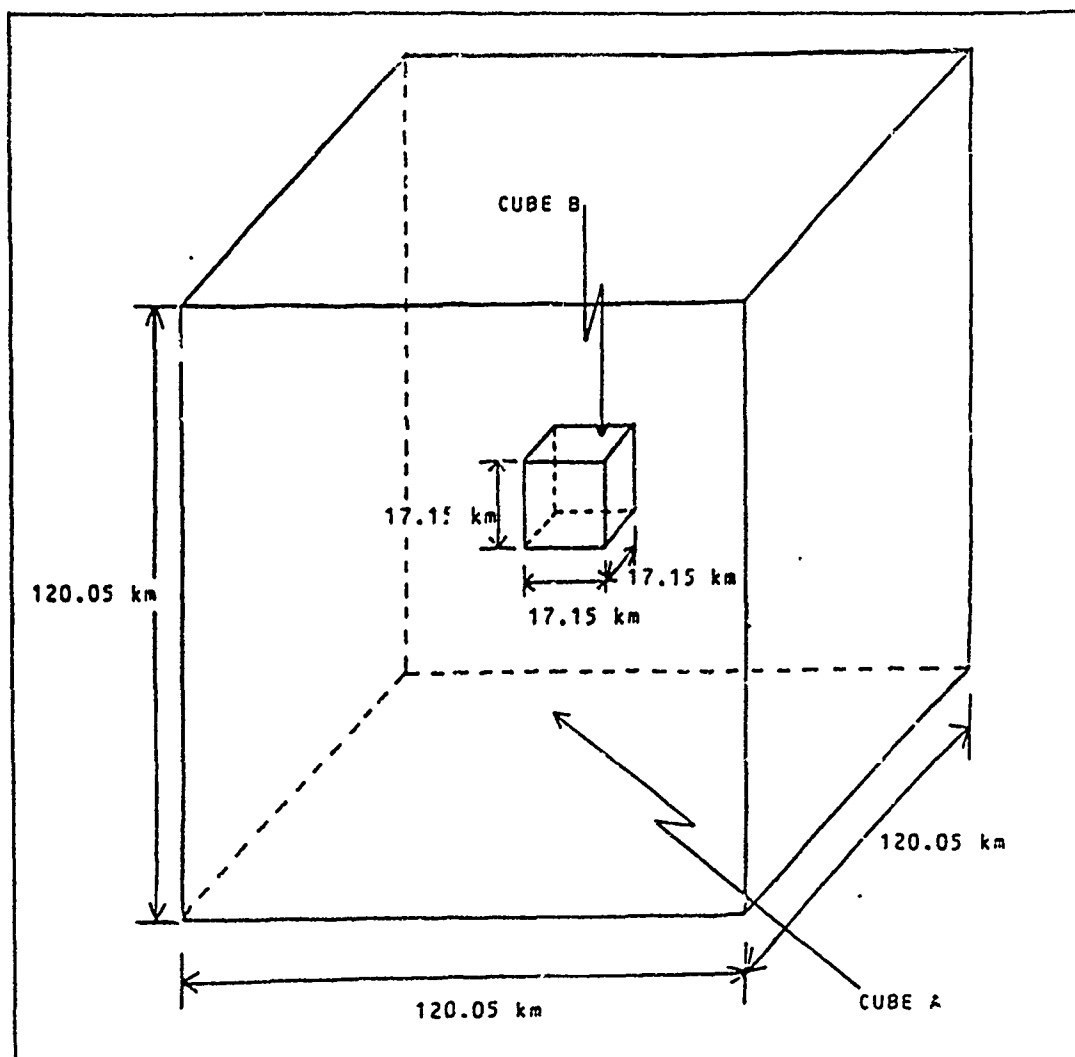


Figure C1. Initial Downscaling of Cube A

Figure C2. The number of particles within each of these three subvolumes was then recorded for the next subscaling.

It is important to note here that only those subvolumes which contained a significant number of particles at each subscaling were considered further in the attenuation calculations. A significant number of particles was determined to be the number of particles which caused an attenuation of 0.1 percent or greater when Eq (42) was applied. For a subvolume of 0.35 km on a side, this number was determined to be approximately 545,000 particles. For a subvolume 2.45 km on a side, 26.6 million particles was considered a significant number.

Now, the spreadsheet was again used to downscale the cloud using dimensions of 0.35 km on a side. For the center subvolume from before (cube C), the origin was left at $(\xi, \eta, \zeta) = (0, 0, 0)$. However, for cubes D and E, the origin was moved 2.45 km (5.82×10^{-5} RU) in the plus and minus ξ directions, respectively. The number of chaff particles within the central column of cubes C, D, and E ((η, ζ) equal to (4,4)) for each of the seven values of ξ were now recorded. For this example, 21 sub-subvolumes 0.35 km on a side (cubes F through Z) were found to contain a significant number of particles to be recorded. Cubes F through Z are shown in Figure C3 and the number of chaff particles contained in each cube is shown in Table C1.

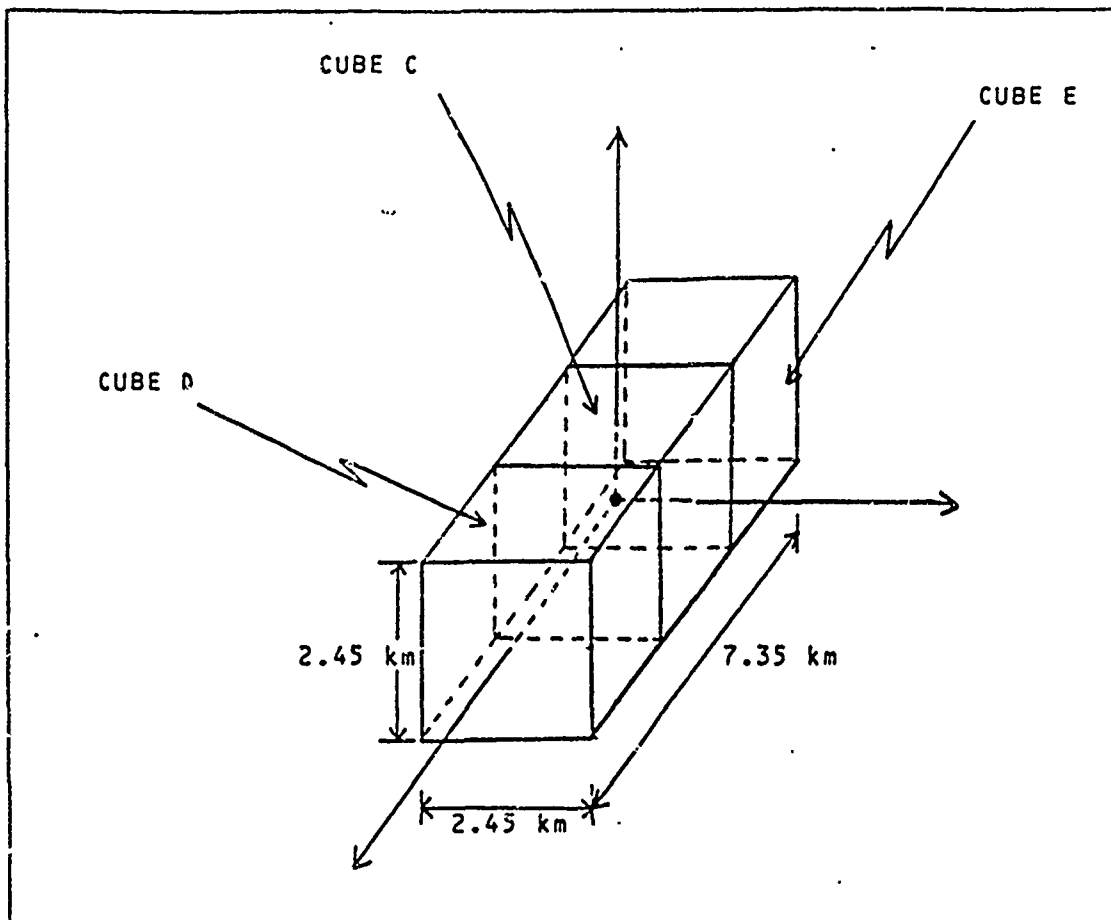


Figure C2. Central Column at 2.45 km Scaling

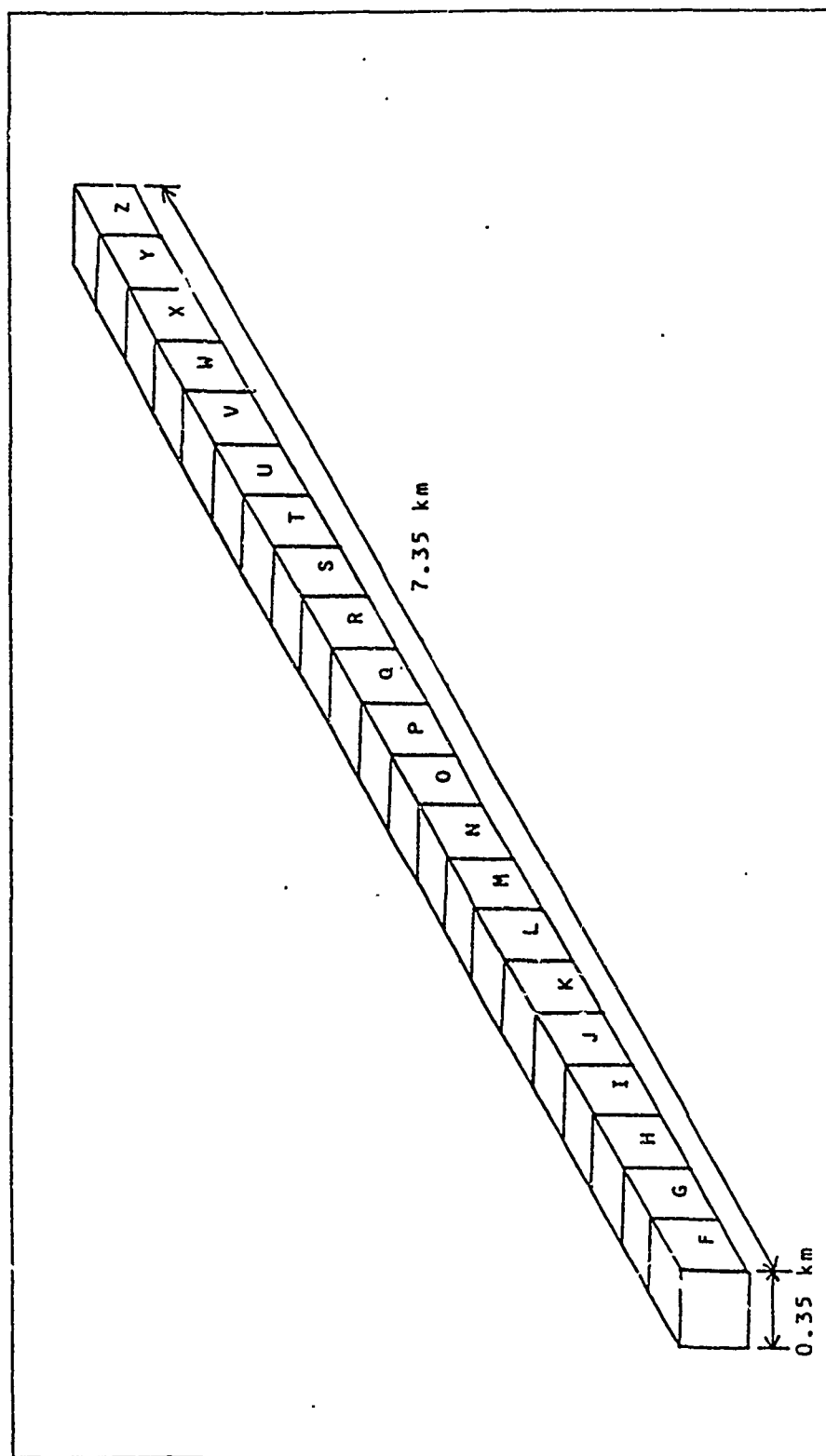


Figure C3. Central Column at 0.35 km Scaling

Table CI. Number of Particles Along the Central
Column at 0.35 km Scaling

CUBE	# OF PARTICLES
F	5.72×10^5
G	1.60×10^6
H	4.03×10^6
I	9.10×10^6
J	1.84×10^7
K	3.35×10^7
L	5.47×10^7
M	2.41×10^8
N	3.16×10^8
O	3.72×10^8
P	3.93×10^8
Q	3.72×10^8
R	3.16×10^8
S	2.41×10^8
T	5.42×10^7
U	3.32×10^7
V	1.83×10^7
W	9.02×10^6
X	4.00×10^6
Y	1.59×10^6
Z	5.67×10^5

Each of these 21 sub-subvolumes through the thickness of the cloud was now examined individually. The scale of the spreadsheet was again reduced to provide cubes 0.05 km on a side. The origin of the grid was moved in each case to the appropriate ξ location. Since only the central column of the chaff cloud was examined in detail, the coordinates for both η and ξ were always zero as the origin was moved back and forth through the chaff cloud.

Finally, using the attenuation spreadsheet, the signal attenuation through each of cubes F through Z was calculated. Then, each of the 21 attenuation values for the 21 cubes with (η, ξ) equal to (1,2) were multiplied together to obtain the signal attenuation through the entire chaff cloud at those coordinates. Attenuation for the other 44 significant (η, ξ) values were then calculated in a similar manner.

Since the effectiveness of the chaff cloud is only as good as the worst attenuation value, the highest value for P_{out} obtained in the above calculations was chosen as the overall attenuation value for the chaff cloud. Using the above method, the signal attenuation for the chaff cloud with a 0.05 m/s dispensing velocity and at a time six hours after dispensing turned out to be -18.3 dB ($P_{out}/P_{in} = 0.0149$). Therefore, the cloud is "effective" for these parameters of velocity and time after dispensing.

The above procedure was repeated for every combination of dispensing velocity and time after dispensing that was examined in this study. Although the signal attenuation and the number of times the cloud was scaled up and down varied for each change in dispensing velocity and time after dispensing, the overall procedure was very similar for the additional runs required.

Bibliography

- Bate, Roger R. and others. Fundamentals of Astrodynamics. New York: Dover Publications, Inc., 1971.
- Brown, Capt Tommy C. "Effects of Reflective Chaff on Satcom Uplinks" (Unclassified), Chapter IV in Applications of Electronic Countermeasures Against Uplinks of the Defense Satellite Communications System (Classified SECRET). MS thesis, AFIT/GSO/ENS/87D-05. School of Engineering, Air Force Institute of Technology (AU), Wright-Patterson AFB OH, December 1987.
- Butters, Brian C.F. "Chaff," IEE Proceedings Part F, 129: 197-201 (June 1982).
- Chen, Francis F. Introduction to Plasma Physics. New York: Plenum Press, 1977.
- Dasenbrock, Robert and others. Dynamics of Satellite Disintegration. NRL Report 7554: Naval Research Laboratory, 30 January 1976 (AD-A020921).
- Evans, LtCol Howard E. II. Personal Interviews. Air Force Institute of Technology (AU), Wright Patterson AFB OH, January to November 1988.
- . Class handout distributed in PHYS 519, The Space Environment, School of Engineering, Air Force of Technology (AU), Wright Patterson AFB OH, October 1987.
- Hameen-Antilla, K.A. "Statistical Mechanics of Keplerian Orbits," Astrophysics and Space Science, 43: 145-174 (1976).
- Heard, William B. Satellite Breakups: Survey of a Dynamical Theory, NRL Memorandum Report 3802: Naval Research Laboratory, July 1978 (AD-A060742).
- . "Asymptotic Distribution of Particles From Fragmented Celestial Bodies," The Astronomical Journal, 82: 1025-1035 (December 1977).
- . "Dispersion of Ensembles of Non-Interacting Particles," Astrophysics and Space Science, 43: 63-82 (1976).

Illustrated Encyclopedia of Space Technology: A Comprehensive History of Space Exploration, The (Third Impression) edited by Philip de Ste. Croix. New York: Harmony Books, 1982.

Johnson, Nicholas L. and Darren S. McKnight. Artificial Space Debris. Malabar, Florida: Orbit Book Company, 1987.

Kessler, Donald J. "Space Debris: More Than Meets the Eye," Sky and Telescope, 73: 587 (June 1987).

Knott, E.F. and others. Chaff Theoretical/Analytical Characterization and Validation Program. Contract DAAG29-80-C-0009. Atlanta Engineering Experiment Station, Georgia Institute of Technology, September 1981 (AD-A105893).

MacLellan, D.C. and others. "Effects of the West Ford Belt on Astronomical Observations," Proceedings of the IEEE, 52: 564-570 (May 1964).

Overhage, C.F.J. and W.H. Radford. "The Lincoln Laboratory West Ford Program: An Historical Perspective," Proceedings of the IEEE, 52: 452-454 (May 1964).

Peebles, Peyton Z. "Bistatic Radar Cross Sections of Chaff," IEEE Transactions on Aerospace and Electronic Systems, AES-20: 128-140 (March 1984).

Ross, Stanley. "The Orbital Motion of Pell + Clouds," The Journal of the Astronautical Sciences 3: 79-83 (Fall 1961).

Shapiro, I.I. and others. "Orbiting Properties of the West Ford Dipole Belt," Proceedings of the IEEE, 15: 469-518 (May 1964).

Stanley, William D. Electronic Communications Systems. Reston, Virginia: Reston Publishing Company, Inc., 1962.

Thomson, William Tyrrell. Introduction to Space Dynamics. New York: Dover Publications, Inc., 1986.

Vita

Captain Alan R. Sterns was born in Ludington, Michigan on 12 December 1960. He graduated from high school in Green River, Wyoming in 1979. He then attended the United States Air Force Academy and graduated on 1 June 1983 with a Bachelor of Sciences degree in Engineering Sciences. Upon graduation, he went to work for Space Command inside Cheyenne Mountain in Colorado Springs as an orbital analyst. He worked there until assuming a position for United States Space Command as a staff officer in J3S0S in July 1986. From there he entered the School of Engineering at the Air Force Institute of Technology in May of 1987.

Permanent address: 3845 Rosemere Street

Colorado Springs, Colorado 80906

Unclassified

SECURITY CLASSIFICATION OF THIS PAGE

REPORT DOCUMENTATION PAGE

Form Approved
OMB No. 0704-0188

1a. REPORT SECURITY CLASSIFICATION Unclassified			1b. RESTRICTIVE MARKINGS		
2a. SECURITY CLASSIFICATION AUTHORITY			3. DISTRIBUTION/AVAILABILITY OF REPORT Approved for public release; distribution unlimited.		
2b. DECLASSIFICATION/DOWNGRADING SCHEDULE					
4. PERFORMING ORGANIZATION REPORT NUMBER(S) AFIT/GSO/ENP/88D-6			5. MONITORING ORGANIZATION REPORT NUMBER(S)		
6a. NAME OF PERFORMING ORGANIZATION School of Engineering		6b. OFFICE SYMBOL (If applicable) AFIT/ENS	7a. NAME OF MONITORING ORGANIZATION		
6c. ADDRESS (City, State, and ZIP Code) Air Force Institute of Technology (AU) Wright-Patterson AFB, Ohio 45433-6583			7b. ADDRESS (City, State, and ZIP Code)		
8a. NAME OF FUNDING/SPONSORING ORGANIZATION		8b. OFFICE SYMBOL (If applicable)	9. PROCUREMENT INSTRUMENT IDENTIFICATION NUMBER		
8c. ADDRESS (City, State, and ZIP Code)			10. SOURCE OF FUNDING NUMBERS		
			PROGRAM ELEMENT NO.	PROJECT NO.	TASK NO.
11. TITLE (Include Security Classification) THE USE OF CHAFF IN SPACE AS A JAMMING DEVICE BETWEEN GROUND STATIONS AND SATELLITES					
12. PERSONAL AUTHOR(S) Alan R. Sterns, Capt USAF					
13a. TYPE OF REPORT MS Thesis		13b. TIME COVERED FROM _____ TO _____		14. DATE OF REPORT (Year, Month, Day) 1988, DEC	
15. PAGE COUNT 171					
16. SUPPLEMENTARY NOTATION					
17. COSATI CODES			18. SUBJECT TERMS (Continue on reverse if necessary and identify by block number) Chaff, Statistical Mechanics, Orbits, Spacecraft Debris, Electronic Countermeasures		
FIELD	GROUP	SUB-GROUP			
17	04	03			
22	01				
19. ABSTRACT (Continue on reverse if necessary and identify by block number) LtCol Howard E. Evans II					
20. DISTRIBUTION/AVAILABILITY OF ABSTRACT <input checked="" type="checkbox"/> UNCLASSIFIED/UNLIMITED <input type="checkbox"/> SAME AS RPT <input type="checkbox"/> DTIC USERS			21. ABSTRACT SECURITY CLASSIFICATION Unclassified		
22a. NAME OF RESPONSIBLE INDIVIDUAL LtCol Howard Evans, Physics Instructor			22b. TELEPHONE (Include Area Code) (513) 255-2012		22c. OFFICE SYMBOL AFIT/ENP

Approved for release in
accordance with E.O. 12958-1
ESR Review
12 Jan 1989

This study predicts the time evolution of the attenuation characteristics of a cnaff cloud deployed in orbit around the earth. The study consists of three parts: applying the statistical mechanics solution of a satellite breakup model by William Heard of the Naval Research Laboratory, solving for particle density at any time after dispensing, and calculating the attenuation of an 8 GHz signal through the cloud. The study shows that significant levels of signal attenuation can be achieved, with attenuations of greater than -50 dB lasting for several hours.